Design of a hybrid system to generate electricity by gasification of residual biomass and photovoltaic generation for different uses in developing countries

TRABAJO FINAL DE MÁSTER EN
ENERGY ENGINEERING – GREEN POWER SYSTEM
INGENIERÍA ENERGÉTICA

Author: **Salvatore Pecoraro**

Student ID: 10567875
Advisors: Ramón Gavela González, Carlos García Martínez
Academic Year: 2021-22

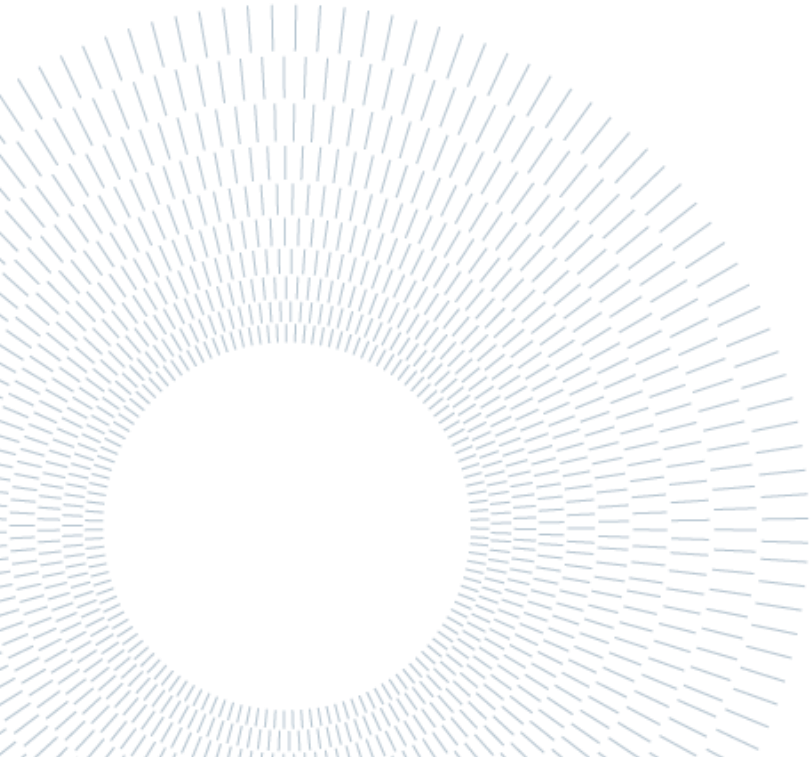

ABSTRACT

The present work aims to identify cost-effective and sustainable solutions to supply electricity and water to developing countries, in particular using a hybrid system consisting of a 20 kW downdraft gasifier and photovoltaics. The completed project will be used by the NGO Manos Unidas as a mean to estimate the costs, performance and potential of this system and will help investigate the advantages that gasification can provide in economic, environmental and exploitation terms of the residual biomass present on site. Initially, a focus is made on the numbers and the situation of energy need in the world, observing what are the initiatives and objectives to fulfill the deficiencies. The picture of the energy conversion processes starting from biomass is illustrated in a clear and schematic way. Among these there is gasification, which is exhaustively explained and classified according to existing types, processes and technologies, with a main focus on downdraft gasification, whose principles and sub-processes are explained in detail. After providing the above information, it is possible to move on to the calculation part. In order to provide broader results, nine of the most common types of residual biomass are selected. Using the experimental data, a detailed calculation procedure is developed which, starting from the raw biomass, transforms it into syngas. Then, this gas mix passes through a heat exchanger to heat water for sanitary purposes, to finally be burned inside an engine to produce electricity. In this calculation phase, all main and auxiliary equipment are selected from real catalogs. At this point, a rural community in Nigeria is identified in the vicinity of a chicken farm, whose manure is a valuable resource that can be used inside the gasifier. The loads and needs of this population are identified and, after hypothesizing a load profile, a process of LCOE minimization was developed through a MATLAB code. After having identified the investment and O&M costs and all the necessary parameters, it has been found an optimal solution that couples in the cheapest way the gasification and photovoltaic technology with their relative auxiliary elements. Finally, having defined in detail all the elements that make up the project, it is possible to estimate the total investment.

Separately from all the calculations developed, it has been elaborated a zero-dimensional model which allows to predict the composition of the syngas and its calorific value starting from the elemental composition of each biomass. The results are compared and validated with the experimental data of the same biomasses chosen in the calculation phase. This tool allows to obtain immediate, economic and on average acceptable estimates on the productivity of gasification.

Key-words: downdraft gasification, developing countries, PV panels, 0-D gasification model.

ABSTRACT EN ESPAÑOL

El presente trabajo tiene como objetivo identificar soluciones económicamente ventajosas y sostenibles para suministrar electricidad y agua a los países en desarrollo, en particular utilizando un sistema híbrido que consta de un gasificador de tiro descendente de 20 kW y paneles fotovoltaicos. El proyecto finalizado será utilizado por la ONG Manos Unidas como un medio para estimar los costes, el rendimiento y el potencial de este sistema y ayudará a investigar las ventajas que la gasificación puede proporcionar en términos económicos, medioambientales y de mejora de la biomasa residual presente en el sitio. Inicialmente, se hace un enfoque sobre los números y la situación de las necesidades energéticas en el mundo, observando cuáles son las iniciativas y los objetivos para suplir las carencias. La imagen de los procesos de conversión de energía a partir de la biomasa se ilustra de forma clara y esquemática. Entre ellas se encuentra la gasificación, que se explica exhaustivamente y se clasifica según los tipos, procesos y tecnologías existentes, hasta la gasificación downdraft, cuyos principios y subprocesos se explican detalladamente. Después de proporcionar la información anterior, puede pasar a la parte de cálculo. Con el fin de proporcionar resultados más amplios, se seleccionan nueve de los tipos más comunes de biomasa residual. A partir de los datos experimentales, se desarrolla un procedimiento de cálculo detallado que, a partir de la biomasa bruta, la transforma en gas de síntesis. Esta mezcla de gases luego pasa a través de un intercambiador de calor para calentar agua con fines sanitarios, para luego ser quemada dentro de un motor para la producción de electricidad. En esta fase de cálculo, todos los equipos principales y auxiliares son cuidadosamente seleccionados de catálogos reales. En este punto, se identifica una comunidad rural en Nigeria en las inmediaciones de una granja de pollos, cuyo estiércol es un recurso valioso que se puede utilizar dentro del gasificador. Se identifican las cargas y necesidades de esta población y, tras asumir un perfil de carga, se ha desarrollado un proceso de minimización de LCOE mediante un código MATLAB. Después de haber ingresado los costos de inversión y mantenimiento y haber ingresado todos los parámetros necesarios, se encontró una solución óptima que soporta la tecnología de gasificación y fotovoltaica con sus elementos auxiliares relativos de la manera más económica. Habiendo definido en detalle todos los elementos que componen el proyecto, es posible estimar la inversión total.

Aparte de todos los cálculos desarrollados, se elabora un modelo de dimensión cero que permite predecir la composición del gas de síntesis y su poder calorífico a partir de la composición elemental de cada biomasa. Los resultados se comparan y validan con los datos experimentales de las mismas biomasas elegidas en la fase de cálculo. Esta herramienta permite obtener estimaciones inmediatas, económicas y en promedio aceptables sobre la productividad de la gasificación.

Palabras clave: gasificador downdraft, países subdesarrollados, paneles fotovoltaicos, gasificación modelo 0-D.

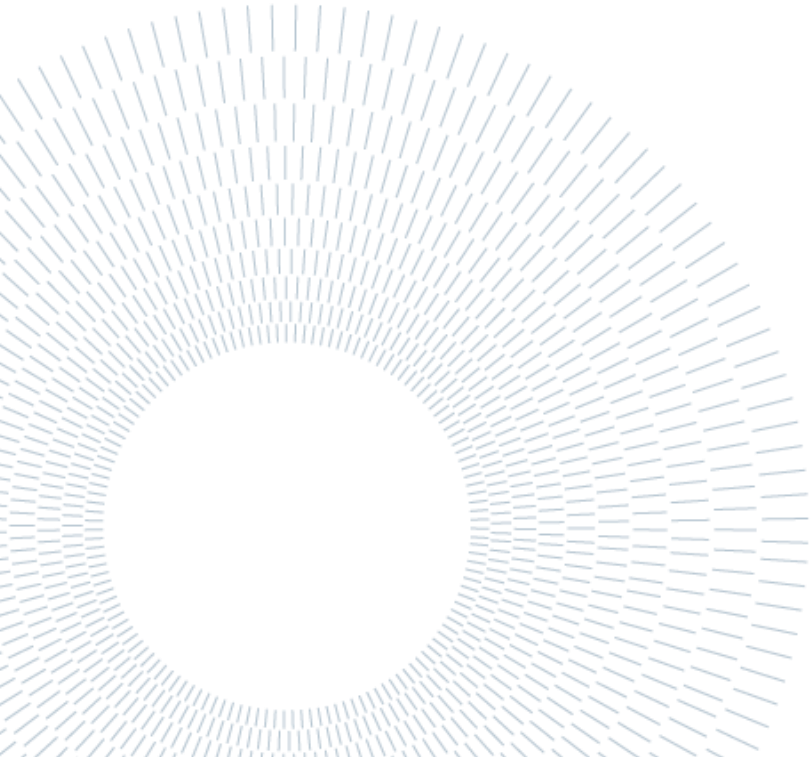

CONTENTS

1 INTRODUCTION

1.1 WORLD EXPANSION AND INNOVATION

In the recent centuries, and especially in the last few decades, the globe has seen an increasing number of rapid changes. With the late 18th and early 19th centuries' industrial revolutions, the economy shifted from being mostly agrarian to being focused on the production of products. The industrial revolution was one of the most important events in human history, affecting numerous countries throughout the world. While the industrial revolution began in Britain in the 18th century and continued throughout the decades that followed, its effects may still be observed today in humanity's lives. The industrial revolution had both beneficial and bad effects on society as a whole. It has resulted in increased economic growth, more efficient labor division, and the utilization of technology innovation to address issues rather than relying on circumstances beyond human control. On the other side, it has resulted in a slew of issues as a result of unsustainable and huge exploitation of global resources, as well as the concentration of power in the hands of a few people. Then, while the industrial revolution has many great outcomes, it also has many bad outcomes, such as terrible working and living circumstances, low salaries, child labor, severe pollution, resource depletion, and so on. Coal was the primary driver of technical advancement and growth since it fueled the steam engines that powered trains, ships, and other types of technology. It is the primary resource on which all developing countries rely, and it is extremely detrimental to the environment because of the high CO_2 output, which has a significant impact on the greenhouse effect.

The industrial revolution ushered in a time of rapid and continuous social development, as well as a steady rise in demand for all products and technology. For some, it resulted in enormous increases in wealth and financial well-being. It also prompted a fast demographic transition by increasing occupational specialization and allowing cities to host greater populations. Then, as industrial progress is followed by demographic increase, the two occurrences are inextricably connected in a vicious cycle that has resulted in a constant demand for more things to be produced. Indeed, as compared to prior centuries, the demographic growth over the last few decades has been staggering. A tremendous change occurred with the industrial revolution: whereas it had taken all human history until around 1800 for world population to reach one billion, the second billion was achieved in only 130

years (1930), the third billion in 30 years (1960), the fourth billion in 15 years (1974), and the fifth billion in only 13 years (1987) [1].

- During the 20th century alone, the population in the world has grown from 1.65 billion to 6 billion.
- In 1970, there were roughly half as many people in the world as there are now.
- Because of declining growth rates, it will now take over 200 years to double again.

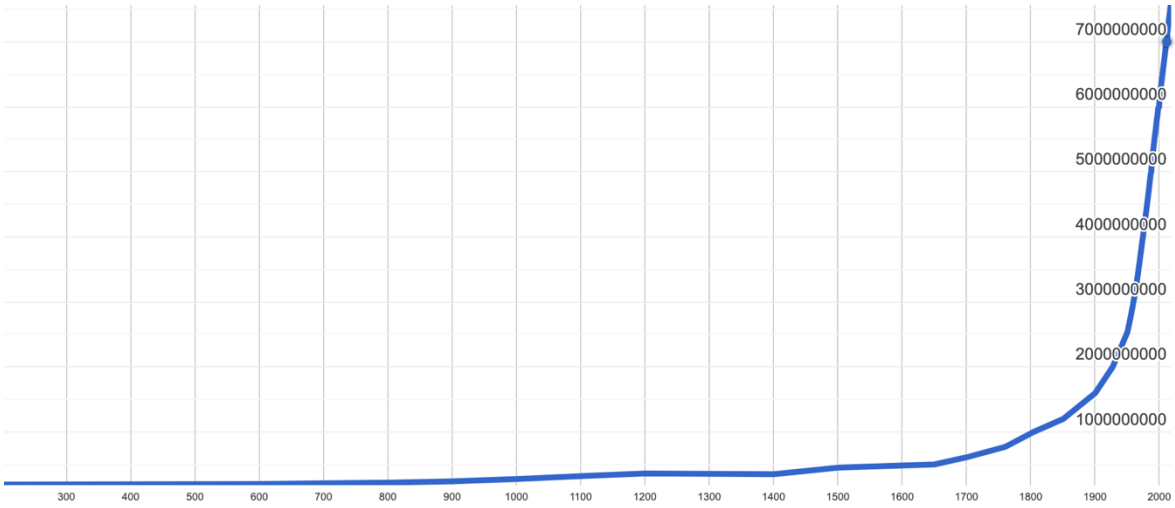

Figure 1: World population change (source: World Population Prospects [2])

For these reasons, the exigence to find sustainable alternatives to provide energy, food and any goods or products and to put them in action in a concrete way, is a challenge that is more concrete than ever today. Lots of initiatives in Europe and, more in general, throughout the world have been carried out and are nowadays in continuous evolution. Among them, the most important one, that is currently into force, is the Agenda 2030.

1.2 AGENDA 2030: OBJECTIVES

The United Nations' 2030 Agenda for Sustainable Development is a comprehensive plan that describes how poverty may be eradicated and the globe transformed into a peaceful, sustainable environment for everybody. In September 2015, 193 member nations signed the 2030 Agenda, pledging to strive toward social inclusion, environmental preservation, and long-term economic growth. The United Nations and its member nations throughout the world are committing to this agreement, ensuring that they develop equitable and peaceful communities while also working toward long-term sustainability. The Agenda has a grand objective of changing the world. It is the most comprehensive handbook ever published, including ideas for alleviating severe poverty, protecting the environment, and reducing

inequality. To carry out this ambitious agenda, governments will need to adopt extraordinary measures that are crucial to improve our planet. It includes 17 macro-sustainable development goals in a broad action plan with 169 milestones.

Figure 2: Agenda 2030, goals [3]

In this regard, energy is a critical component of practically all of the world's most pressing concerns and opportunities: jobs, security, climate change, food production, and increasing earnings are all goals that incorporate it in some way. In a nutshell, renewable energy provides a massive potential. And it is precisely for this reason that one (the seventh aim) of the UN's 17 Sustainable Development Goals has to do with it. One specific aim of this goal is to build infrastructure and upgrade technologies to deliver modern and sustainable energy services by 2030, particularly in least developed countries, small island states, and landlocked developing countries, in line with their unique assistance programs [4].

1.3 ELECTRICITY ACCESS

Energy access initiatives are bearing fruit, with 2019 statistics showing significant improvement. The number of individuals without access to electricity fell from about 860 million in 2018 to 770 million in 2019, a recent low.

In India, the government promised that 100% energy access will be achieved in 2019, and successful measures have been enacted in a number of African nations. Nonetheless,

previous success is being reversed as a result of the Covid-19 epidemic. While the number of people without access to electricity in Sub-Saharan Africa has consistently fallen since 2013, it is now expected to rise in 2020, pushing several nations further away from the goal of universal access by 2030 [5]. Since 2000, about 1.2 billion people in developing Asia have acquired access to electricity, with 96 percent of the area having access to power in 2019 compared to 67 percent in 2000. In India, the government declared that more than 99 percent of the population will have access to power in 2019. In Africa, access to electricity more than quadrupled from 9 million per year between 2000 and 2013, to 20 million between 2014 and 2019, exceeding population growth. Therefore, the number of individuals without access to electricity has gradually decreased from 610 million in 2013 to roughly 580 million in 2019. Much of the recent dynamism may be attributed to a small handful of nations, namely Kenya, Senegal, Rwanda, Ghana, and Ethiopia.

In the following image it is possible to give a look to the actual situation in the world.

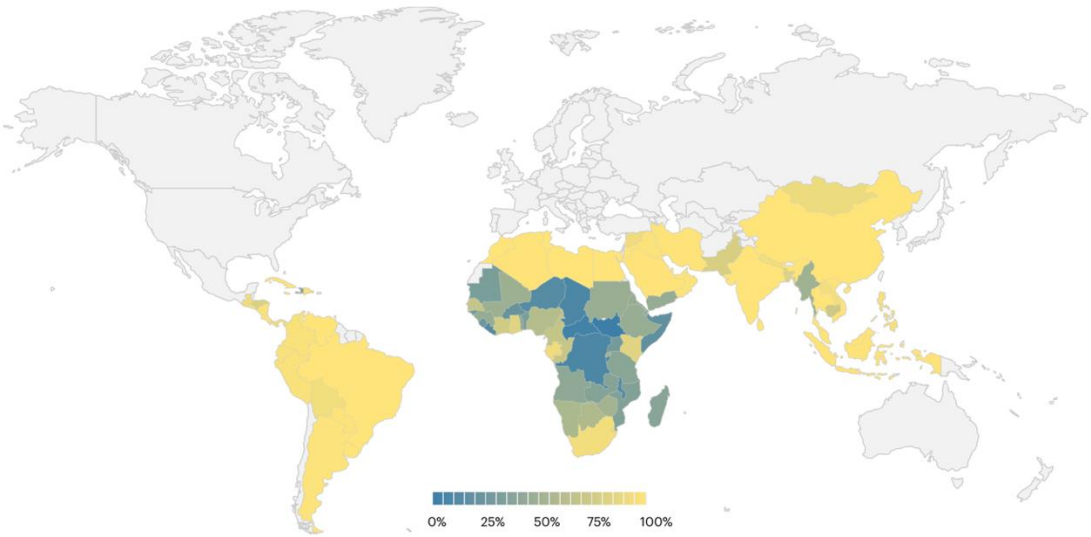

Figure 3: Proportion of population with access to electricity, 2019 (source: IEA data and projections [6])

Focusing on the rural population, the situation is even worse and the access to electricity, mostly in sub-Saharan, is still a big problem and many rural communities live without any access to electricity. It is possible to have an outlook thanks to the following image.

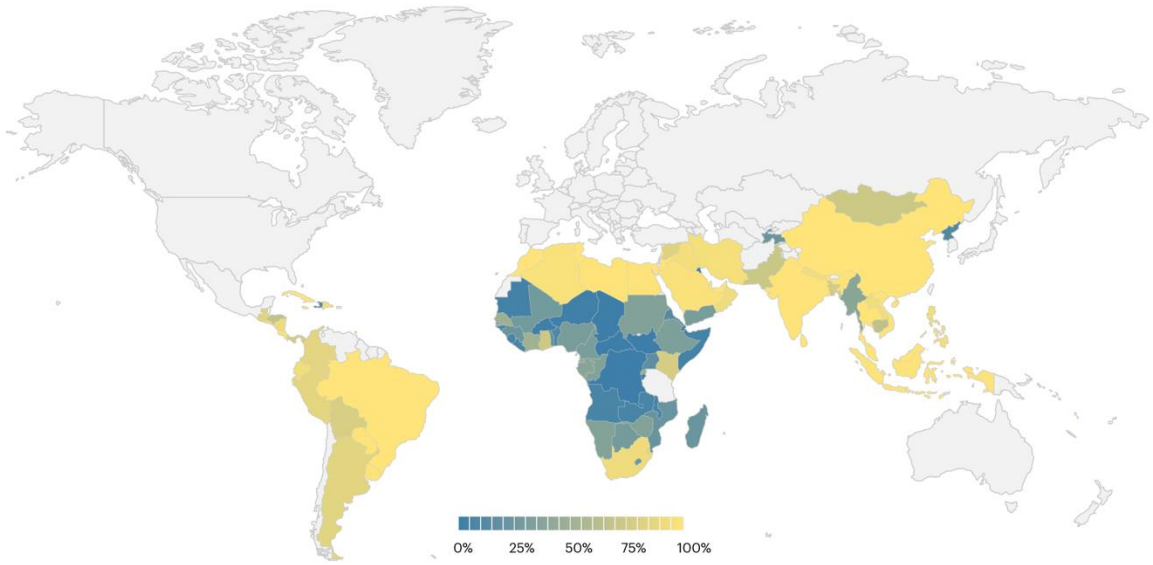

Figure 4: Proportion of rural population with access to electricity, 2019 (source: IEA data and projections [6])

Renewable energy sources appear to be the least expensive way to achieve universal electricity access in many areas: in addition to increasing grid-connected renewable electricity generation, declining costs of small-scale solar photovoltaic (PV) for stand-alone systems, and mini-grids relying on renewable sources such as biomass are critical in helping deliver affordable electricity access to millions. This is especially true in isolated rural parts of African countries, where many people remain without access to energy. According to the IEA Sustainable Development Scenario, decentralized solutions are the most cost-effective approach to offer power to more than half of the world's population by 2030.

1.4 AIM OF THE PROJECT

The project studies the production of electrical energy through a biomass downdraft gasifier fed by poultry manure, a gas engine and a generator, hybridized with a photovoltaic installation, to supply electrical energy to a population in Nigeria. The project ends in an electrical panel to which the population will connect its electrical network. It also includes a water heating system based on the heat of the gases coming out of the gasifier, to feed community showers, which will be built by the town, as well as the construction of a deep well, the installation of a submersible pump and the construction of an elevated tank, from which the water will be fed to the population, through a drinking water supply network, which will be built by the population. It ends up with the development of a model, reported

in the appendix, to predict the syngas composition starting from the elemental composition of each kind of biomass.

The present work is needed by the NGO Manos Unidas to match in a sustainable and smart way the primary needs for rural populations.

1.5 MANOS UNIDAS

Manos Unidas is an Association of the Spanish Catholic Church for help, promotion and development of the most disadvantaged countries, which was established in 1960. To guarantee the technical and economic quality of the projects, it has a group of volunteer engineers, who review the projects and give their binding approval for their approval by the Permanent Commission. This group is organized into four subgroups to address the different techniques: Water, Building, Energy and Agriculture.

Manos Unidas complies with all the principles of transparency and good practices established by the Fundación Lealtad and the Coordinator of NGO Spain. It has the qualification of the Spanish Agency for International Development Cooperation (AECID), which accredits it to qualify for funding from this Agency. Manos Unidas' accounts are externally audited every year.

The projects are requested by the different institutions of the church: missionaries, missionaries, parishes, educational institutions, health centers, etc. These institutions frequently request projects in collaboration with NGOs from any country in the world.

It has an annual budget of 40 million euros, of which 16.5% come from public funds and 83.5% from private funds. Among the latter, an important part comes from periodic contributions from its partners.

It has a total of 144 employees and 6,344 volunteers, dedicating a very small part of its budget to internal expenses. Most of the budget goes to solve the problems of the third world, fighting against hunger, nutritional deficiency, misery, disease, underdevelopment and lack of education.

Every year it serves some two million direct beneficiaries from 53 countries in Africa, America and Asia, serving more than 400 projects a year.

In 2010 he won the Prince of Asturias Award.

2 BIOMASS AS ENERGY SOURCE & GASIFICATION TECHNOLOGY

2.1 WHAT IS BIOMASS

According to Directive 2009/28/EC on the promotion of the use of energy from renewable sources, biomass is defined as the biodegradable fraction of products, waste and residues of biological origin from agricultural activities (including substances of plant origin and animal origin), from forestry and related industries, including fishing and aquaculture, as well as the biologically degradable fraction of industrial and municipal waste.

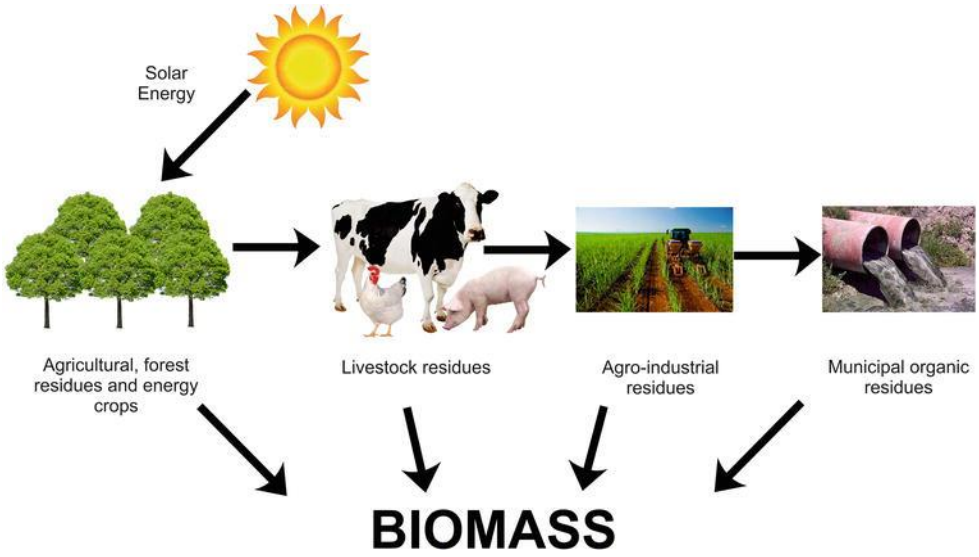

Figure 5: Energy from different biomass sources [81]

So, biomass resources will come from very diverse and heterogeneous sources. When the utilization rate is equal to or less than the production capacity, it is termed a renewable energy source (biological capacity of renewal). Biomass is a modern non-fossil and organic-inorganic solid substance produced by natural and manmade processes. It consists of:

- Natural constituents originated from growing from growing flora through photosynthesis or from animal and human sources.
- Technogenic products (also known as byproducts) produced from the processing of the aforementioned natural ingredients (like waste).

Renewable biomass energy extraction is a CO_2-neutral process since there are no additional carbon emissions in the environment due to the close carbon dioxide cycle. When all energy

consumption connected to CO_2 emissions (transport of biomass, ammonia production and harvesting, for example) is taken into account, biomass production is no longer CO_2-neutral.

Biomass can be a renewable source, however increasing biomass growth using fertilizers might have more negative consequences than CO_2 emissions because most fertilizers are based on ammonia. Another disadvantage is eutrophication (a consequence of heavy fertilizer use), which causes a rise in algae in the water and ultimately oxygen depletion through photosynthesis. Soil acidification, organic contaminants, heavy metal buildup, and N_2O emissions are other harmful impacts.

In the realm of renewable energies, the term biomass has two distinct meanings since the same designation is used to both the resource (raw material) and the energy generated by its use:

- Biomass is defined as "any sort of organic matter of recent biological origin" in respect to the resource. It therefore includes a diverse range of organic matter, ranging from plant, animal, or microbial products to those found in wastewater, sewage sludge, or the organic part of municipal solid waste (MSW). Fossil fuels and their derivatives (plastics and synthetic goods) are excluded from this idea because, although having a biological beginning, their production occurred in the distant past.
- Biomass is defined in the energy context as a renewable energy source based on the energy consumption of biofuels derived from biomass-type raw materials. Biomass has the characteristics of renewable energy since its energy content is derived, in the end, from solar energy fixed by plants during the photosynthetic process and collected in the links of the organic molecules that compose their biomass. Biofuels are the results of biomass transformation that are utilized for energy purposes. They can be solid, liquid, or gaseous biofuels depending on their physical condition.

2.2 ADVANTAGES AND DISADVANTAGES OF BIOMASS

Of course, the biomass, such us all the other resources employed to produce energy, is characterized by some advantages but also by some drawbacks. All the aspects must be considered when a specific process is analyzed. Here below are evidenced the main features.

Advantages

- Reduction of sulfur and particulate emissions.
- Decrease in polluting gas emissions.
- Cleaner and theoretically neutral combustion in CO_2.
- Soil restoration, by reducing the risk of forest fires and insect pests.
- Use of agricultural residues.
- Production of electricity from waste with low economical potential.
- Independence from fluctuations in fuel prices from abroad since they are not imported.
- Reduction of foreign energy dependency.
- Energy diversification.
- Development of rural areas and job creation.

Disadvantages

- Competition with the basic uses of the forest and agriculture.
- Intensive use of fertilizers and water requirements.
- Its relocation, the lack of established distribution channels and the need for storage in large quantities may incur additional operating costs.
- Low energy density. In general, large amounts of biomass are needed to obtain considerable amounts of energy compared to traditional fuels.

2.3 DIFFERENT BIOMASS SOURCES FOR ENERGY PURPOSES

Biomasses can be classified according to the process through which they are obtained. As said above, there are lots of types of biomasses and in turn there are many ways to obtain the biomass source. Here below the following classification is proposed:

- *Natural biomass.*

  It grows naturally on uncultivated ground (mostly forest area) and has traditionally been utilized to meet man's caloric needs (firewood). Because of the possibility of deforestation if proper safeguards are not followed, this sort of biomass is not suited for large-scale energy consumption. Natural biomass is the foundation of developing peoples' energy consumption, and as their demography and energy demands grow, so does the strain on ecosystems, potentially leading to desertification.

- *Residual biomass.*

  It is the one produced as a byproduct of any process that consumes biomass. It comes from agricultural, forestry, and animal farms, as well as organic waste created in businesses and cities. Because this sort of biomass necessitates chipping or packing prior to transportation, as well as seasonality, collecting, and variation, it is preferable to establish biomass collection facilities to centralize its distribution.

  The following benefits of residual biomass for energy use stand out: reduced pollution and deterioration of the environment, as well as the risk of fire, reduced production costs, because they are normally charged to the main product, reduced space occupied by waste accumulation, and low transportation costs because residual biomass is usually concentrated in certain places.

  While, concerning the drawbacks that residues present, in the event that the user is not the owner, the following stand out: being a raw material, they are no longer waste and enter the market in competition with other products, the different alternatives bring insecurity in supply and price, location in terrains of difficult accessibility, variety of sizes and composition, impurities and high degree of humidity.

- *Scraps of agricultural crops.*

  They are often wastes and leftovers of the food processing process, therefore the energy products derived from them are typically not competitive with the fuels they are meant to replace. Its seasonality is determined by industrial activities. Chips, bark, or sawdust from the first and second transformation industries of wood, bones, shells, olive oil, or nuts are examples.

- *Biomass produced by dedicated energy crops.*

  Energy crops are low-cost, low-maintenance crops planted only for the production of energy through burning (not for food). Pellets, bioethanol, and biogas are produced from the crops. The fuels are burnt to produce electricity or heat. Although there are crops that can be used as energy producers that must be selected according to profitably obtaining the maximum amount of energy possible, which implies a positive energy balance, high levels of productivity with low production costs, the

species dedicated to producing biomass for energy purposes can be herbaceous or woody in nature.

2.4 BIOMASS CONVERSION PROCESSES

This section only deals with a general vision of the processes, according to the raw materials used, the necessary transformations and the main energy products obtained. Here below it is reported a scheme representing all the possible processes that is possible to make starting from the biomass. They can be classified in three big macro-families that, in turn, can be further classified depending on the different processes: biological conversion processes, thermo-chemical conversion processes, oil extraction processes.

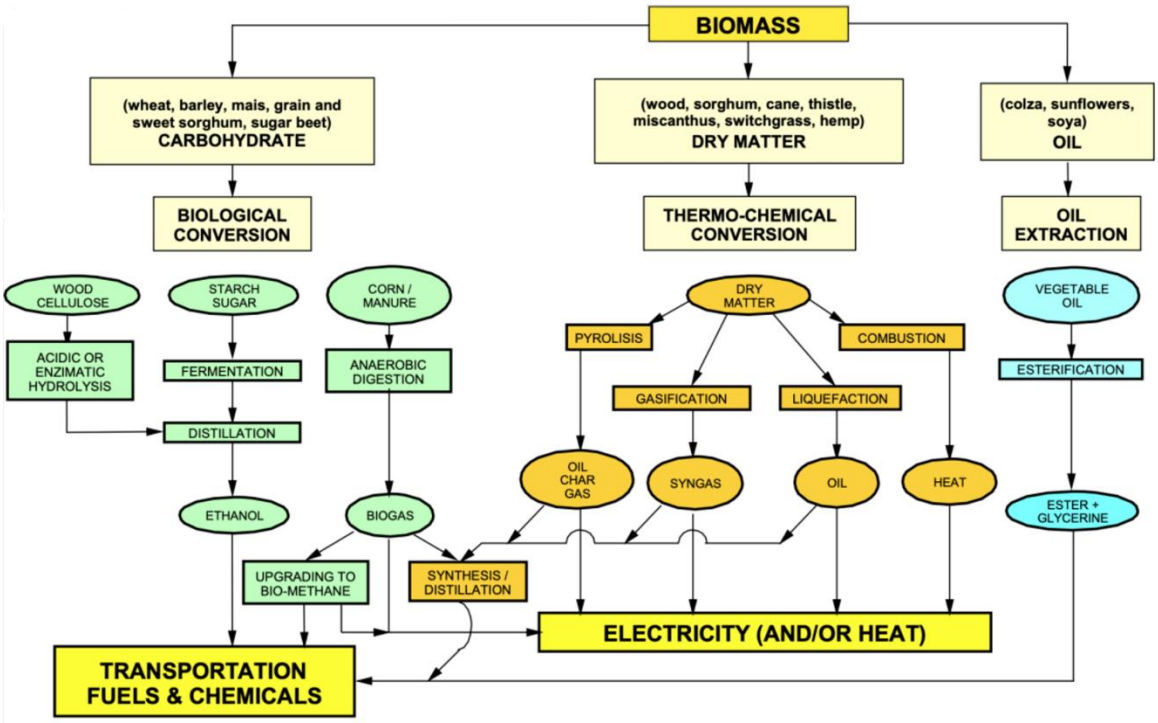

Figure 6: Biomass conversion processes

2.4.1 Biological conversion processes

They intend to transform biomass, fundamentally of the wet type, into fuels through various processes at low temperatures, among which the following stand out: hydrolysis, fermentation, anaerobic digestion.

1. *Hydrolysis*

   It is the process through which, from polymeric carbohydrates, sugar monomers are obtained. The process can be catalyzed either by acid or enzymes, but they are very costly, and they represent the major impediment to an economically viable production of biofuels from lignocellulose. Acid-catalyzed hydrolysis is the most used method, and it involves either the use of concentrated or dilute acid (i.e., H_2SO_4 or HCl). By reaction with water, from lignocellulosic biomass it is obtained glucose. Hydrolysis is performed on both cellulose and hemicellulose: for hemicellulose, hydrolysis is easier than for cellulose due to its possession of more amorphous property.

   The mechanism of the hydrolysis of lignocellulosic biomass to glucose occurs in three steps:

   1. The reaction with water catalyzed by endoglucanase resulting to the formation of cellodextrin with a shorter chain, and free-chains ends (reducing and non-reducing ends).
   2. The degrading of cellodextrin to two-unit glucoses (cellobioses) with the help of exoglycanase.
   3. The formation of glucose obtained when the β-glucosidases strikes the cellobioses.

2. *Fermentation*

   This biological process involves the conversion of the monomeric units of sugars obtained from the hydrolysis step into ethanol, acids and gases using microorganisms such as yeast, fungi, or bacteria. Good microorganisms to obtain ethanol need to have high growth and fermentation rate, high ethanol yield and productivity, low fermentation pH to reduce the bacterial contamination, high fermenting temperature and high tolerance to inhibitor. Bacteria used for fermentation are called thermophilic

because they can resist to temperatures. The most used microorganism is yeast especially Saccharomyces cerevisiae due to high yield of ethanol and high tolerance limits. Yeast is added to the sugar solutions obtained from the hydrolysis, which is then heated. The yeast contains an enzyme called invertase, which acts as a catalyst and helps to convert the sucrose sugars into glucose and fructose. The fructose and glucose sugars then react with another enzyme called zymase, which is also contained in the yeast to produce ethanol and carbon dioxide.

The fermentation process takes around three days to complete and is carried out at 250-300°C.

3. *Anaerobic digestion*

   Anaerobic digestion is the process of conversion of the biomass into biogas (mainly methane and carbon dioxide) by means of anaerobic microorganisms.

2.4.2 Thermo-chemical conversion processes

They are conversion processes at high temperatures that are applied fundamentally to dry biomass, and in particular, to straw or wood, as well as to residual-type biomass.

1. *Pyrolysis*

   Pyrolysis is a general term for thermal degradation in an inert atmosphere. It is the first step both for combustion and gasification. It is the thermal degradation of biomass in the absence of oxygen or that is carried out in a reduced amount of it. During the process, the larger molecules are broken down by heat into smaller ones, giving rise to gases and a carbonaceous solid (char), whose quantities and composition depend on the original biomass, the residence time, the pyrolysis temperature, the heating rate, and the type of reactor to be used.

2. *Gasification*

   It is a thermochemical process by which biomass is transformed into a low calorific value fuel by combining pyrolysis and gasifying agents such as water vapor, oxygen, carbon dioxide or hydrogen, which must be present in the atmosphere in small quantities so that combustion does not occur.

It will be deeply explained later in more detail, due to the big importance it has in this project.

3. *Liquefaction*

Liquefaction is a thermochemical conversion process that is applied to convert biomass into bio-oil (target product), biochar, and gases. The process is usually carried out in water or another suitable solvent at 250-400 °C under pressures of 5-25 MPa. The liquefaction can either be indirect or direct. The indirect liquefaction refers to the Fischer-Tropsch where the source must be converted in syngas through gasification processes and then from syngas to liquid fuel. The direct liquefaction of biomass refers to the conversion biomass into bio-oil, and the main technologies are hydrolysis fermentation and thermodynamic liquefaction.

4. *Combustion*

Combustion is a chemical reaction in which a material combines quickly with oxygen and produces heat. The original material is referred to as the fuel (biomass), while the supply of oxygen is referred to as the oxidizer. As a result of the interaction between oxygen and biomass, heat, CO_2, and water are created. While wood is the most widely utilized feedstock, a variety of other materials can also be burnt satisfactorily. These include residuals and byproducts from sawmills, such as straw and bark residuals, as well as energy crops. Farmers and other rural residents are increasingly interested in biomass heat as a cost-effective alternative to propane or furnace oil. Stoves and fireplaces can provide direct space heating or be hooked up with a back boiler that feeds heated water to radiators throughout the building.

2.4.3 Oil extraction processes

These processes allow, starting from lipids (vegetable oils and animal fats), to obtain biodiesel. The biodiesel can be obtained through two different processes that lead to different properties of the fuel: transesterification and hydroprocessing process. The first step is

common for both processes, and it is the extraction of the oil from the biomass, that is achieved mechanically (milling) and then mainly chemically.

2.5 DEFINITION AND MAIN CHARACTERISTICS OF GASIFICATION

Gasification is a thermochemical process that produces syngas (also known as producer gas, product gas, synthetic gas, or synthesis gas) from the interactions between the fuel and the gasification agent. The syngas consists mostly of CO, H_2, N_2, CO_2, and minor hydrocarbons (CH_4, C_2H_4, C_2H_6, etc.). H_2S, NH_3, and tars may also be present in trace concentrations.

In general, biomass gasification is the thermochemical conversion of organic (waste) feedstock in a high-temperature environment, which allows biomass to be converted not only to syngas for energy generation, but also to chemicals such as methane, ethylene, adhesives, fatty acids, surfactants, detergents, and plasticizers.

Biomass gasification methods can be classified as air gasification (using air), oxygen gasification (using oxygen), steam gasification (using steam), carbon dioxide gasification (using carbon dioxide), or a combination of these. In general, oxygen gasification, steam gasification, and carbon dioxide gasification produce higher HHVs of syngas than air gasification; however, air gasification is the most widely studied and applied process because the gasification agent (air) is cheap, the reaction process is simple, and the reactor structure is simple (According to previous studies [7], the calorific value of syngas formed is 4-7 MJ/m3 when air is used as the gasification agent, 10-18 MJ/m3 when steam is used as the gasification agent, and 12-28 MJ/m3 when oxygen is used as the gasification agent). Gasification processes is an endothermic process that can be either **direct** (using air or oxygen to generate heat through exothermic reactions) or **indirect** (transferring heat to the reactor from the outside). The primary benefits of direct gasification are that it is a one-stage process, that direct heat transfer from gases to biomass is extremely efficient, and that the process is generally self-regulating.

Many aspects influence syngas composition, including the kind of gasifier, the gasification agent used, the temperature of gasification, the moisture content of the biomass to be gasified, and the amount of air (where air is employed as a gasification agent) utilized to gasify the biomass. Indeed, the so-called equivalent ratio (ER) - the oxygen utilized compared to that necessary for full combustion - is a critical component in gasification. The

ER for excellent gasification typically varies from 0.25 to 0.35, whereas the ER for pyrolysis is zero or near to zero, and the ER for combustion is always more than one.
In the following figure it is possible to see how the syngas composition changes at varying the equivalent ratio.

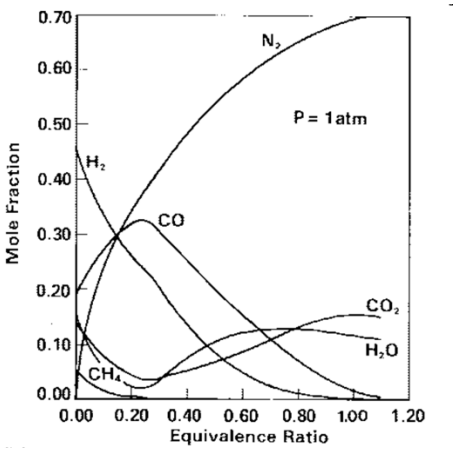

Figure 7: Syngas composition at varying ER [8]

The gasification process is an overall endothermic process that involves multiple chemical reactions, the most important of which involve carbon, CO, CO_2, hydrogen (H_2), water (steam), and methane (CH_4), as shown below:

The combustion reactions

1. $C + 1/2\ O_2 \rightarrow CO$ ($\Delta H°(298K)$ = -111 MJ/kmol)
2. $CO + 1/2\ O_2 \rightarrow CO_2$ ($\Delta H°(298K)$ = -283 MJ/kmol)
3. $H_2 + 1/2\ O_2 \rightarrow H_2O$ ($\Delta H°(298K)$ = -242 MJ/kmol)

Other important gasification reactions

4. Water-Gas Reaction: $C + H_2O \leftrightarrow CO + H_2$ ($\Delta H°(298K)$ = +131 MJ/kmol)
5. Boudouard Reaction: $C + CO_2 \leftrightarrow 2CO$ ($\Delta H°(298K)$ = +172 MJ/kmol)
6. Methanation Reaction: $C + 2H_2 \leftrightarrow CH_4$ ($\Delta H°(298K)$ = -75 MJ/kmol)

With the above, the combustion reactions are essentially carried out to completion under normal gasification operating conditions. Furthermore, under high carbon conversion conditions, the three heterogeneous reactions (reactions 4–6) can be reduced to two homogeneous gas phase reactions of water-gas-shift and steam methane-reforming

(reactions 7 and 8 below), which collectively play an important role in determining the final equilibrium synthesis gas (syngas) composition.

7. Water-Gas-Shift Reaction: $CO + H_2O \leftrightarrow CO_2 + H_2$ ($\Delta H°(298K)$ = -41 MJ/kmol)
8. Steam Reforming Reaction: $CH_4 + H_2O \leftrightarrow CO_2 + 3H_2$ ($\Delta H°(298K)$ = +206 MJ/kmol)

The use of the gasification process to obtain thermal and electrical energy through the production of syngas has the following advantages and disadvantages.

Advantages

- Zero CO_2 emissions balance. This is due to the fact that during the synthesis gas combustion process, an amount of carbon dioxide equivalent to that absorbed by the biomass during the photosynthesis process is emitted.
- Small-sized plants (<5 MW) that are technically and economically viable, thus favoring distributed generation and the consequent reduction in losses due to electricity transmission.
- Biomass availability on site. The location of generation plants next to biomass sources results in savings in transport costs.
- Use of waste and residues. Many plants carry out the gasification process from biomass produced as waste from an industrial or agricultural process, which facilitates its disposal and also helps to minimize the environmental impact.
- Minimum costs of biomass, especially because it is a waste, which means the energy revaluation of a fuel at a very low price.
- Gas versatility, since it can feed steam turbines, internal combustion engines or boilers.
- Simple operation and maintenance.

Disadvantages

- It could be necessary to adapt the gasifier to the fuel to be used in order to optimize its operation.

- Synthesis gas contains tar and remains in the form of ashes, which implies prior washing and conditioning so as not to damage the turbine or the engine.
- Special safety measures are required, making sure the process is sealed and preventing highly toxic gases from escaping. There is a risk of explosion if the process is not properly controlled.

2.6 PHASES OF THE GASIFICATION PROCESS

Gasification is not a continuous process, but rather a sequence of steps, each of which occurs at a different temperature range. If the substrate is heated gradually, as in moving bed reactors, the steps are carried out successively, each in a different zone of the reactor. When the heating is very fast, like in fluidized bed reactors, the phases occur concurrently. The following are the four stages:

1. Drying zone

The contribution of water in the form of humidity means a significant energy consumption for its heating up to 100 °C, evaporation, and heating of the steam to the process temperature. To keep the temperature stable, this consumption must be offset by an energy supply mostly from the combustion step. In addition, the water released during this step serves as a gasifying agent during the gasification stage.

2. Pyrolysis zone

yrolysis is the process of applying heat to raw biomass in the absence of air to convert it into charcoal and different tar vapors and liquids. It is simply a charring process. Once the temperature of biomass climbs over roughly 250 °C-300 °C, it begins to disintegrate rapidly with heat. The biomass decomposes into a mixture of solids, liquids, and gases. The solids that remain are generally referred to as charcoal. Tars are the aggregate name for the gases and liquids that are emitted.

Lower temperature pyrolysis produces gases and liquids that are essentially pieces of the original biomass that break off with heat. These pieces are the more complex H, C, and O molecules in biomass known as volatiles.

3. Combustion zone

Combustion is the sole net exothermic activity among the four Gasification processes; ultimately, all of the heat that drives drying, pyrolysis, and reduction

originates either directly from combustion or indirectly from combustion via heat exchange activities in a gasifier. Combustion can be powered by either tar vapors or pyrolysis char. Different types of reactors employ one or both. The objective of a downdraft gasifier is to burn pyrolysis tar gasses to create heat to operate reduction, as well as CO_2 and H_2O to decrease in reduction.

4. Reduction zone

Carbon dioxide (CO_2) or water vapor (H_2O) is reduced in a gasifier by passing it past a bed of heated charcoal (C). The carbon in heated charcoal is extremely reactive with oxygen; it has such a high oxygen affinity that it removes oxygen from water vapor and carbon dioxide and redistributes it to as many single bond sites as possible. Because the oxygen is more attracted to the C bond site than to itself, no free oxygen can survive in its typical diatomic O_2 state. All available oxygen will bond to all accessible C sites as individual O until there is no more oxygen. When all of the available oxygen has been redistributed as single atoms, reduction comes to an end. CO_2 is reduced by carbon to make two CO molecules, while H_2O is reduced by carbon to produce H_2 and CO. Both H_2 and CO are combustible fuel gases that may be routed off to accomplish desired work elsewhere.

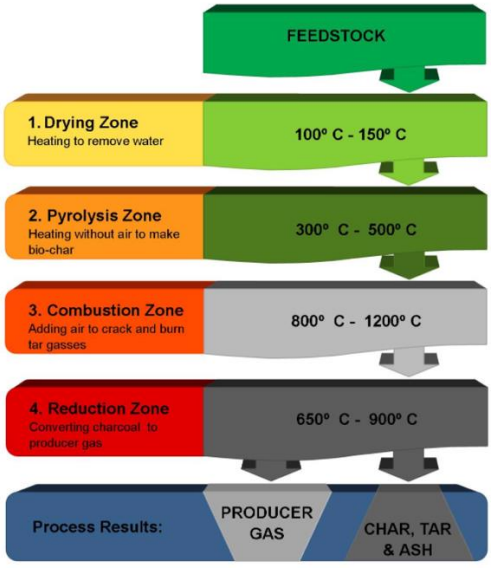

Figure 8: Different zones of the gasification process [9]

2.7 GASIFICATION REACTORS

Biomass gasification can take place in a variety of reaction systems. The nature of the substrate (biomass, mineral coal, charcoal, organic waste), the conditioning needs (granulometry, humidity, mechanical properties), the capacity of the system, the composition and calorific value of the product gas, the concentration of polluting elements (tars, particles), as well as the investment, operation, and maintenance costs are all determined by the reactor design.

The table below lists the most commonly used commercial gasification reactors for biomass gasification. Moving bed reactors are the most basic for low and medium capacity systems. Bubbling fluidized bed reactors need larger expenditures but allow for more processing capacity in larger power plants that can only run on biomass. Circulating fluidized bed and entrained bed reactors are utilized in extremely high capacity operations where coal is commonly employed as the gasification substrate.

Table 1: Design and operation characteristics of gasification reactors (source: Knoef, 2005)

	Moving bed		Fluidized bed		Entrained flow
	Downdraft	**Updraft**	**Bubbling**	**Circulating**	
Temperature of operation (ºC)	700 – 1200	700 – 900	850 – 950	850 – 1000	1500
Process control	Simple	Very simple	Medium	Complex	Medium
Optimal capacity (MW_t)	0.2 – 5	5 – 20	1 – 20	> 20	> 100
Maximum humidity (% humid base)	25	60	40	40	15
Max ashes (% dry basis)	6	50	20	15	5
Minimum particle size (mm)	40 – 100	10 – 250	-10.0	1.0 – 10.0	0.1 – 1.0
Fuel morphology	Uniform	Heterogeneus	Milled	Milled	Powdered
Apparent density (kg/m^3)	> 500	> 400	> 100	> 100	> 400
Syngas outlet temperature (ºC)	700	200 – 400	700	700	1000
Tar content (g/Nm^3)	0.015 – 3.0	30 – 150	1 – 2	1 – 2	0.01 – 0.05
Typical pressure of operation (bar)	1	1	1	20 – 70	20 – 70
Typical gasifying agent	Air/steam	Air/steam	Air/steam	Oxigen/steam	Oxigen/steam
Syngas LHV (MJ/Nm^3)	4 – 5.0	5.0 – 6.0	5.0 – 5.5	15 – 20	15 – 22
Syngas application	Engine (electr.)	Thermal	Engine (electr.)	Turbine (electr.) + syntesis	Turbine (electr.) + syntesis
Ash melting temperature (ºC)	> 1250	> 1000	> 1000	> 1050	< 1250

The types of gasifiers can be divided into three macro-families:

1. Moving bed gasifiers
2. Fluidized bed gasifiers
3. Entrained flow gasifiers

In general terms, comparing the three technologies (going from the first to the last one) the temperature increases as well as the costs, while the size of the feed particles decreases.

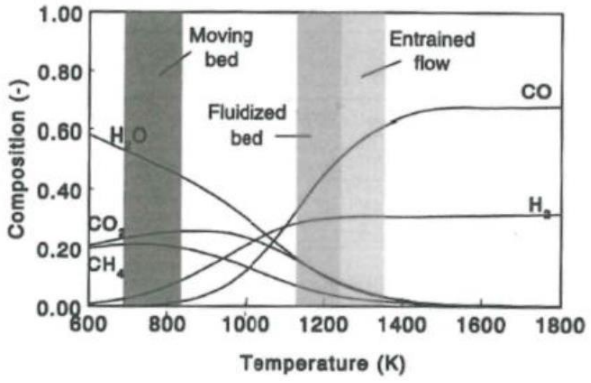

Figure 9: Composition of the syngas for different reactors [8]

The gasification gives rise to different syngases depending mostly on the operating temperature and leads to different applications. For low temperature syngas rich in hydrocarbons, fuel purpose is the best choice thanks to the high heating value. For medium-temperature medium-purity syngas, metallurgic treatments are the best applications. While high-temperature high-purity syngas is used in chemical application (like ammonia, methanol process) applications.

1) Moving bed gasifiers

The biomass enters the gasifier continuously from the top and is gently heated and dried (partial pyrolysis) on its way down, while the resultant gas is cooled as it departs the reactor. The high-temperature steam further heats and de-volatilizes the biomass as it lowers. The biomass is gasified by steam and carbon dioxide in the gasification section. Because it is an endothermic process, the temperature rises from top to bottom. When the remaining feedstock is burned, carbon dioxide is produced in the combustion zone. The maximum temperatures (about 1300 K) are achieved in the combustion zone, towards the reactor's bottom. Because the temperature is lower than the "slagging" temperature of the ash, all that remains of the original feedstock is dry ash (the temperature at which the mineral matter becomes sticky and even melts). The biomass bed is supported by a spinning grate, which cools the ash by releasing heat to the entering steam and oxygen. The temperature in this sort of reactor must be kept low to prevent solid particles from melting and damaging the

continually spinning device. The unit's heat recovery is quite effective, however the low temperature of the exit gas (used to pre-heat the entering biomass) results in the presence of hydrocarbons.

The moving-bed reactor has the problem of producing several byproducts such as condensable hydrocarbons, phenols, ammonia tars, oils, naphtha, and dust. As a result, gas cleaning for the moving bed gasification process is significantly more difficult than for other gasification processes, making it uneconomic in many applications. The counter-current action, on the other hand, makes the process extremely efficient.

Updraft biomass gasifiers can handle high moisture feeds, giving them an advantage for generating gas for burning in a burner. Updraft gasifiers, on the other hand, create 5 to 20% volatile tar-oils and are hence inappropriate for engine operation. Downdraft gasifiers generally create less than 1% tar-oil and are thus frequently employed for engine operation. The following are the causes for this disparity. Updraft biomass gasifiers can handle high moisture feeds, giving them an advantage for generating gas for burning in a burner. Updraft gasifiers, on the other hand, create 5 to 20% volatile tar-oils and are hence inappropriate for engine operation. Downdraft gasifiers generally create less than 1% tar-oil and are thus frequently employed for engine operation.

- *Downdraft (Imbert) gasifier.* The downdraft gasifier was created to convert high volatile fuels (wood, biomass) to low tar gas and has so proven to be the most successful power generating system. The upper cylindrical component of the inner chamber, as shown in the image below, is merely a magazine for the wood chips or other biomass fuel. This compartment is replenished every few hours during operation. The spring-loaded lid is opened to charge the gasifier and then closed while the gasifier is running. The spring allows the cap to snap up and release pressure in the event of a gas explosion, acting as a safety valve. A set of radially directed air nozzles about one-third of the way up from the bottom allows air to be pulled into the chips as they move down to be gasified. The entering air burns and pyrolyzes part of the wood, most of the tars and oils, and some of the charcoal that fills the gasifier below the nozzles during operation. The gasifier is self-adjusting in various ways. If there isn't enough charcoal at the air nozzles, additional wood is burnt and pyrolyzed to produce more. If too much char accumulates during high-load situations, the char level rises over the nozzles, causing incoming air to burn the char, lowering the char level. The reaction zone is therefore maintained at the nozzles.

To allow efficient gravity feeding via the constricted hearth, the Imbert gasifier requires a low-moisture (25 percent moisture) and evenly blocky fuel.

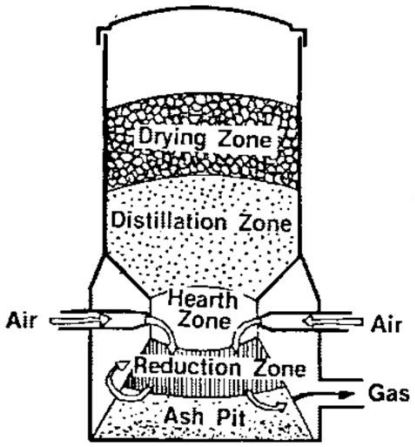

Figure 10: Downdraft gasifier scheme [10]

2) Fluidized bed gasifiers

A fluidized-bed gasifier is a back-mixed reactor in which feedstock particles are properly mixed with feedstock particles that are already being gasified. This gasifier runs at atmospheric pressure, has a short contact duration, and a moderate, constant temperature.
The char particles that exit the reactor with the product gas are largely collected in cyclones and recycled back into the reactor. At the bottom of the reactor, dry ash exits.
Because the reactor is back-mixed, considerable quantities of unreacted carbon are removed with the product gas and ash, lowering the conversion. The fluidized-bed gasifier generates far less contaminants than the moving bed gasifier due to its greater operating temperature.

- *Bubbling fluid bed gasifier.*

  The bubbling fluidized bed gasifier is made out of a vessel with a grid at the bottom through which the gasifying agent (e.g., an H_2O/air combination) is injected. The prepared biomass feed is delivered into a moving bed of fine-grained material above the grid. The air/biomass ratio is controlled to keep the bed temperature between 700 and 900 °C. In the hot bed, the biomass is pyrolyzed, yielding char, gaseous chemicals, and tar. Contact with the hot bed material, which may contain tar

reforming catalyst, converts the high molecular weight tar, providing a producer gas with a reduced tar concentration.

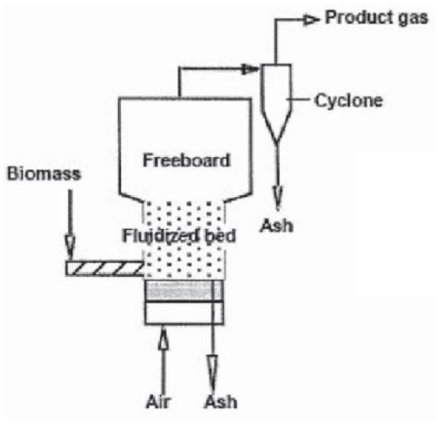

Figure 11: Bubbling fluid bed gasifier scheme [11]

- *Circulating fluid bed gasifier.*

Circulating fluidized bed reactors operate similarly to fluidized bed reactors. The primary distinction between circulating fluidized bed reactors and fluidized bed reactors is that fluidized bed reactors use a single heated reactor with cyclones for char separation. This char can be burned to generate thermal energy or used for another purpose. Circulating fluidized bed reactors use a first fluidized bed unit to perform the pyrolysis process, but then feed the generated char into a second fluidized bed unit. This second fluidized bed unit is used to burn the char contained in the inorganic heat carrier in order to generate heat that will provide the majority of the heat necessary for the first unit, to which the heated inorganic heat carrier is returned to complete the pyrolysis process.

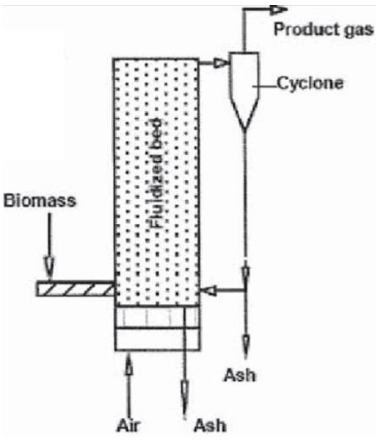

Figure 12: Circulating fluid bed gasifier scheme [11]

3) Entrained flow gasifier

The entrained-flow gasifier is a plug-flow device in which coal particles react with steam and oxygen simultaneously at air pressure. The reactor has a short residence time and a high temperature to enhance coal conversion. Only CO and H_2 are generated at this high temperature. Molten slag is used to remove the ash (liquid phase). The coal particles in fluidized-bed and entrained-flow reactors are heated very quickly, generally at speeds exceeding 1000 K/s. Pyrolysis happens after severe heating, and when mixed, significant volumes of volatiles, coke, and so on are generated on a microsecond scale. The process should be designed so that this does not result in decreased efficiency and difficulties downstream of the reactor.

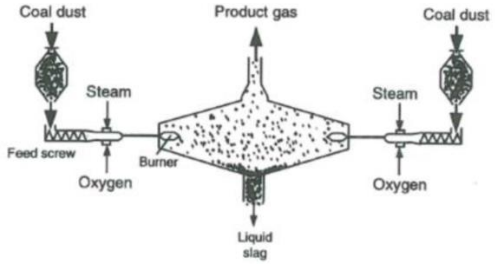

Figure 13: Entrained flow gasifier scheme [11]

2.8 HISTORY

Gasification was autonomously discovered in both England and France in 1798, and by 1850, the technology had advanced to the level that it was possible to light most of London with synthetic gas or "town gas" derived from coal. Manufactured gas quickly crossed the Atlantic and, by 1920, most American towns and cities provided gas to people for cooking and illumination via local "gasworks." Tiny gasifiers based on charcoal and biomass feedstocks were created around the time of World War I to power cars, boats, trains, and small electric generators. Because gasoline was less expensive and easier to use than biomass between the two world wars, development was largely pursued by amateur enthusiasts. At the start of World War II, there was a lot of interest in all kinds of alternative fuels. During WWII, around one million downdraft gasifiers were utilized to power automobiles, trucks, boats, railroads, and electric generators across Europe. By 1943, gasifiers powered 90 percent of the automobiles in Sweden. By the conclusion of the war, there were almost

700,000 wood-gas generators powering what were considered simply temporary improvements for wartime conditions. However, a few automobile manufacturers went so far as to alter the bodywork to accommodate gasifier installation. After the war, low-cost gasoline became accessible again, and most consumers returned to using gasoline since it was more convenient. Gasification was strongly tied to economic considerations at the time, which altered dramatically and swiftly as a result of the conflict. The rapid adoption of gasification technologies is ultimately dependent on their capacity to compete with fossil fuels, which is dependent on unknown elements such as resources, economics, and political situations. As a result, during periods of fossil fuel scarcity, gasification has been pushed very quickly toward technological improvement, and new technologies have been developed; however, during times of emergency, priorities shift dramatically, and the development of gasification technology has met many struggles.

2.9 STATE OF ART

The International Energy Agency's (IEA) Bioenergy Program Task has been judged to properly characterize the current state-of-the-art of gasification technology [6]. The Worldwide Energy Agency's (IEA) Bioenergy Program Task 33 on Gasification of Biomass and Waste is a working group of international specialists whose goal is to promote the commercialization of efficient, cost-effective, and environmentally friendly thermal biomass gasification technologies. This paper is based on research completed for the IEA Bioenergy Program Task 33 during the 2019-2021 triennium. Task 33 keeps track of the essential unit activities and unit processes that comprise biomass and waste gasification.

Gasification is a well-established energy conversion technique that may create clean fuels, power, and chemicals from solid and liquid fuels, coals, pet coke, and petroleum refinery leftover hydrocarbons as well as biomass and trash. Currently, 686 gasifiers working in 272 large-capacity facilities across around 30 nations have a synthesis gas production capacity close to 200 GWth, or roughly of almost 200 MWth per gasifier installation. Another 83 GWth of synthesis gas capacity is being added by an additional 74 facilities with 238 gasifiers that are currently being built. This is the outcome of a long-term endeavor; it took more than 60 years of global work to achieve this level of gasification production capability. This excellent figure demonstrates the maturity as well as the promise of gasification

technologies, even if the utilization of non-fossil feedstocks such as biomass and wastes is more limited and typically limited to lower capacity units. Indeed, the number of facilities that use these feedstocks is approximately 100, with a total capacity of a few GWth.

Although biomass gasification's technical viability and the associated environmental benefits are widely recognised, the extent of its commercial use has largely been restricted to CHP, district heating, and a few co-firing applications, mainly driven by a mixture of local or regional environmental, economic, and climatic factors. The LCV (low calorific value) or MCV (medium calorific value) gas generated by small- to medium-sized gasifiers, with capacities ranging from 0.02 to 20 MWth, is fed to internal combustion engines to create electricity and CHP. More than 1000 such machines are already in use in Germany alone. Furthermore, and particularly in Japan and the United Kingdom, there are thermal facilities ranging from a few MW to tens of MW that gasify wastes to enhance the process performance and productivity of traditional incineration plants for power and CHP. There are also tens of stationary and circulating fluidized bed gasifiers on a 10-140 MWth scale that employ various types of biomass residues and wastes to create LCV product gas for use as a fuel in lime and cement kilns, as well as for co-firing with coal in power plants.

Figure 14: Distribution of industrial gasification plants in the world (source: Gasification & Syngas Technologies Council [12])

2.9.1 Alternative applications – biofuels

Until recently, competition from low-cost fossil fuels, legislative uncertainty, and insufficient incentives from policy interventions hampered the development of sophisticated techniques and widespread application of biomass gasification for synthesis gas. Due to this, cooperation between developers, business, and other value-chain players have not been encouraged, which has prevented the development and expansion of bioenergy and waste conversion technologies. Therefore, the development of such technologies, such as enhanced biofuels based on gasification production technologies, has been gradual towards industrial scales. There is normally a development sequencing from the laboratory to bench scale, to pilot plant to a demonstration, before achieving a first prototype. Overcoming these risks within the existing support and market systems has shown to be a bottleneck for the two last phases in the sequence.

Many gasification-based biofuel project innovations were initiated in the EU between 2010 and 2016, fueled by the renewable energy regulation (RED) and peaked oil prices at the time. Except for the Gothenburg Biomass Project (GoBiGas) phase 1, none of the projects were realized in the EU, including those that received NER 300 funding (*NER 300 is a funding program pooling together approximately EUR 2 billion for innovative low-carbon technology, focusing on the commercial demonstration of environmentally safe Carbon Capture and Storage (CCS) and advanced renewable technologies within the EU*). Furthermore, GoBiGas phase 1 was halted in 2018 due to financial constraints. The primary motivation for constructing the GoBiGas phase 1 plant was not to test its viability as a standalone economic endeavor; rather, it was to obtain the knowledge needed to de-risk the five-fold scale-up in GoBiGas phase 2. However, once the second phase of the project was canceled in 2015, the reasons for continuing to operate at a loss were no longer there.

In 2018, two waste gasification projects were proposed in Rotterdam and Tarragona, both employing Enerkem technology, however they are still in the planning and permission stages. Several project studies are also being conducted, however these are less progressed than the scheduled projects. Also worthy of notice is the waste-to-jet fuel project being performed by the Fischer-Tropsch (FT) technology business Velocys in the United Kingdom.

In a global sense, the situation is comparable. Although not for biofuels, one factory in Japan uses the Ebara Ube Process (EUP) to gasify plastic waste to generate syngas, which is then used to manufacture hydrogen for ammonia synthesis. However, it was stated in 2019 that EUP technology will serve as the foundation for a collaboration between JGC Corporation, Ebara Environmental Plant Co., Ltd., Ube Industries, Ltd., and Showa Denko K.K. for an EPC company for plastic waste gasification plants. Sekisui Chemical collaborated with LanzaTech Inc. to develop the gasification of combustible trash into carbon monoxide and hydrogen, which is then transformed to ethanol by gas fermentation.

Enerkem also has a factory in Edmonton, Alberta, that is now in operation and uses refuse-derived fuel (RDF). A second factory in Canada is being planned.

Several initiatives have been launched in the United States over the last decade. Two industrial projects, Range Fuel and Ineos Bio, finished construction but were abandoned after a few years, ostensibly due to technical difficulties. Two more projects, Red Rock Biofuels and Sierra Biofuels, attained financial close in 2017 and are now under building after several years of planning and finance difficulties. In addition, Velocys' biomass-to-FT liquids project and Aemetis' biomass-to-ethanol facility are also in the planning stages.

In the EU, only four significant pilot plants are operational, one of which, Gaya, is relatively tiny, one is under development, and two, Comsyn and BioTfueL, have begun since 2016. In the United States, there are three significant operational pilot facilities, one of which is built on the same technology as the Güssing and GoBiGas plants.

The dilemma of poor advancement is not restricted to gasification technology. The similar tendency is evident for various types of biofuels, since many of the causes are repeating themes, such as energy pricing and regulatory and legislative restrictions impacting the market.

Many factors favor gasification as a technology; the combination of fuel and product flexibility, high fuel conversion, technologies suitable for a variety of scales, and so on are technical aspects that imply that gasification has fewer feedstock and potential and challenges than other advanced biofuel technologies. Despite technical challenges in previous installations, this potential is a fundamental component of gasification that maintains the technology on the table.

It should also be noted that the innovation in the technology is the use of biomass in gasification systems and the accompanying gas cleaning, whereas gas upgrading and product synthesis are widely employed in the petrochemical and chemical sectors and are therefore well-proven. By example, contemporary coal gasification began in the 1970s-80s, progressed through the learning curve, and is now a proven commercial technology with several installations, particularly in China. There is no reason why biomass gasification might not follow in the footsteps of this technology if it is successful in the initial installations.

The RED II, and ideally the follow-up on the renewable fuel standard (RFS2), as well as policy interventions in several countries individually, focus on decreasing GHG emissions in the transportation sector and, as a result, place a greater premium on advanced biofuels. Such legislative and commercial improvements may result in more favorable market conditions and the economic viability of gasification-based and other advanced biofuels plants. The common issues confronting advanced biofuels include the use of the aforementioned framework policies to establish conditions, first for financing developments and market establishment in industrial scale first-of-a-kind plants, and then, more long-term, to establish a commercial structure that leads to more widespread activities and deployment.

3 PLANT DESIGN METHODOLOGY

3.1 CONSIDERED BIOMASSES

In principle, whichever type of biomass can be used in the downdraft gasifier. The most important prerequisite that must be respected is related to the humidity content, whose value must be kept under about the 30% to allow the proper working of the gasifier.

To have a wider view on how the different biomasses can lead to different outcomes of the gasification process and to see how different the results among them are, a good number of biomasses has been considered and, for each of them, all the calculations have been carried out.

In order to make all the required estimations for each biomass, it is necessary to get the data upon the proximate analysis, ultimate analysis and syngas composition. Those analysis have been taken from other studies and publications that report in a detailed way all the information needed. The considered biomasses are: wood shavings [13] [14], hazelnut shells [15] [16], coconut shells [15] [17], corn cob [18], rice husk [19], pine tree [19] [20], beech wood [21], chicken manure [22], almond shell [23].

The data provided by all those studies are often referred to different bases, therefore they all have to be expressed in the same way to get consistent results and to make valuable comparisons. The elemental analysis, in mass percentages, is provided on a dry ash free basis for all the biomasses. Then the sum of the elemental composition is less than 100% since it does not include the humidity and ash content. Among the biomasses above described, there were some whose elemental composition was given just on ash free (AF) basis and some others on as received (AR) basis. Consequently, each element percentage has been properly scaled to get the elemental composition on dry ash free (DAF) basis in the following way:

$$\%element_{i,DAF} = \%element_{i,AF} * (100\% - \%_{humidity}) \quad (3.1)$$

$$\%element_{i,DAF} = \%element_{i,AR} * (100\% - \%_{humidity} - \%_{ash}) \quad (3.2)$$

Finally, all the compositions are reported in the following tables.

Table 2Table 2: Proximate analysis of the different biomasses

	Proximate analysis				
	Volatile matter	**Humidity**	**Ash**	**Fixed carbon**	**Sum**
Wood shavings	76%	6%	4%	14%	100.00%
Hazelnut shells	63%	12%	1%	24%	100.00%
Coconut shells	74.3%	7.4%	0.7%	17.6%	100.00%
Corn cob	71.4%	10.0%	1.6%	17.0%	100.00%
Rice husk	55.7%	9.4%	19.7%	15.2%	100.00%
Pine tree	67.7%	14.0%	0.4%	17.9%	100.00%
Beech wood	74.2%	8.3%	1.2%	16.3%	100.00%
Chicken manure	56.7%	29.4%	13.8%	0.1%	100.00%
Almond shell	72.3%	10.6%	1.2%	15.9%	100.00%

Table 3: Ultimate analysis of the different biomasses

	Ultimate analysis							
	C	**H**	**O**	**N**	**S**	**Cl**	**sum DAF**	**sum with ash and humidity**
Wood shavings	57.42%	4.32%	28.22%	0.81%	0.00%	0.00%	90.76%	100.00%
Hazelnut shells	40.84%	5.04%	40.12%	0.19%	0.58%	0.00%	86.78%	100.00%
Coconut shells	44.41%	6.02%	41.35%	0.09%	0.00%	0.00%	91.87%	100.00%
Corn cob	42.87%	4.99%	40.18%	0.36%	0.00%	0.00%	88.40%	100.00%
Rice husk	33.08%	3.35%	33.97%	0.29%	0.21%	0,00%	70.90%	100.00%
Pine tree	40.67%	5.58%	39.26%	0.08%	0.00%	0.00%	85.60%	100.00%
Beech wood	42.98%	5.78%	41.61%	0.16%	0.02%	0.01%	90.55%	100.00%
Chicken manure	35.00%	4.00%	15.70%	2.10%	0.00%	0.00%	56.80%	100.00%
Almond shell	51.40%	6.50%	29.60%	0.70%	0.00%	0.00%	88.20%	100.00%

Table 4: Syngas composition of the different biomasses

	SYNGAS COMPOSITION				
	CO	**CO_2**	**CH_4**	**H_2**	**N_2**
Wood shavings	22.2%	11.5%	4.5%	10.9%	50.9%
Hazelnut shells	19.6%	10.0%	2.0%	12.7%	55.7%
Coconut shells	21.3%	11.8%	1.5%	13.5%	51.9%
Corn cob	17.4%	12.0%	1.5%	15.5%	53.6%

Rice husk	20.0%	12.0%	2.0%	16.0%	50.0%
Pine tree	20.0%	14.0%	2.0%	18.0%	46.0%
Beech wood	12.8%	12.7%	3.7%	7.2%	61.5%
Chicken manure	22.0%	12.0%	1.0%	15.0%	50.0%
Almond shell	16.2%	10.7%	5.9%	13.1%	54.1%

3.2 CALCULATION PROCEDURE

Calculations are very important to understand the feasibility of the project and to assess all the resources that are needed to produce a certain amount of electricity. It is very important to assess the amount of biomass necessary to produce a certain quantity of syngas and so, consequently, a certain amount of electricity. The outcomes strictly depend on many parameters and in particular on the experimental data upon the biomass composition, the syngas composition, the value of the lower heating value, the moisture content, the ash content, the fixed carbon content and the volatile matter content. In turn the experimental syngas composition depends on the parameters at which the downdraft gasifier run, whose operation must be optimized to extract the maximum power.

In this section, the procedure of calculation is explained in a detailed way. To do that it has been taken in consideration the chicken manure. The method here illustrated holds true for all the other biomasses, of course the outcomes will be different due to the different compositions and to a different equivalent ratio. Here below are illustrated all the steps.

3.2.1 Biomass characterization

The biomass to be gasified must first be characterized as exactly as possible. For this reason, the proximate and ultimate analysis of the selected samples must be carried out, which properly represent the material to be gasified. The following results are obtained from the immediate analysis, whose values have been obtained for a chicken manure sample [24]:

Table 5: Chicken manure proximate analysis

Proximate analysis	
Humidity [%]	29.4
Ashes [%]	13.8
Volatile matter [%]	56.7
Fixed carbon [%]	0.1
LHV [MJ/kg]	15.8

In the proximate analysis, the lower heating value of the biomass is also obtained. Elemental analysis determines the mass percentage of the main elements of the biomass. The elemental analysis, in mass percentages, is provided on a dry ash free basis, therefore the sum of percentages and fixed carbon add up to 56.8%, and not 100% [25].

Table 6: Chicken manure ultimate analysis

Ultimate analysis	
Carbon [%]	35.0
Hidrogen [%]	4.0
Oxigen [%]	15.7
Nitrogen [%]	2.1

3.2.2 Molecular mass and molecular composition of the biomass

Having the mass percentage of each element and the molecular mass, it is possible to determine the moles of each element by dividing the mass percentage for the molecular mass. Then it is possible to compute the moles on dry ash free basis (DAF) in the following way.

$$Moles_{DAF} = \frac{Moles_{AR}}{1 - humidity[\%] - ash[\%]}$$

(3. 3)

Then, it is possible to find the molecular composition of the biomass. To do that it has been taken 1 atom of carbon as basis and the other atoms are computed by dividing the moles of that element for the moles of carbon on DAF basis. Therefore, the chemical formula of the biomass is: $CH_{1.371}O_{0.336}N_{0.051}$.

Finally, the overall biomass molecular weight is computed by summing the molecular weight of each atom that compose the biomass molecule.

Table 7: Chicken manure molecular weight

	Mass percentage	Molecular mass	Moles	Moles on dry ash free (DAF) basis	Atoms in the molecule	Molecular weight
C	35.0%	12.0107	0.02916	0.05135	**1.000**	12.011
H	4.0%	1.00784	0.04	0.07042	**1.371**	1.371
O	15.7%	15.999	0.00981	0.01727	**0.336**	5.383
N	2.1%	14.0067	0.0015	0.00264	**0.051**	0.720
Sum	56.8%		0.08048	0.14168		**19.474**

3.2.3 LHV of the components constituting the syngas starting from enthalpies of formation

The LHV of the components that constitute the syngas is found starting from the enthalpies of formation of the molecules involved in the combustion reaction that is carried out to form that specific product. Here below the values of the enthalpies of formation are reported [26].

Table 8: Molecular weight of the components present in the syngas

Molecule	$\Delta h^{\circ}f$ [MJ/kmol]
CO(g)	-110.53
CO_2(g)	-393.52
H_2O(g)	-241.82
H_2O(l)	-285.83
CH_4(g)	-74.85
O(g)	249.17

N(g)	472.68

After that, it is necessary to consider the following combustion reactions to determine the LHV of the molecules present in the syngas.

Table 9: Combustion reactions to determine the LHV

Reaction to determine the LHV of CO	$CO + 1/2\ O_2 \rightarrow CO_2 + LHV_{CO}$
Reaction to determine the LHV of H_2	$H_2 + 1/2\ O_2 \rightarrow H_2O + LHV_{H2}$
Reaction to determine the LHV of CH_4	$CH_4 + 2\ O_2 \rightarrow CO_2 + 2\ H_2O + LHV_{CH4}$

Having those reaction, the LHV is computed as follows:

- $LHV_{CO} = \Delta h°_{f,CO} + \frac{1}{2}\ \Delta h°_{f,O_2} - \Delta h°_{f,CO_2}$

(3. 4)

- $LHV_{H_2} = \Delta h°_{f,H_2} + \frac{1}{2}\ \Delta h°_{f,O_2} - \Delta h°_{f,H_2O}$

(3. 5)

- $LHV_{CH_4} = \Delta h°_{f,CH_4} + 2\ \Delta h°_{f,O_2} - \Delta h°_{f,CO_2} - 2\Delta h°_{f,H_2O}$

(3. 6)

The LHV obtained are in MJ/kmol, it is possible to convert them in other useful unit of measures in the following way (normal contitions: T=298.15K, P=101325Pa).

$$LHV_i\left[\frac{MJ}{Nm^3}\right] = LHV_i\left[\frac{MJ}{kmol}\right] * \frac{101325}{298{,}15 * 8314}\left[\frac{kmol}{Nm^3}\right]$$

(3. 7)

$$LHV_i\left[\frac{MJ}{kg}\right] = \frac{LHV_i\left[\frac{MJ}{kmol}\right]}{MM_i\left[\frac{kg}{kmol}\right]}$$

(3. 8)

And finally, the following results are obtained.

Table 10: LHV of the components present in the syngas

	MJ/kmol	MJ/Nm3	MJ/kg
LHV_{CO}	282,99	11,565	10,107
LHV_{H2}	285,83	11,681	142,915
LHV_{CH4}	890,33	36,385	55,646

3.2.4 Properties of the syngas

The composition of the synthesis gas depends on many factors: type of biomass, air flow, temperature, pressure, residence time, flow geometry, etc. The most reliable method to know the composition of this gas is to carry out experiments in an experimental gasifier, varying the parameters to optimize the process; In addition, the calculation using chemical equilibrium equations could provide good results, if the parameters are well adjusted with known experimental results, considering all the chemical reactions involved. Another method can be the consultation of publications of similar biomass.

As an example, the following volume composition (molecular fraction) for chicken manure has been obtained from the literature [24]:

Table 11: Molecular fraction of the chicken manure syngas

Syngas Composition		LHV[MJ/Nm³]	MM[kg/kmol]
CO	22%	11.565	28
CO_2	12%	-	44
H_2	15%	11.681	2
N_2	50%	-	28
CH_4	1%	36.385	16

It is possible to compute LHV contribution of each component by multiplying the volume fraction for the respective LHV. Then, summing up the three contributions, it is found the overall value for the syngas. The obtained value is expressed in [MJ/Nm^3] and so, to express it in [MJ/kg] it is necessary to find the density of the

syngas. First, it is computed the density of each component in normal conditions according to ideal gas law, then each of them is multiplied by the respective volume fraction and finally all the contributions are summed up to give the syngas density.
At this point it is possible to express the LHV of the syngas in [MJ/kg] by just dividing the before computed value for the density of the syngas just found.
Another important characteristic of the syngas is its molecular mass, that is simply computed by summing up all the contributions given by the multiplication of the molecular mass of each element and their relative volume fraction. The density of the components of syngas have been obtained whith perfect gas law at normal conditions (298.15 ºK, 1 atm)
All the results are shown in the following table.

Table 12: Chicken manure syngas characteristics

	LHV contrib. [MJ/m3]	Density [kg/Nm3]	Density contrib. [kg/Nm3]	LHV contrib. [MJ/kg]	MM syngas [kg/kmol]
CO	2.544	1.144	0.252	2.404	6.16
CO_2		1.798	0.216		5.28
H_2	1.752	0.082	0.012	1.655	0.3
N_2		1.144	0.572		14
CH_4	0.364	0.654	0.007	0.344	0.16
Sum	**4.660**	-	**1.058**	**4.403**	**25.9**

3.2.5 LHV of the syngas mixed with stoichiometric air

It is also useful, for the engine performance calculations, to compute the lower heating value of the mixture of the syngas with a stoichiometric amount of air. It is carried out according to the following formula.

$$H_{syngas} = \frac{LHV_{syngas}}{1 + 2.38 * v_{CO} + 2.38 * v_{H2} + 9.52 * v_{CH4}}$$

(3. 9)

With:

- v_{CO}, the volume fraction of CO in the gas.

- v_{H2}, the volume fraction of H_2 in the gas.
- v_{CH4}, the volume fraction of CH_4 in the gas.

The coefficients of the denominator of the previous equation are the moles of air for each mole of O (atomic oxygen) necessary for the complete combustion of each component, considering that the volumetric composition of the air is 21% oxygen and 79% nitrogen. So, the amount of air necessary for the combustion of the component for each mole of monoatomic oxygen is (1+79/21)/2.
Then the coefficients 2.38 and 9.52 are found respectively as (1+3.76)/2 and (1+3.76)*2.

Table 13: Lower heating value of the mixture of the syngas with a stoichiometric amount of air

H_{syngas}	
[MJ/Nm³]	2.359
[MJ/kg]	2.228

3.2.6 Stoichiometric amount of air per each kilo of biomass

After having computed how the molecule of the biomass is made, it is possible to go through the calculation of the amount of stoichiometric air needed to burn the biomass. In particular, the calculations are made according to the combustion reaction here reported.

$$C\,H_x\,O_y\,N_z + n(O_2 + 3.76\,N_2) \rightarrow C\,O_2 + a\,H_2O + b\,N_2$$

Then, knowing the atoms of oxygen that react for each element constituting the biomass, the number of moles of oxygen are found by multiplication with the atoms of each element constituting the biomass. So, the overall moles of oxygen are found summing up all the contributions. At this point it is possible to compute the amount of stoichiometric air.

It is also possible, knowing the molecular mass and the density of the air that are respectively 28.84 kg/kmol and 1.179 Nm^3/kg (normal conditions), to find the kg and the Nm^3 of the stoichiometric air.

Overall, the results are summarized in the following table.

Table 14: Stoichiometric amount of air to burn the chicken manure

	Atoms in the molecule	Molar fraction of O	Moles O	[kmol air/kmol biom]
C	1.000	2	2.000	**5.591**
H	1.371	0.5	0.686	[kg air/kmol biom]
O	0.336	-1	-0.336	**161.253**
N	0.051	0	0.000	[Nm3 air/kmol biom]
Sum			**2.349**	**136.820**

3.2.7 Actual air amount for the gasification process

Gasification occurs in conditions of poor amount of oxygen with respect to the stoichiometric amount. The ratio between the actual amount of oxygen used for gasification and the stoichiometric amount is called equivalent ratio (ER) and it is a paramount parameter of the process. Indeed, it strongly affects the outcomes of the gasification and it has to be found, for each kind of biomass, an optimal value that optimize the process. This value is found through direct assessment of the performances of a gasifier or through simulations. In this case, the equivalent ratio used for the gasification of chicken manure will be calculated using the following equation knowing that the air-fuel ratio used in the simulation of downdraft gasification of chicken manure is 1.5 $Nm^3_{air}/kg_{biomass}$ [24], the calculation is detailed below:

$$ER = \frac{\left(\frac{RA}{Biom}\right)_{gasification}}{\left(\frac{RA}{Biom}\right)_{stoich}} = \frac{\left(\frac{m_{air,gasification}}{m_{biom}}\right)}{\left(\frac{m_{air.stoich}}{m_{biom}}\right)}$$

(3. 10)

To find the Nm^3 of air needed for each kg of biomass, the following relation has been used:

$$\left(\frac{RA}{Biom}\right)_{stoich}\left[\frac{Nm^3_{air}}{kg_{biom}}\right] = \frac{\left(Stoich.air\ \left[\frac{kmol_{air}}{kmol_{biom}}\right] * MM_{air}\left[\frac{kg_{air}}{kmol_{air}}\right]\right)}{\rho_{air}\left[\frac{kg_{air}}{Nm^3}\right] * MM_{biomass}\left[\frac{kg_{biom}}{kmol_{biom}}\right]}$$

(3. 11)

Finally, knowing that the amount of stoichiometric air is 7.026 $Nm^3_{air}/kg_{biomass}$, the equivalent ratio (ER) can be computed:

$$ER = \frac{1.5}{7.026} = 0.21$$

(3. 12)

3.2.8 Stoichiometric amount of air of combustion per each kmol of syngas

At this point, the syngas composition is defined and so, analogously to what has been done in the calculation of the stoichiometric air to burn the biomass, the stoichiometric air of combustion of the syngas has been computed. In the following table all the results are summarized.

Table 15: Stoichiometric amount of air to burn the chicken manure syngas

	volume composition	Molar fraction of O	Moles O for moles of gas [kmol O/kmol syngas]
CO	22.0%	1	0.22
CO_2	12.0%	0	0
H_2	15.0%	1	0.15
N_2	50.0%	0	0
CH_4	1.0%	4	0.04
			0.41

Finally, the stoichiometric amount of air is obtained.

It is obtained a value equal to 0.9758 $kmol_{air}/kmol_{syngas}$ (0.9758 Nm^3_{air}/Nm^3_{syngas}) and so, dividing for the syngas density, it is obtained a value equal to 0.922 Nm^3_{air}/kg_{syngas}.

3.2.9 Molar flow rate of each component for 1kg/h of biomass AR (humid and with ash)

An important step, in this flow of calculations, is to determine the flow rate of each element for each kg/h of biomass that is introduced in the gasifier. Then, after having taken 1 kg/h as a basis is possible to compute all the other flow rates that, in this case, are expressed in molar basis.

$$\dot{n}_{biomass,DAF}\left[\frac{kmol_{DAF}}{h}\right] = \frac{\dot{m}_{biomass,AR} * \left(1 - \%_{humidity} - \%_{ash}\right)\left[\frac{kg_{DAF}}{h}\right]}{MM_{DAF}\left[\frac{kg_{DAF}}{kmol_{DAF}}\right]}$$

(3. 13)

$$\dot{n}_{fixed\ carbon}\left[\frac{kmol_C}{h}\right] = \frac{\dot{m}_{biomass,AR}\left[\frac{kg_{AR}}{h}\right] * \%_{fixed\ carbon}\left[\frac{kg_C}{kg_{AR}}\right]}{MM_C\left[\frac{kg_C}{kmol_C}\right]}$$

(3. 14)

$$\dot{n}_{air}\left[\frac{kmol_{air}}{h}\right] = \dot{n}_{biomass,AR}\left[\frac{kmol_{DAF}}{h}\right] * Stoich.\,air\left[\frac{kg_{air_{stoich}}}{kmol_{DAF}}\right] * ER\left[\frac{kg_{air}}{kg_{air_{stoich}}}\right]$$

(3. 15)

$$\dot{n}_{H_2O}\left[\frac{kmol_{H_2O}}{h}\right] = \frac{\dot{m}_{biomass,AR}\left[\frac{kg_{AR}}{h}\right] * \%_{humidity}\left[\frac{kg_{H_2O}}{kg_{AR}}\right]}{MM_{H_2O}\left[\frac{kg_{H_2O}}{kmol_{H_2O}}\right]}$$

(3. 16)

At this point, it is possible to compute the flow rate of the syngas. To compute this value, it is convenient to start from the amount of air that reacts in the gasification reaction and then, passing from the amount of nitrogen in the air, the final result is obtained. It is convenient to do that with nitrogen since it is an inert and so it is simpler to make the calculations with respect to the other components.

First, it has to be written the gasification reaction.

$$CH_xO_yN_z + \dot{n}_{air}(0{,}21O_2 + 0{,}79N_2) \rightarrow v_{CO}CO + v_{CO2}CO_2 + v_{H2}H_2 + v_{CH4}CH_4 + v_{N2}N_2$$

This gasification reaction is performed with an amount of air given by the stoichiometric one multiplied by the ER. The nitrogen produced is due to two contributions:

1. The amount of air that enters. Then, knowing that the air is composed, approximately, by 21% of oxygen and 79% of nitrogen, it is possible to find the kmoles of nitrogen per kmol of dry biomass (molecule of biomass) produced by making $0{,}79\% * \dot{n}_{air}$.
2. The nitrogen contained in the biomass. Knowing that the kmols of nitrogen, v_{N2}, come from the N of the biomass molecule, they are obtained z katomos of nitrogen per kmol of biomass.

Then, summing up those two contributions it is obtained the overall amount of N_2:

$$v_{N2} = \frac{z}{2} + 0{,}79 * \dot{n}_{air}$$

(3. 17)

But v_{N2} is, based on 100% in this way. To find the actual amount of syngas produced it has to be divided this value by the volumetric fraction of N_2 that is present on the syngas (50%). Overall, the following formula is obtained:

$$\dot{n}_{syngas}\left[\frac{kmol_{syngas}}{h}\right] = \frac{\frac{z}{2} + 0{,}79 * Q_{aire}}{50\%}$$

(3. 18)

$$\dot{m}_{syngas}\left[\frac{kg_{syngas}}{h}\right] = \dot{n}_{syngas}\left[\frac{kmol_{syngas}}{h}\right] * MM_{syngas}\left[\frac{kg_{syngas}}{kmol_{syngas}}\right]$$

(3. 19)

$$\dot{v}_{syngas}\left[\frac{Nm^3_{syngas}}{h}\right] = \frac{\dot{m}_{syngas}\left[\frac{kg_{syngas}}{h}\right]}{\rho_{syngas}\left[\frac{kg_{syngas}}{Nm^3_{syngas}}\right]}$$

(3. 20)

Overall, the following results are obtained:

Table 16: Molar flow rate of each component for 1kg/h of biomass AR

$\dot{n}_{biomass,DAF}$	0.0292	$kmol_{DAF}/h$
$\dot{n}_{fixed\ carbon}$	0.0001	$kmol_{FC}/h$
$\dot{n}_{air}$	0.0342	$kmol_{air}/h$
$\dot{n}_{H_2O}$	0.0163	$kmol_{H2O}/h$
$\dot{n}_{syngas}$	0.0556	$kmol_{syngas}/h$

Then, the most important outcome is the syngas flow rate that is possible to get starting from 1kg/h of biomass and it is equal to 0.0556 kmol/h. By multiplying this value by the syngas molecular mass and the syngas density, they are respectively obtained the values of 1.440 kg/h and 1.361 Nm^3/h.

3.2.10 Gasifier efficiency

Now that all the calculations have been made. it can be easily calculated the gasifier efficiency that is equal to 40.1% and it is obtained according to the following formula:

$$\eta_{gasifier} = \frac{LHV_{syngas}}{LHV_{biomass}} = \frac{LHV_{syngas}\left[\frac{MJ}{Nm^3}\right] * \dot{v}_{syngas}\left[\frac{Nm^3}{h}\right]}{LHV_{biomass}\left[\frac{MJ}{kg_{AR}}\right] * \dot{m}_{biomass,AR}\left[\frac{kg_{AR}}{h}\right]} \quad (3.21)$$

3.2.11 Syngas obtained for each biomass starting from 1kg/h of biomass AR

Now that all the calculation procedure has been explained step by step it is possible to summarize the amount and the properties of the syngas obtained for each biomass. To compare all the outcomes, it has been assumed a value of the equivalent ratio ER of 0.3 (typical value for downdraft gasifier). Then the following tables summarize all the results that are obtained by adopting the same procedure described before.

Table 17: Syngas properties for all the biomasses

	LHV_{syngas}		H_{syngas}		ρ_{syngas}	MM_{syngas}
	[MJ/Nm³]	[MJ/kg]	[MJ/ Nm³]	[MJ/kg]	[kg/ Nm³]	[kg/kmol]
Wood shavings	5.480	5.066	2.473	2.286	1.082	26.466
Hazelnut shells	4.479	4.206	2.286	2.147	1.065	26.058
Coconut shells	4.587	4.285	2.327	2.174	1.071	26.198
Corn cob	4.370	4.159	2.269	2.160	1.051	25.710
Rice husk	4.911	4.709	2.399	2.300	1.043	25.520
Pine tree	5.145	4.972	2.456	2.374	1.035	25.320
Beech wood	3.669	3.309	2.007	1.810	1.109	27.128
Chicken manure	4.662	4.404	2.359	2.229	1.058	25.900
Almond shell	5.552	5.308	2.458	2.349	1.046	25.598

Table 18: Amount of necessary air for all the biomasses

	RA/Biomst	ER	RA/Biom real	St. air for syngas comb.	
	$[Nm^3_{air}/kg_{biomass}]$	$[kg_{air}/kg_{air,stoich}]$	$[Nm^3_{air}/kg_{biomass}]$	$[kmol_{air}/kmol_{syngas}]$ or $[Nm^3_{air} / Nm^3_{syngas}]$	$[Nm^3_{air}/kg_{syngas}]$
Wood shavings	6.394	0.3	1.918	1.216	1.124
Hazelnut shells	4.586	0.3	1.376	0.959	0.901
Coconut shells	4.962	0.3	1.489	0.971	0.907
Corn cob	4.696	0.3	1.409	0.926	0.881
Rice husk	4.167	0.3	1.250	1.047	1.004
Pine tree	4.841	0.3	1.452	1.095	1.058
Beech wood	4.794	0.3	1.438	0.828	0.747
Chicken manure	7.026	0.3	2.108	0.9758	0.922
Almond shell	6.581	0.3	1.974	1.259	1.204

Table 19: Amount of syngas produced for all the biomasses

	Amount of syngas produced for each kg/h of biomass AR		
	[kmol/h]	[kg/h]	[Nm³/h]
Wood shavings	0.110	2.913	2.693
Hazelnut shells	0.070	1.818	1.707

Coconut shells	0.085	2.231	2.084
Corn cob	0.075	1.935	1.842
Rice husk	0.058	1.468	1.407
Pine tree	0.087	2.211	2.137
Beech wood	0.068	1.856	1.674
Chicken manure	0.079	2.041	1.928
Almond shell	0.104	2.672	2.554

3.3 ENGINE: SELECTION AND DESIGN

Once all the preliminary calculations have been made, it is necessary to go through the estimation of the main parameters that characterize the motor and through which a proper choice can be made. First, they have to be analyzed which motors are suitable for syngas applications. Spark ignition engines, normally used with gasoline or kerosene, can run on syngas only. Diesel engines can be adapted to run on syngas by lowering the compression ratio and installing a spark ignition system. Another possibility is to run a normal, unconverted diesel engine with the "dual fuel" system, whereby the engine provides 0 to 90 percent power on producer gas, the rest being required of diesel for the ignition of the gas/air fuel mixture. The advantage of the latter system lies in its flexibility: in the event of a non-functional gasifier or lack of biomass fuel, an immediate changeover is usually possible, operating entirely on diesel. However, not all types of diesel engines can be adapted to the exposed system of operation. The compression ratios of diesel engines with antechamber and turbulence chamber are too high for proper operation with dual fuel and the use of lean gas in such engines causes detonations, caused by too high pressures and ignition delay. Direct injection diesel engines have lower compression ratios and can generally be converted successfully.

The calculations, in this section, will consists of the following steps:

1) Calculation of the approximate optimal engine displacement for each type of syngas used assuming a reasonable value of the used excess air, according to literature values. It will be carried out by using typical efficiencies values since at this preliminary step it has not yet decided the motor to be used.

2) Once the engine displacement is known, it is possible to see which motor in the market offers a value of engine displacement similar to those that have been found.
3) Compute, for each syngas and at given technology, the real value of the excess air (and the consequent penalty on the LHV), the amount of gas and the amount of air that has to enter in the motor to reach the nominal power.

1. The heating value of the produced syngas depends on the design of the gasifier and the characteristics of the fuel feeding the gasifier. It is important to minimize heat losses from the gasifier in order to achieve a high heating value. Moisture content and size distribution are two of the most important characteristics of fuel.

Concerning the engine, when mixing the syngas with combustion air, there is an additional reason for power loss, due to changes in gas composition, being very difficult to continuously maintain a stoichiometric mixture of syngas and air.

Since both excess and lack of air cause a decrease in the calorific value of the mix (per unit volume), both will cause a decrease in power as illustrated in the following figure [27].

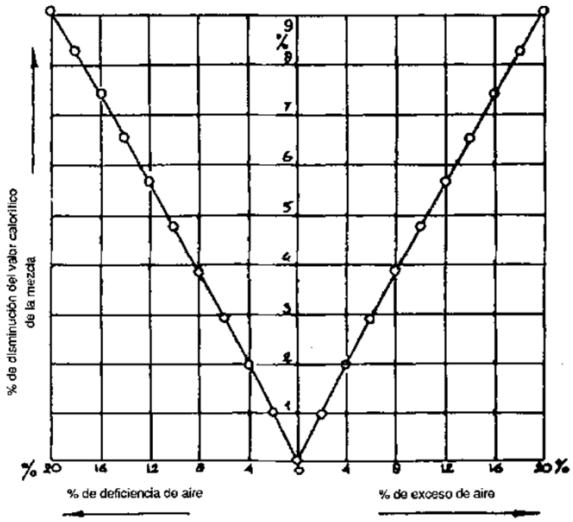

Figure 15: Decrease of the heating value of a mixture of syngas and air as a function of the deficiency or excess of air [21]

The only possible way to adjust the mixture for stoichiometric combustion is to install a hand-operated valve on the engine's combustion air inlet and run it regularly for maximum engine power output.

It is often best to run the engine with a slight excess of air to prevent flashback into the engine exhaust gas system. For this reason, to estimate the optimal engine displacement of the motor it has been considered an excess of air equal to 20%.
Here below it is reported the calculation procedure and all the typical values of the involved efficiencies.
First, it has been written the line equation through which it is possible to compute the LHV reduction as function of the excess air.

$$LHV_{reduction}[\%] = \frac{9}{20} * x[\%]$$

(3. 22)

Where x[%] is the excess air.
Therefore, the LHV reduction can be written as:

$$F_{LHV,loss}[\%] = \frac{\left(100 - \left(\frac{9}{20}\right) * x[\%]\right)}{100}$$

(3. 23)

It is then assumed an alternator efficiency η_{GE} equal to 0.75 [28], while the motor efficiency is assumed to be equal to a typical value of 0.5.

The motor power output can be computed in the following way.

$$P_{el}[kW] * 3{,}6\left[\frac{MJ}{kW}\right] = \eta_{GE} * \dot{V}_{syngas}\left[\frac{Nm^3_{syngas}}{h}\right] * LHV_{syngas}\left[\frac{MJ}{Nm^3_{syngas}}\right] * \eta_m * F_{LHV,loss}[\%]$$

(3. 24)

The required power output is priorly decided and it is equal to 20 kW_{el}. Then the volume flow rate of the syngas can be computed through the inverse formula:

$$\dot{V}_{syngas}\left[\frac{Nm^3_{syngas}}{h}\right] = \frac{\left(\eta_{GE} * LHV_{syngas} * \eta_m * F_{LHV,loss}[\%]\right)}{P_{el}[kW] * 3{,}6\left[\frac{MJ}{kW}\right]}$$

(3. 25)

Then it is possible to compute the volume flow rate of the air entering in the motor.

$$\dot{V}_{air}\left[\frac{Nm^3_{air}}{h}\right] = \dot{V}_{syngas}\left[\frac{Nm^3_{syngas}}{h}\right] * Stoich.air\ \left[\frac{Nm^3_{air}}{Nm^3_{syngas}}\right] * (1 + x[\%])$$

(3. 26)

Finally, summing up the two volume flow rates, the motor flow rate is found.

$$\dot{V}_{motor}\left[\frac{Nm^3}{h}\right] = \dot{V}_{syngas}\left[\frac{Nm^3_{syngas}}{h}\right] + \dot{V}_{air}\left[\frac{Nm^3_{air}}{h}\right]$$

(3. 27)

At this point, it is assumed a value of the volumetric efficiency η_V equal to 0.7 [29], a rotational speed n equal to 1500 rpm and it is used the following formula.

$$\dot{V}_{motor}\left[\frac{Nm^3}{h}\right] = \frac{1}{2} * \left(\frac{Engine\ displacement}{1000}\right) * \eta_V * n(rpm) * 60$$

(3. 28)

And so, reversing the expression it is found the engine displacement.
Overall, applying this procedure for all the considered biomasses, they are obtained the values that can be seen here below in the summarizing table.

Table 20: Estimation of the optimal engine displacement for all the biomasses

	$\dot{V}_{syngas}$	$\dot{V}_{air}$	$\dot{V}_{motor}$	Engine displacement
	[Nm³/h]	[Nm³/h]	[Nm³/h]	[L]
Wood shavings	38.50	56.19	94.70	3.006
Hazelnut shells	47.10	54.21	101.32	3.216
Coconut shells	45.99	53.59	99.59	3.161
Corn cob	48.28	53.64	101.92	3.236

Rice husk	42.96	53.99	96.95	3.078
Pine tree	41.01	53.88	94.89	3.012
Beech wood	57.51	57.16	114.67	3.640
Chicken manure	45.26	53.00	98.26	3.119
Almond shell	38.00	57.41	95.41	3.029
Average	-	-	-	**3.166**

The most important outcome of this analysis, as said, is the average energy displacement, whose value is equal to 3.166 L. It is the driving information that has helped to proper select an engine that can produce electric energy starting from the syngas as a fuel. For this reason, it has been selected the Power Products GZ25 generator, equipped with a KOHLER GMC430-27 engine [30], designed to run on gas, so it will not be necessary to adapt the set so that it can operate using syngas. It can provide a nominal power equal to 20 kW_{el} and it has an engine displacement close to the average value written above.

Figure 16: KOHLER generator [24]

It is an open generator, which has its engine and alternator exposed. In this way, immediate and easy access is achieved in the event of repair or maintenance. On the other hand, as this is the open version, it does not have a silencer, so it has to to be installed in an area where the noise does not disturb the people in the surroundings. For this reason, it has been chosen to use the soundproofed version. It has been chosen instead of the open version one because, even if it doesn't guarantee an immediate and easy access in the event of repair or maintenance, it has the advantage of having a silencer that allow to install it in the nearby of the usage site since the noise does not disturb the people in the surroundings.

Figure 17: KOHLER soundproofed version generator [24]

The generator is also equipped with a Decision-Maker® 3000 panel offering an advanced control, monitoring, and diagnostic system for optimized performance.

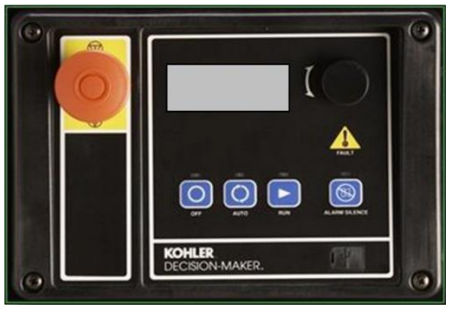

Figure 18: Generator controls/ Decision Maker 3000 [24]

In the following image, all the engine and alternator specifications are reported.

DIMENSIONS SOUNDPROOFED VERSION	
Commercial reference of the enclosure	SSE25-60
Length (mm)	2585
Width (mm)	1078
Height (mm)	1513
Dry weight (kg)	841
Acoustic pressure level @1m in dB(A)	76
Sound power level guaranteed (Lwa)	96

GENERAL ENGINE DATA	
Engine brand	GENERAL MOTORS by PSI
Engine ref.	GMC430-27
Air inlet system	Athmo
Cylinders configuration	L
Number of cylinders	4
Displacement (L)	2.97
Charge Air coolant	Air/Air DC
Bore (mm) x Stroke (mm)	101.60 x 91.44
Compression ratio	8.2 : 1
Speed (RPM)	1500
Pistons speed (m/s)	4.57
Maximum stand-by power at rated RPM (kW)	27.50
Frequency regulation, steady state (%)	+/- 0.5%
BMEP (bar)	0
Governor type	Electronic

GENERAL DATA	
Alternator commercial brand	KOHLER
Alternator ref.	4P4
Number of Phase	Three phase
Power factor (Cos Phi)	0.80
Altitude (m)	0 à 2500
Overspeed (rpm)	2250
Number of pole	4
Capacity for maintaining short circuit at 3 In for 10 s	No
Insulation class	H
T° class (H/125°), continuous 40°C	H / 125°K
T° class, standby 27°C	H / 163°K
AVR Regulation	
Total Harmonic Distortion in no-load DHT (%)	2,62
Total Harmonic Distortion, on load DHT (%)	3,57
Wave form : NEMA=TIF	84,6
Wave form : CEI=FHT	1,89
Number of bearing	1
Coupling	Direct
Voltage regulation at established rating (+/- %)	1
Recovery time (Delta U = 20% transcient) (ms)	500
Indication of protection	IP 23
Technology	Without collar or brush

Figure 19: Engine and alternator general data

3. At this step, having selected the engine, all the efficiencies and parameters are well defined and so they do not have to be estimated according to typical values anymore.
The starting point is now the engine displacement whose values is determined by the motor itself and it is equal to 2.97 L [30]. So, the volumetric flow rate entering in the motor is equal to 106.7 Nm^3/h and can be easily computed as:

$$\dot{V}_{motor}\left[\frac{Nm^3}{h}\right] = \frac{1}{2} * \left(\frac{Engine\ displacement}{1000}\right) * \eta_V * n(rpm) * 60 \qquad (3.29)$$

Where n is the engine rotational speed [30] and η_V is the volumetric efficiency, whose value has been assumed equal to the previous case, with a typical value of 0.7 [29].

At this point the three following equations can be written to respectively compute the three unknowns (the actual excess air $x[\%]$, the volume flow rate of the syngas $\dot{V}_{syngas}$ and the volume flow rate of air $\dot{V}_{air}$).

$$P_{el}[kW] * 3.6\left[\frac{MJ}{kW}\right] = \eta_{GE} * \dot{V}_{syngas}\left[\frac{Nm^3_{syngas}}{h}\right] * LHV_{syngas}\left[\frac{MJ}{Nm^3_{syngas}}\right] * \eta_m * F_{LHV,loss}[\%] \quad (3.30)$$

$$\dot{V}_{motor}\left[\frac{Nm^3}{h}\right] = \dot{V}_{syngas}\left[\frac{Nm^3_{syngas}}{h}\right] + \dot{V}_{air}\left[\frac{Nm^3_{air}}{h}\right] \quad (3.31)$$

$$\dot{V}_{air}\left[\frac{Nm^3_{air}}{h}\right] = \dot{V}_{syngas}\left[\frac{Nm^3_{syngas}}{h}\right] * Stoich.air\left[\frac{Nm^3_{air}}{Nm^3_{syngas}}\right] * (1 + x[\%]) \quad (3.32)$$

Where $F_{LHV,loss}$ is function of the excess air as written before and η_m is found as a function of the compression ratio according to the following chart [27].

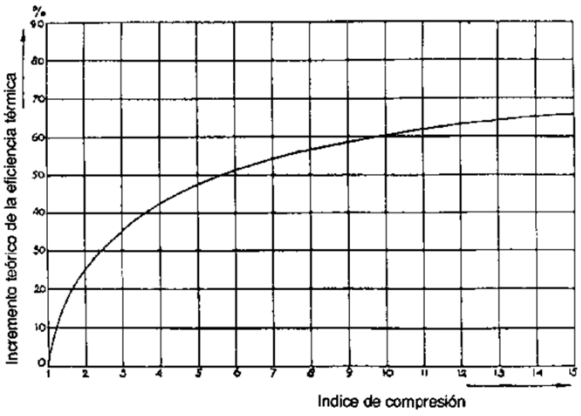

Figure 20: Relation between compression ratio and thermal efficiency of an engine [21]

Knowing that the compression ratio of the selected engine is 8.2, it is estimated an efficiency η_m equal to 0.54.

Overall, the following results are obtained for each biomass.

Table 21: Estimation of the main engine parameters at nominal conditions for all the biomasses

	$\dot{V}_{syngas}$	$\dot{V}_{air}$	Excess air (x)	$F_{LHV,loss}$	LHV_{loss}
	[Nm³/h]	[Nm³/h]	[%]	[%]	[%]
Wood shavings	35.55	57.82	33.74	84.82	15.18
Hazelnut shells	42.04	51.32	27.27	87.73	12.27
Coconut shells	41.44	51.93	29.07	86.92	13.08
Corn cob	41.44	51.93	29.07	86.92	13.08
Rice husk	39.24	54.13	31.71	85.73	14.27
Pine tree	37.88	55.49	33.81	84.78	15.22
Beech wood	48.04	45.33	13.91	93.74	6,.6
Chicken manure	41.07	52.29	30.47	86.29	13.71
Almond shell	34.93	58.44	32.89	85.20	14.80
Average	-	-	29.10	86.90	13.10

Finally, it is possible to compute the amount of biomass needed to produce the nominal power of 20 kW_{el} (or also the amount of biomass needed to produce each kW_{el}).

Table 22: Amount of biomass required to produce each kWel of power for all the biomasses

	Amount of syngas produced for each kg/h of biomass AR	Syngas flow rate to produce 20 kW		kg of biomass needed to produce 20 kW	kg of biomass needed to produce 1 kW
	[Nm³/h]	[Nm³/h]	[kg_{syngas}/h]	[$Kg_{biomass}$/h]	[$Kg_{biomass}$ /h*kW_{el}]
Wood shavings	2.693	35.55	38.45	13.20	0.65991
Hazelnut shells	1.707	42.04	44.77	24.63	1.23148
Coconut shells	2.084	41.44	44.36	19.88	0.99422
Corn cob	1.842	41.44	43.54	22.50	1.12499
Rice husk	1.407	39.24	40.93	27.89	1.39429
Pine tree	2.137	37.88	39.19	17.73	0.88642
Beech wood	1.674	48.04	53.26	28.69	1.43464
Chicken manure	1.928	41.07	43.47	21.30	1.06507
Almond shell	2.554	34.93	36.54	13.68	0.68376

3.4 GASIFIER: SELECTION AND DESIGN

For the choice of the gasifier, a brief compilation of existing models already on the market has been made, the model has been chosen based on the factors previously calculated,

seeking to have a minimum gas flow capacity equal or greater than that necessary according to the results just obtained for the nominal motor production requirements.

The gasification equipment that has been chosen is the GEK Gasifier Kit version v5.0 from the American manufacturer All Power Labs [31].

It has also been chosen also for the simplicity of use. Indeed, the GEK Gasifier makes it easy for beginners and experts alike to run high-performance solutions in small-scale gasification. The GEK Gasifier kit is a complete gas-making system: from biomass-fuel-feed input through syngas/air-mixer output, all controlled by a full automation system. Moreover, the GEK kit comes largely assembled, skidded and commissioned. It arrives ready-to-run, with minimal assembly, not as parts to puzzle together. The GEK gasifier a size of 145 x 145 x 223 cm and a weight of 450 kg and it is made as reported in the following images.

Figure 21: GEK gasifier: kit, processes and flows [25]

Such equipment includes:

- Hopper: standardized hopper ready for continuous feed airlock.
- GEK Gasifier: proven power pallet gasifier with automated char ash removal system.
- Automation system: fully automated gasifier control hardware and software.
- Gas filter: improved packed-bed filter using activated charcoal.
- Standard skid mount: all components come mounted on a forklift ready skid.

In the following tables, all the main gasifier features are reported.

GASIFIER SPECIFICATIONS	
Type:	Multistage Downdraft with thermal recycling
Materials:	304 SS/310 SS/ 321 SS/mild steel
Ash Removal:	Automated 12-hour batch vessel
Fuel Feed:	Automated
Hopper Capacity:	0.33 m³/88 gallons
Hopper Filling:	Batch - refill while operating
Maintenance Cycle:	~12 hours
Control System:	On-Board Automation

MAJOR COMPONENTS INCLUDED	
Gasifier	v5 GEK Gasifier with thermal recycling
Automation	Custom APL with open-source microcontroller
Feed System	Batch Hopper with feedstock auger
Filtration	Packed Bed
Gas Mixing	Active PID Controlled wide-band O_2 sensor
Mounting Skid	Powder-Coated Steel
Flare Stack	Premixed, Auto-Igniting
User Kit	Tools Consumables

PERFORMANCE	
Maximum Gas Flow Rate:	60 m³/hr ~20kWe or 380,000 BTU
Minimum Gas Flow Rate:	10 m³/hr ~3kWe or 60,000 BTU
Gas Energy Density	6.5 MJ/m³
Gas Composition	CO: 22%, H_2: 20%, CH_4: 3% CO_2: 10%, N_2: 45%
Biomass Consumption:	1.2 kg biomass = 3 m³ gas = 1 kWhe
Run Time per Hopper Fill: approximate @ 200 kg/m³ fuel density	5 kW: 15 m³/hr = 11 hrs 10 kW: 31 m³/hr = 5.5 hrs 20 kW: 62 m³/hr = 2.8 hrs
Max. Continuous Operation:	~12 hours
Start Up Time:	5 -20 min.

Figure 22: GEK gasifier: specifications, components and performance [25]

All Power Labs also provides the composition of the gas produced under standard operating conditions (CO: 22%, H_2: 20%, CH_4: 3% CO_2: 10%, N_2: 45%). It is observed that the composition of the product gas corresponding to the gasification of the different biomasses studied is similar to that provided by the manufacturer of the gasifier, so the use of the chosen biomasses will be suitable for this equipment.

3.4.1 Calculation of the autonomy time of the gasifier feeding system.

The hopper capacity of the selected gasifier is equal to 0.33 m^3. Starting from this information, it is possible to compute the time of autonomy of the gasifier feeding system or, in other words, the frequency with which the hopper must be replenished to guarantee a continuous operation of the gasifier. Then, knowing the inlet flow rate of each biomass to be fed into the gasifier to get the amount of syngas needed to run the engine at the nominal power of 20 kW_{el}, it is possible to obtain the time of autonomy according to the following formula.

$$T_a[h] = \frac{V_{hopper}}{\frac{\dot{m}_{biomass}}{\rho_{biomass}}}$$

(3. 33)

Then the following times of autonomy for each biomass are obtained starting from the mass flow rate and then going through the biomass density [32] [33] [34].

Table 23: Feeding system time of autonomy

	kg of biomass needed to produce 20 kW	Density	Nm³ of biomass needed to produce 20 kW	Hopper time of autonomy
	[kg/h]	[kg/m3]	[Nm3/h]	[h]
Wood shavings	13.19821895	256	0.051555543	6.40
Hazelnut shells	24.62965668	336	0.07330255	4.50
Coconut shells	19.88432337	336	0.059179534	5.58
Corn cob (dry)	22.49975628	304	0.074012356	4.46
Rice husk	27.88573223	679	0.041068825	8.04
Pine tree (dry)	17.72830125	330	0.053722125	6.14
Beech wood	28.69288901	330	0.086948149	3.79
Chicken manure	21.30149295	480	0.04437811	7.44
Almond shell	13.67521503	336	0.040700045	8.11

3.5 HEAT EXCHANGER: SELECTION AND DESIGN

Heat exchangers are devices designed to transfer heat between two or more fluids (i.e., liquids, vapors, or gases) of different temperatures. Depending on the type of heat exchanger employed, the heat transferring process can be gas-to-gas, liquid-to-gas, or liquid-to-liquid and occur through a solid separator, which prevents mixing of the fluids, or direct fluid contact. Other design characteristics, including construction materials and components, heat transfer mechanisms, and flow configurations, also help to classify and categorize the types of heat exchangers available. Finding application across a wide range of industries, a diverse selection of these heat exchanging devices are designed and manufactured for use in both heating and cooling processes. All heat exchangers operate under the same basic principles. However, these devices can be classified and categorized in several different ways based on their design characteristics.

3.5.1 Types of heat exchangers

Based on the different design characteristics, there are several different variants of heat exchangers available. Some of the more common variants employed throughout industry include:

- ***Shell and tube heat exchangers***: the most common type of heat exchangers, shell and tube heat exchangers are constructed of a single tube or series of parallel tubes (i.e., tube bundle) enclosed within a sealed, cylindrical pressure vessel (i.e., shell). The design of these devices is such that one fluid flows through the smaller tubes, and the other fluid flows around their outsides and between them within the sealed shell. Other design characteristics available for this type of heat exchanger include finned tubes, single- or two-phase heat transfer, countercurrent flow, cocurrent flow, or crossflow arrangements, and single, two, or multiple pass configurations.
- ***Double pipe heat exchangers***: a form of shell and tube heat exchanger, double pipe heat exchangers employ the simplest heat exchanger design and configuration which consists of two or more concentric, cylindrical pipes or tubes (one larger tube and one or more smaller tubes). As per the design of the shell and tube heat exchanger, one fluid flows through the smaller tube, and the other fluid flows around the smaller tube within the larger tube.
- ***Plate heat exchangers***: plate heat exchangers are constructed of several thin, corrugated plates bundled together. Each pair of plates creates a channel through which one fluid can flow, and the pairs are stacked and attached (via bolting, brazing, or welding) such that a second passage is created between pairs through which the other fluid can flow.
- ***Condensers, evaporators, and boilers***: boilers, condensers, and evaporators are heat exchangers which employ a two-phase heat transfer mechanism. Condensers are heat exchanging devices that take heated gas or vapor and cool it to the point of condensation, changing the gas or vapor into a liquid. On the other hand, in evaporators and boilers, the heat transfer process changes the fluids from liquid form to gas or vapor form.

3.5.2 Selection of the proper HX

The syngas leaves the gasifier at high temperature, and it cannot be injected in the engine at such high temperature. Then, it is necessary to cool down the syngas flow prior to put it in the generator. In this direction, it has to be selected a heat exchanger that must be able to cool it down and to transfer the heat to another fluid. The heated fluid is very useful for other final uses and allows to do not waste the available thermal energy that otherwise would be wasted. In the specific case, it has been chosen to use this thermal energy to heat up the sanitary water that can be used for showers and public bathrooms. For this scope, it has been chosen the heat exchanger of BOWMAN company [35].

Bowman HX are designed for a wide range of commercial or industrial applications, including district heating and hot water, space heating, thermal oil heating, electricity generation using ORC or Stirling engine technology, or when using a chiller to cool.

All Bowman units are based on the company's shell and tube heat exchanger design that combines excellent heat transfer performance with ease of installation and simple maintenance. To choose the useful model for the present application, it has to be computed the heat that can be recovered from the hot syngas exiting from the gasifier.

The heat exchanged by the syngas refrigeration is computed as follows:

$$Q_{HX} = \dot{m}_{gas} * Cp_{gas} * \Delta T$$

(3. 34)

Where:

Q_{HX} is the heat exchanged in kW.

$\dot{m}_{gas}$ is the gas flow that passes through the exchanger in kg/s.

Cp_{gas} is the specific heat of the gas under standard conditions in kJ/kg*K.

ΔT is the temperature change in the gas produced in the exchanger in K.

The specific heat of the gas is computed as:

$$Cp_{gas} = \sum Cp_i * m_i$$

(3. 35)

Where:

Cp_i is the specific heat of each gas component under standard conditions in kJ/kg*K.

m_i is the mass fraction of each gas component on a dry basis.

The calculation of the mass fraction of each component of the gas is calculated as:

$$m_i = \frac{MM_i * v_i}{\sum MM_i * v_i}$$

(3. 36)

Where:

MM_i is the molar weight of each gas component in kg/kmol.

v_i is the volume fraction of each gas component on a dry basis.

Finally, concerning the ΔT across the HX, it has been considered a typical syngas inlet temperature in the HX equal to 750 °C [36] and an outlet temperature of the syngas equal to 70 °C, that is the maximum temperature at which a typical fan can work [37]. Finally, the thermal power available for each biomass is computed.

Table 24: Heat recovered from hot syngas

	$Q_{recovered}$ [KW]
Wood shavings	8.33
Hazelnut shells	9.76
Coconut shells	9.66
Corn cob	10.02
Rice husk	9.16
Pine tree	8.89
Beech wood	11.05
Chicken manure	9.57
Almond shell	8.19

At this point it is possible to decide which is the most adequate HX among the BOWMAN choices. According to the specifications, the values of heat recovered are obtained by exchanging the heat between the exhausts (which enter in the HX at 600 °C and go outside at the temperature reported in the following figure) and the water (which is heated up from 25 °C to 80 °C).

Tipo	Potencia Típica de Motor	Flujo de Salida de Gas de Escape	Temperatura de Salida Gas	Recuperación de Calor	Caída de presión del Gas de Escape
	kW	kg / min	ºC	kW	kPa
2-25-3737-4	16	1.2	210	9.5	1.6
2-32-3737-5	16	1.2	170	11.5	1.8
3-32-3738-5	32	2.4	198	19	1.2
3-40-3738-6	32	2.4	163	21	1.3
3-60-3738-8	32	2.4	116	23	1.6
4-32-3739-5	60	4.5	199	36	1.0
4-40-3739-6	60	4.5	164	39	1.2
4-60-3739-8	60	4.5	116	43	1.4
5-32-3740-5	90	6.7	195	55	1.0
5-40-3740-6	90	6.7	161	59	1.1
5-60-3740-8	90	6.7	115	65	1.4

Figure 23: Types of BOWMAN HX [35]

Having all those information, it is possible to compute the maximum $UA|_{max}\left[\frac{kW}{K}\right]$ for all the HX models according to the following formula.

$$Q = U \times A \times \Delta T_{mln}$$

(3. 37)

Where ΔT_{mln} is the mean logarithmic temperature difference between the gas and the water and it is computed as follows.

$$\Delta T_{mln} = \frac{(T1g - T2w) - (T2g - T1w)}{ln\frac{(T1g - T2w)}{(T2g - T1w)}}$$

(3. 38)

At this point, it is known the heat recovery limit of each HX model. The following step consists in defining the inlet and outlet temperature of the water that is heated up. It has been assumed an inlet temperature of water equal to 25 °C and an outlet temperature equal to 50 °C. While the gas enters at 750 °C and exits at 70 °C.

Having defined the real case temperature differences, it is possible to estimate the actual mean logarithmic temperature difference and, consequently, all the actual $UA\left[\frac{kW}{K}\right]$ for each syngas/biomass using the values of heat that is possible to recover for each biomass. Finally, for each case it is checked if the actual UA is lower than the $UA|_{max}$ that the specific HX model allows. The $UA|_{max}$ for the models 2-25-3737-4 and 2-25-3737-5 are respectively 0.0293 kW/K and 0.0392 kW/K.

Once the model of HX has been selected, it is possible to compute the water flow rate that is heated for all the different biomasses. Overall, the following results are obtained.

Table 25: HX models and flow rate of heated water for all the biomasses

	$Q_{recovered}$	$\Delta T\|_{mln\|real}$	UA	$T_{water\ oulet\ final}$	m_{water}	HX MODEL
	[KW]	[K]	[kW/K]	[°C]	[kg/h]	-
Wood shavings	8.33	317.01	0.0263	50	287.12	2-25-3737-4
Hazelnut shells	9.76	317.01	**0.0308**	50	336.26	2-25-3737-5
Coconut shells	9.66	317.01	**0.0305**	50	332.67	2-25-3737-5
Corn cob	10.02	317.01	**0.0316**	50	345.03	2-25-3737-5
Rice husk	9.16	317.01	0.0289	50	315.48	2-25-3737-4
Pine tree	8.89	317.01	0.0280	50	306.12	2-25-3737-4
Beech wood	11.05	317.01	**0.0349**	50	380.72	2-25-3737-5
Chicken manure	9.57	317.01	**0.0302**	50	329.56	2-25-3737-5
Almond shell	8.19	317.01	0.0258	50	282.21	2-25-3737-4

Bowman offers three ranges of exhaust gas heat exchangers: (i) without end covers for direct connection to customer piping, (ii) with straight end covers and (iii) with 90º end covers. The model with straight end covers has been chosen because it is available the right size for this specific application; these units offer installation flexibility for use in a wide range of applications.

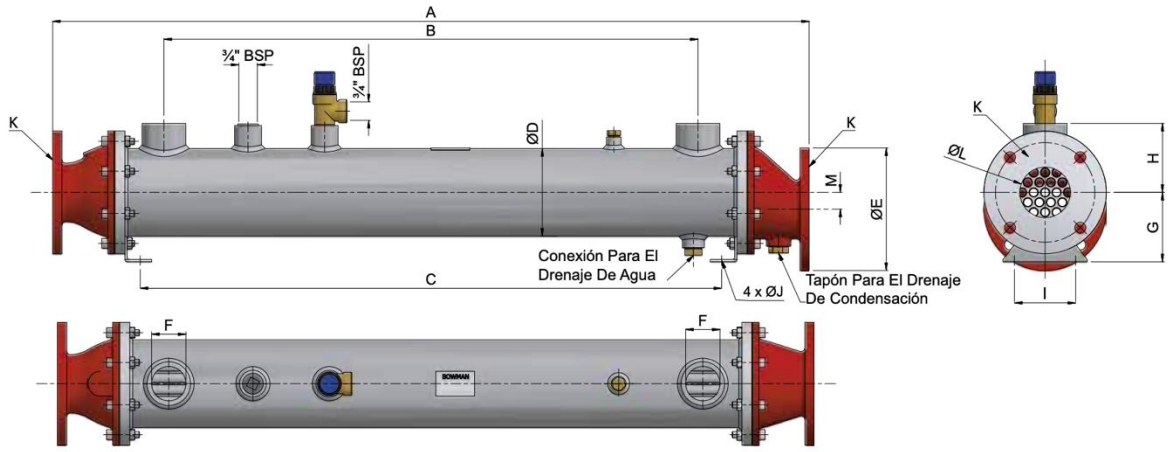

Figure 24: HX with straight end covers BOWMAN [35]

Tipo	A mm	B mm	C mm	D mm	E mm	F BSP	G mm	H mm	I mm	J mm	K	L	M	kg
2-25-3737-4	750	550	588	60.3	100	¾"	65	55	60	9	DN25	34	12	10
2-32-3737-5	928	728	766	60.3	100	¾"	65	55	60	9	DN25	34	12	12
3-32-3738-5	960	718	760	88.9	140	1"	75	75	60	9	DN50	54	16	18
3-40-3738-6	1162	920	962	88.9	140	1"	75	75	60	9	DN50	54	16	20
3-60-3738-8	1670	1428	1470	88.9	140	1"	75	75	60	9	DN50	54	16	27
4-32-3739-5	990	698	760	114.3	160	1 ½"	90	90	80	9	DN65	66	22	25
4-40-3739-6	1192	900	962	114.3	160	1 ½"	90	90	80	9	DN65	66	22	29
4-60-3739-8	1700	1408	1470	114.3	160	1 ½"	90	90	80	9	DN65	66	22	40
5-32-3740-5	1030	688	760	141.3	190	2"	105	105	100	11	DN80	82	26	36
5-40-3740-6	1232	890	962	141.3	190	2"	105	105	100	11	DN80	82	26	39
5-60-3740-8	1740	1398	1470	141.3	190	2"	105	105	100	11	DN80	82	26	51

Figure 25: Characteristics and dimensions of the model of HX with straight end covers BOWMAN [35]

Finally, it has been chosen the fan to move the syngas across the heat exchanger and, according to the calculation it must guarantee a ΔP equal to 1.6 and 1.8 kPa for the two heat exchangers models that have been selected.

At this scope, it has been chosen the fan model PX7000 of the EMC FIME company [37]. It works with a frequency of 50 Hz, has a maximum air/gas flow of 100 m^3/h, works with a maximum pressure jump of 3500 kPa, has a maximum speed of 12,000 rpm and requires a power equal to 70 W.

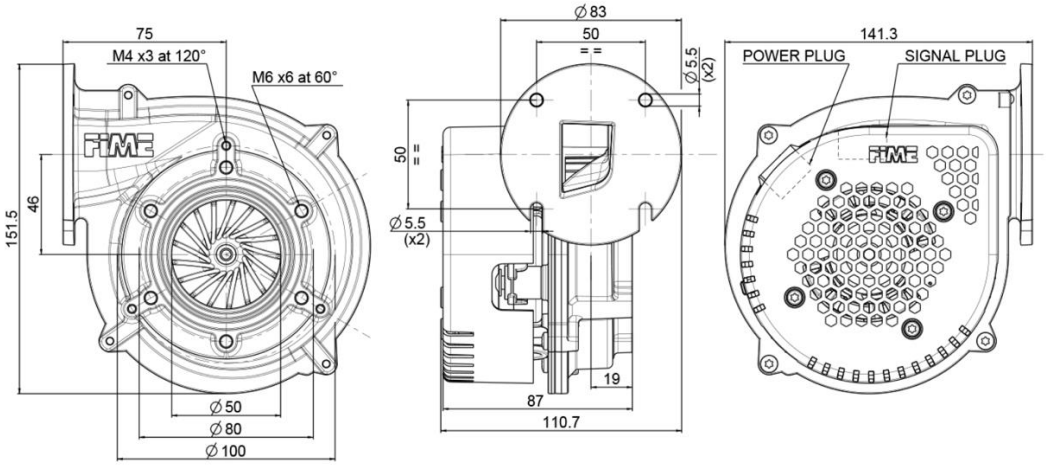

Figure 26: Fan PX7000 of the EMC FIME company [37]

Here below it is also reported the working curve.

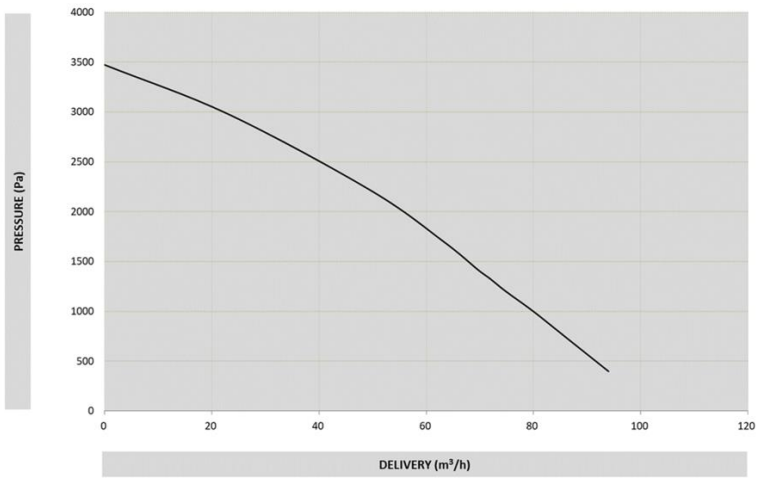

Figure 27: working curve of the fan PXX7000 [37]

Overall, the entire process can be resumed through the following representative scheme.

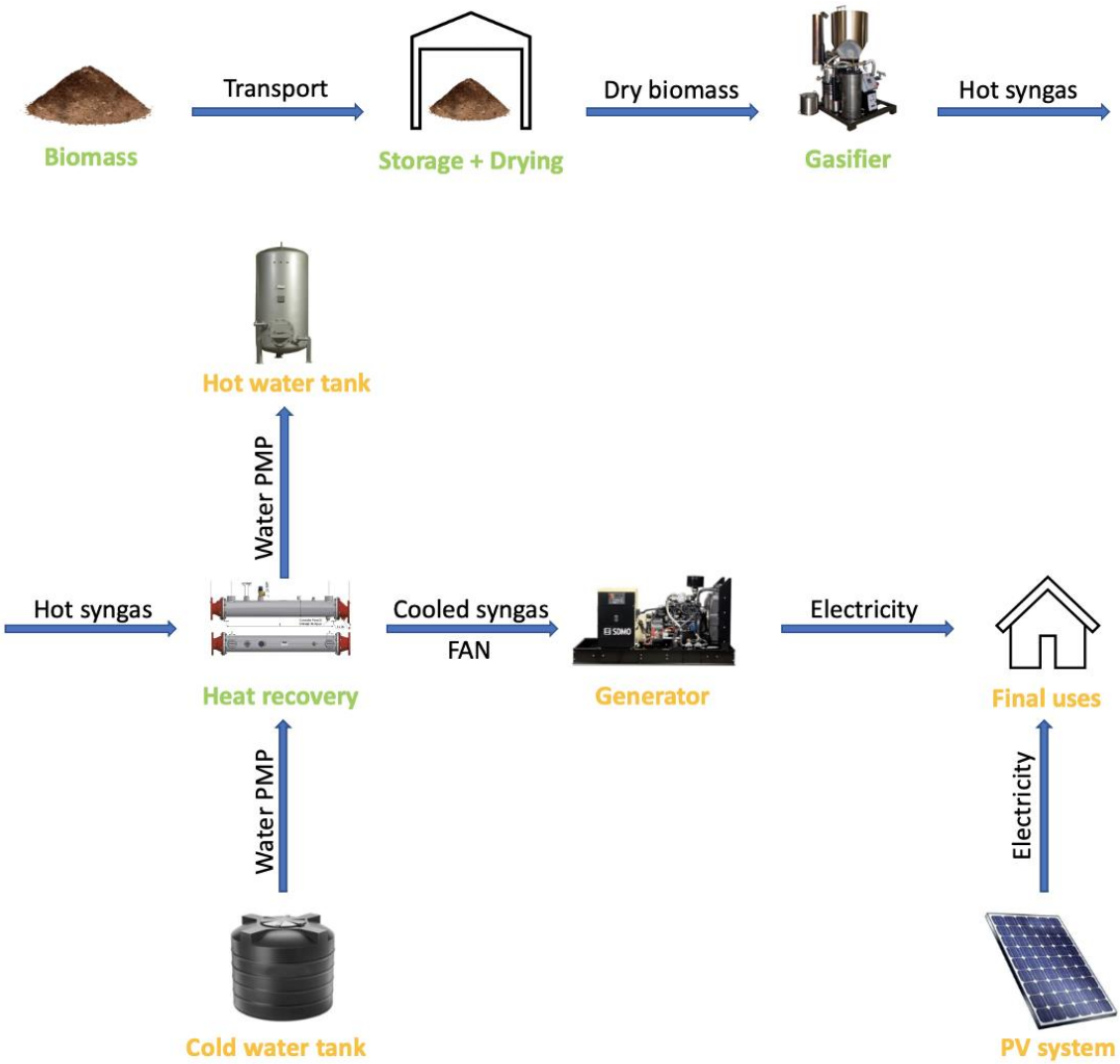

Figure 28: Biomass gasification flow scheme

Finally, it is also reported the electric scheme for the considered project:

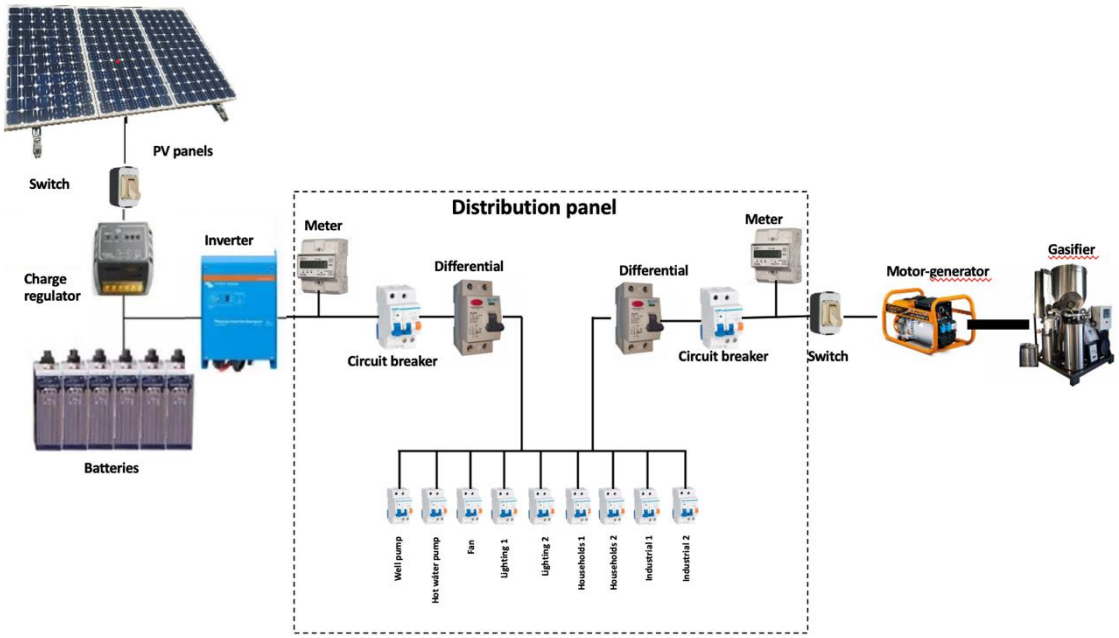

Figure 29: Electric scheme

4 FOCUS ON RURAL COMMUNITY: COMPONENTS, COSTS AND FINAL OUTCOMES

4.1 LOCATION

The energy availability in the rural areas of the world is still a major problem and, mostly in Africa, there is still a lack of electricity. The focus of the project is to supply energy to those rural communities in a sustainable and smart way, using all the potentialities that each place offers. The achievement of this goal can be possible through the employment of different technologies and ways to provide energy. In this direction, a key role is played by renewables that, in most of the cases, produce energy in a very unpredictable and inconstant way, causing problems of lack of energy lack when the primary resources are not available or when the meteorological conditions are not favorable and also issues in balancing the grid. For this reason, the aleatory nature of some renewables, such as PV panels, has to be coupled with the predictable and regulable production from other processes. This is even more critical when the power plant is off-grid and so it doesn't have any possibility to exchange the electricity with the grid.

Then, the purpose of this section is to pick out a place and to propose a solution coupling two technologies: downdraft gasifier and PV panels. The former guarantees a reliable and available production using biomass while the latter allows to exploit the sun irradiation when available reducing the duty of the gasifier and, consequently, the amount of biomass needed. In the specific case, it has been decided to supply energy to a rural population in the neighborhood of Abuja, Niger.

Figure 30: Selected location: Abuja, Niger (source: Google maps)

The reason of this decision is based on the fact that in this place there is a chicken farm, Efugo farms. This ensure the availability of the chicken manure which is a byproduct that can be valorized undergoing downdraft gasification to produce syngas and thus electricity. The community is assumed to be at about 10 km from this farm.

4.2 RURAL POPULATION: LOADS AND NEEDS

As said, in the rural communities the need of energy is still a problem nowadays. The electricity plays a key role in improving the quality of life of those people. In particular, the main needs in such places are:

- Provision of potable water (50 L/(person*day))
- Electricity to charge devices
- Public lights (to ensure more security and to 'enlarge' the day)
- Electricity for other uses (such as appliances in the common area)

This project, in collaboration with the NGO Manos Unidas, has the goal to study the potentialities of a downdraft gasifier of 20 kW coupled with PV panels and how this can comply the needs of the populations in rural areas of the world.

After having explained the priorities of those communities, it is necessary to give an idea, in a simplified but rational way, of the demand curve. The main constraint in assuming the loads is to do not overcome the maximum power that the gasifier can produce, that is 20 kW. It is necessary to underline that this assumed demand is for sure much different from the reality, but it is necessary to have a basis to make the calculations and develop an optimization procedure.
Another assumption is that in each house they live six people.
Finally, a rough estimation brings to a community of 720 people divided in 120 houses. The loads in detail are:

- Water pumping for 720 people (50 L per day each) → 2 kW (36.000 L/d)
  In this case the idea is to have 3 pumps:
  - 1 extraction pump from the water well (50m depth) to the ground well (1.5 kW).
    It can pump 6000 L/h of water and works in a continuous way for 7 hours (from 10 am to 5 pm), then it will pump 42.000 L/d.

- 2 pumps from the ground well to the two tower wells (0.25 kW each). They can pump 4.000 L/h of water and they work for 5 hours (from 10 am to 3 pm), then they will pump 20.000 L/d each.

- Public lighting → 7.2 kW (144 led lights of 50 W each)
  The public illumination will last for 6 hours (from 6 pm to 12 pm).
- Common area appliances → 2.8 kW
  It is assumed that they will work for 8 hours (from 10 am to 6 pm).
- Domestic load → 8.4 kW during day, 12 kW during night
  It is assumed that each house uses 70 W during the day and 100 W during the night (30 W more than day due to illumination).

The loads are reported in the table below and it is assumed that the daily demand curve is the same for each day of the year.

Table 26: Loads and daily demand curve

	Sum	…	09	10	11	12	13	14	15	16	17	18	19	20	21	22	23	00
Public lighting	43.2	0	0	0	0	0	0	0	0	0	0	7.2	7.2	7.2	7.2	7.2	7.2	0
Pumping	13	0	0	2	2	2	2	2	1.5	1.5	0	0	0	0	0	0	0	0
Domestic	135.6	0	0	8.4	8.4	8.4	8.4	8.4	8.4	8.4	8.4	12	12	12	12	12	8.4	0
Appliances	22.4	0	0	2.8	2.8	2.8	2.8	2.8	2.8	2.8	2.8	0	0	0	0	0	0	0
Daily demand	**214.2**	0	0	**13.2**	**13.2**	**13.2**	**13.2**	**13.2**	**12.7**	**12.7**	**11.2**	**19.2**	**19.2**	**19.2**	**19.2**	**19.2**	**15.6**	0

4.3 COMPONENTS

After having described all the needs and the loads, it is necessary to establish which are the components that characterized the specific case and their cost. For each of them it is reported the price of a single unit (after the optimization procedure - minimization of the LCOE - all the quantities will be defined and so it will be possible to establish the overall costs). It has to be specified also that in this project they are considered just the components that concern the energy production and the auxiliary components needed since it is assumed that a grid is already present in the considered community. The components are listed in the table below with their relative costs for a single unit and they are: ground water tank [38], tower water tank [39], tower [40], hot water tank [41], hot water pump [42], extraction pump [43],

secondary pump [44], led light [45], PV panel [46], PV panel structure [47], battery [48], inverter [49], downdraft gasifier [50], generator [51], electrical cabinet [52], bowman HX [53], FAN PX7000 [37], biomass storage [54], well (including the casing and the upper support structure). For this last component the price is given by previous studies of Manos Unidas and it is about 6000 €.

Table 27: Costs of the components

Component	Cost [€/unit]
Water well	6000
Ground water tank (13000 L)	3257.5
Tower water tank (5000 L)	863.56
Tower	10000
Hot water tank (500L)	600
Hot water pump	45
Extraction pump (1.5 kW)	439.32
Sec. Pump (0.25 kW)	60
Led light (50 kW)	41.94
PV panel (0.47kW)	350
PV panel structure (6 PV panels)	130.95
Battery (300 Ah)	750
Inverter (8 kW)	349.97
Downdraft gasifier	40000
Generator	2500
Electrical cabinet	1471.37
Bowmann HX	2138
Fan PX7000	160
Biom. Storage [€/m^3]	22

4.4 PV PANELS CHOICE AND PRODUCTION ESTIMATION

Before proceeding with the optimization procedure, it is important to choose the type of PV panels to be employed and also their relative production throughout the year. The model of PV panels chosen is the X-series. It allows to deliver more power and savings, with fewer panels. In particular, the selected PV panel is the X21-470-COM [55], that has a nominal power of 470 W. It has been chosen because it is a good compromise between cost and efficiency. Here below are reported the specifications of the selected panels.

Electrical Data		
	SPR-X21-470-COM	SPR-X21-460-COM
Nominal Power (Pnom) [7]	470 W	460 W
Power Tolerance	+5/0%	+5/0%
Panel Efficiency	21.7%	21.3%
Rated Voltage (Vmpp)	77.6 V	77.3 V
Rated Current (Impp)	6.06 A	5.95 A
Open-Circuit Voltage (Voc)	91.5 V	90.5 V
Short-Circuit Current (Isc)	6.45 A	6.39 A
Max. System Voltage	1000 V UL & 1000 V IEC	
Maximum Series Fuse	15 A	
Power Temp Coef.	−0.29% / ° C	
Voltage Temp Coef.	−223.2 mV / ° C	
Current Temp Coef.	2.9 mA / ° C	

Operating Condition And Mechanical Data	
Temperature	−40° F to +185° F (−40° C to +85° C)
Impact Resistance	1 inch (25 mm) diameter hail at 52 mph (23 m/s)
Appearance	Class A
Solar Cells	128 Monocrystalline Maxeon Gen III
Tempered Glass	High-transmission tempered anti-reflective
Junction Box	IP-65, 1230 mm cables / MC4 Compatible
Weight	56 lbs (25.4 kg)
Max. Load	Wind: 50 psf, 2400 Pa, 244 kg/m² front & back Snow: 112 psf, 5400 Pa, 550 kg/m² front
Frame	Class 2 silver anodized; stacking pins

Tests And Certifications	
Standard Tests [8]	UL1703 (Type 2 Fire Rating), IEC 61215, IEC 61730
Quality Management Certs	ISO 9001:2015, ISO 14001:2015
EHS Compliance	RoHS, OHSAS 18001:2007, lead free, Recycle Scheme, REACH SVHC-163
Sustainability	Cradle to Cradle Certified™ Silver. "Declare." listed.
Ammonia Test	IEC 62716
Desert Test	10.1109/PVSC.2013.6744437
Salt Spray Test	IEC 61701 (maximum severity)
PID Test	1000 V: IEC 62804, PVEL 600 hr duration
Available Listings	UL, TUV, MCS, FSEC, CEC

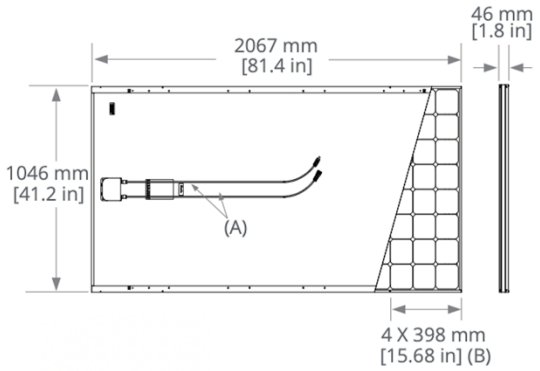

Figure 31: PV panel specifications [55]

After having chosen the type of PV panels, it has to be estimated the production. At this scope it has been used the PVGIS tool [56]. PVGIS (Photovoltaic Geographical Information System) provides information about solar radiation and photovoltaic (PV) system performance for any location in Europe and Africa, as well as a large part of Asia and America.

First, through this tool, it has been seen the optimal position for the PV panels to maximize the production. It has been obtained an optimal slope of 15° and an optimal azimuth of 7°. After that, it has been considered an off-grid system with those values and with an initial peak power installed of 20 kW. Then, selecting the place of interest (Abuja), they have been obtained the daily data of irradiation for each month (considering a typical day for each month). The values have been collected and are reported in a table.

Then those data have been rearranged in a non-dimensional way to get the basis of irradiation distribution in each hour of the day.

After that, they have been collected the data of the overall average energy that can be produced each day by 20 kW peak power installed PV panels system for each month (with slope 15° and azimuth 7°).

Table 28: Tot. Avg. Available energy that can be produced by PV panels [Wh/day] with slope 15° and azimuth 7°

[Wh/day]	Tot. Avg. Available energy that can be produced by PV panels [Wh/day]
January	94817.5
February	93560.9
March	88396.0
April	80672.2
May	69995.9
June	62656.2
July	57016.1
August	54803.7
September	67344.6
October	80846.6
November	94844.1
December	95827.3

Then, by multiplying those values hour by hour for the non-dimensional irradiance, it is possible to obtain the production profile for each month (typical day) of the year for a 20 kW peak power installed PV panels system.

Table 29: Tot. Avg. Available energy that can be produced by PV panels system of 20 kW [Wh/h] hour per hour

[Wh/h]	Sum	…	7	8	9	10	11	12	13	14	15	16	17	18	19	20	…
January	94818	0	0	367	3443	6914	9744	12249	13215	13555	12249	10520	7567	4273	721	0	0
February	93561	0	0	281	3129	6431	9426	11765	13236	13276	12474	10415	7647	4385	1096	0	0
March	88396	0	0	543	3123	6150	9042	11241	12721	12545	11784	9680	6924	3761	882	0	0
April	80672	0	0	946	3284	5878	8365	10202	11378	11391	10567	8689	6067	3216	689	0	0
May	69996	0	0	1049	2973	5247	7197	8744	9727	9821	9040	7493	5354	2731	619	0	0
June	62656	0	0	931	2712	4601	6314	7596	8554	8608	8055	6759	4978	2766	783	0	0
July	57016	0	0	766	2270	3976	5413	6595	7696	7804	7468	6474	4876	2780	900	0	0
August	54804	0	0	719	2200	3957	5341	6309	7098	7388	7278	6268	4690	2712	844	0	0
September	67345	0	0	1010	3098	5325	6985	8589	9295	9308	8658	7095	5021	2531	429	0	0
October	80847	0	0	1367	3989	6765	9039	10894	11563	11159	10406	8272	5147	2218	28	0	0
November	94844	0	0	1505	4774	8030	10766	12627	13489	13119	11806	9426	6375	2928	0	0	0
December	95827	0	0	938	4311	7643	10472	12539	13532	13423	12186	10051	7099	3604	27	0	0

Finally, this last table reported above allows to estimate the production for all the months of the year for a 20 kW peak power installed PV panels system. Then, to obtain the production profile for other peak powers installed, it is just necessary to scale them.

4.5 OPTIMIZATION PROCEDURE

4.5.1 Description

At this point, it is necessary to choose an optimization procedure that allows to find the best combination of all the components to produce the electricity in the most economical effective way. The criterion followed for this purpose is the minimization of the LCOE. Before proceeding, they have to be precisely defined all the principles through which the number of each component is chose to find an optimum. The LCOE minimization has been performed using MATLAB.

In the scheme below it is reported an illustration scheme that summarize the optimization procedure in a short and clear way.

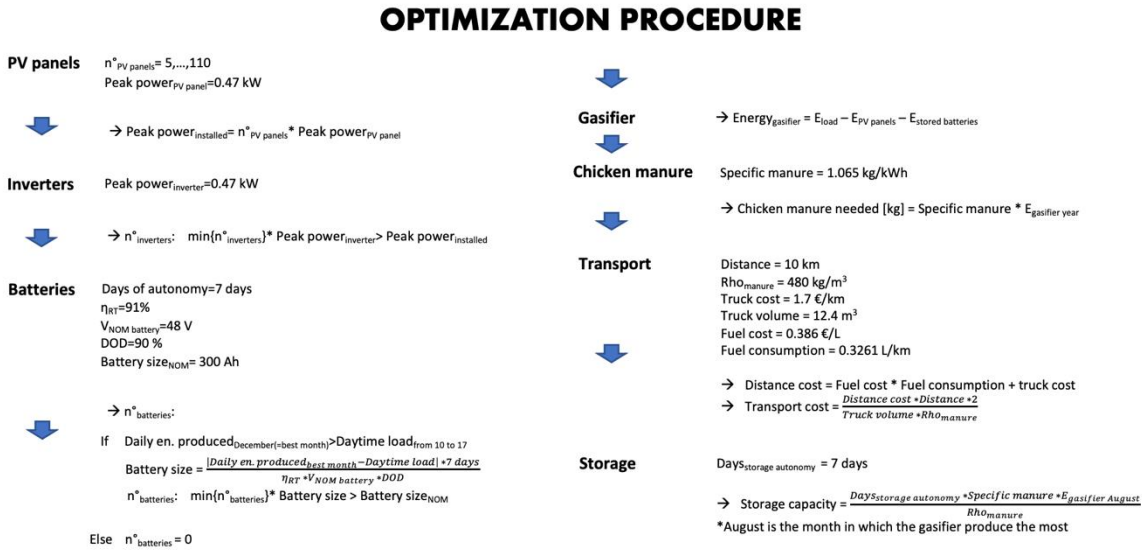

Figure 32: Optimization procedure scheme

The procedure above has been made for each peak power (from 5 to 110 PV panels installed).

4.5.2 Costs

For each of the proposed peak powers, they have to be evaluated the costs to calculate the LCOE for each of them. The list of costs is reported in the table below. For each item, there are both the investment cost (CAPEX) and the operation & maintenance cost (OPEX).

Table 30: Items costs for LCOE minimization

CHICKEN MANURE	CAPEX	-	-	
	OPEX	10*	€/ton	[57]
TRANSPORT	CAPEX	-	-	
	OPEX	0.386	€/L	gasoline cost [58]
		0.326	L/km	fuel consumption [59]
		1.7	€/km	truck cost [59]
		12.4	m3	truck volume
STORAGE	CAPEX	22	€/m3	[54]
	OPEX	4%*totCAPEX	€/year	
GASIFIER	CAPEX	40000	€	[50]
	OPEX	0.063	€/kWh	[60]
GENERATOR	CAPEX	2500	€	[51]
	OPEX	0	€/year	
HEAT EXCHANGER	CAPEX	2138	€	[53]
	OPEX	200	€/year	
FAN	CAPEX	160	€	[37]
	OPEX	0	€/year	
ELECTRICAL CABINET	CAPEX	1471.37	€	[52]
	OPEX	0	€/year	
PV PANELS	CAPEX	350	€/panel	[46]
+ STRUCTURE	OPEX	10	€/(panel*year)	[61]
INVERTERS	CAPEX	349.97	€/inverter	(peak power = 8000 kW) [62]
	OPEX	included in PV OPEX		
BATTERIES	CAPEX	750 (*2.5)	€/battery	*2.5 (because they last 10 yrs) [63]
	OPEX	-	-	

Then, having all the costs, it is possible to compute the LCOE as follows:

$$LCOE\left[\frac{€}{kWh}\right] = \frac{CAPEX * CRF + OPEX}{AEP}$$

(4. 1)

With $CRF = \frac{i*(1+i)^n}{(1+i)^n-1}$

(4. 2)

Where i is the interest rate and it is equal to 0.054 [64] and n is the lifetime (25 years).

4.5.3 Results

After having developed the MATLAB code, it is possible to perform the optimization and to obtain the final results. As said, the optimization consists of founding the minimum LCOE. The chart below shows the LCOE trend as function of the number of PV panels installed. The PV panels installed are the driver to size all the other components because all the other items will be selected as a consequence of the peak solar power installed.

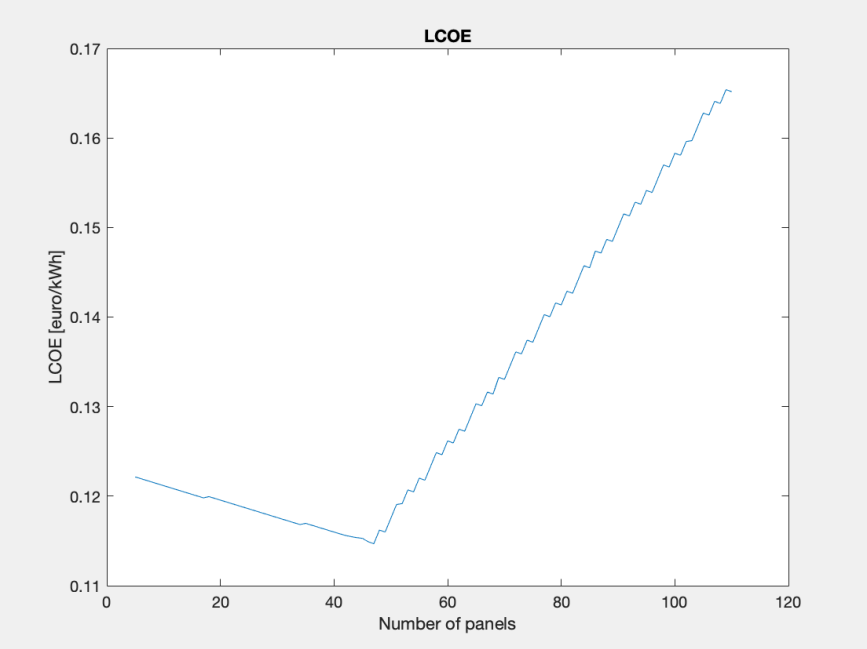

Figure 33: LCOE vs PV panels installed chart (with batteries)

It can be seen that the LCOE decreases until a certain point and then it increases with an higher slope. The first part shows a decreasing trend due to the fact that, increasing the number of PV panels, the transport duty is less and less. Since there is a decreasing trend, it means that the impact of the cost of PV panels is less than the chicken manure and transport cost in this first part. The slope of this first decreasing part would increase increasing the distance or the fuel cost.

Then it is reached a minimum (47 PV panels, 0.1147 €/kWh) that is the optimal solution. It is the best combination of each item to reach the minimum LCOE. After that point, the LCOE shows a positive slope since the costs of the PV panels system (PV panels, inverters, batteries) starts to impact more than the biomass costs for gasification (biomass itself and transport). The slope of this second part strictly depends on the transport and biomass costs, the higher they are and the less steep is the slope. Also, it is possible to see that the shape of the LCOE is not smooth but it presents steps and jumps. They are due to the fact that there are components, such as inverters and batteries, whose units increase in a discrete way depending on the PV panels production and so it reflects on the cost that in certain points suddenly jumps.

It is also interesting to see if the batteries could impact in an important way on the cost and if they can have a negative impact on the LCOE minimization. It could be that it is convenient to put, for example, more PV panels without any battery because the battery cost would impact more than the transport and biomass cots. For this reason it has been made a simulation without the batteries to see how the result changes. The chart shows the LCOE trend without batteries.

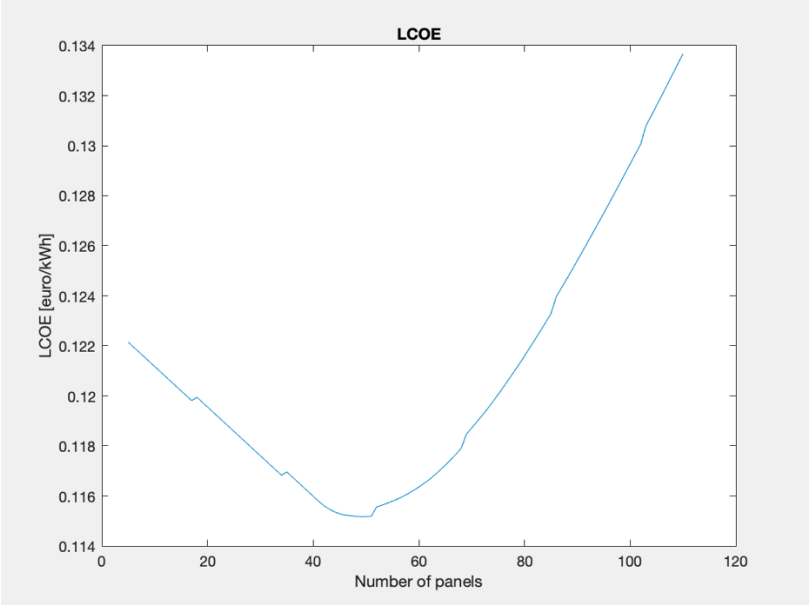

Figure 34: LCOE vs PV panels installed chart (without batteries)

It is possible to notice that the first part remains the same since there the batteries are still not used and so the trend is roughly linear. What changes is the second part where the trend

is much smoother (from this chart it is possible to see that the aforementioned steps were mainly due to the batteries rather than to inverters). This configuration leads to a close solution to the previous one (49 PV panels, 0.1152 €/kWh) with a slightly higher number of PV panels but also a slightly higher value of LCOE.

Afterall the configuration with batteries is chosen because it brings to a lower LCOE (even if it could be reasonable to do not put batteries for simplicity reasons since the LCOE difference is very small).

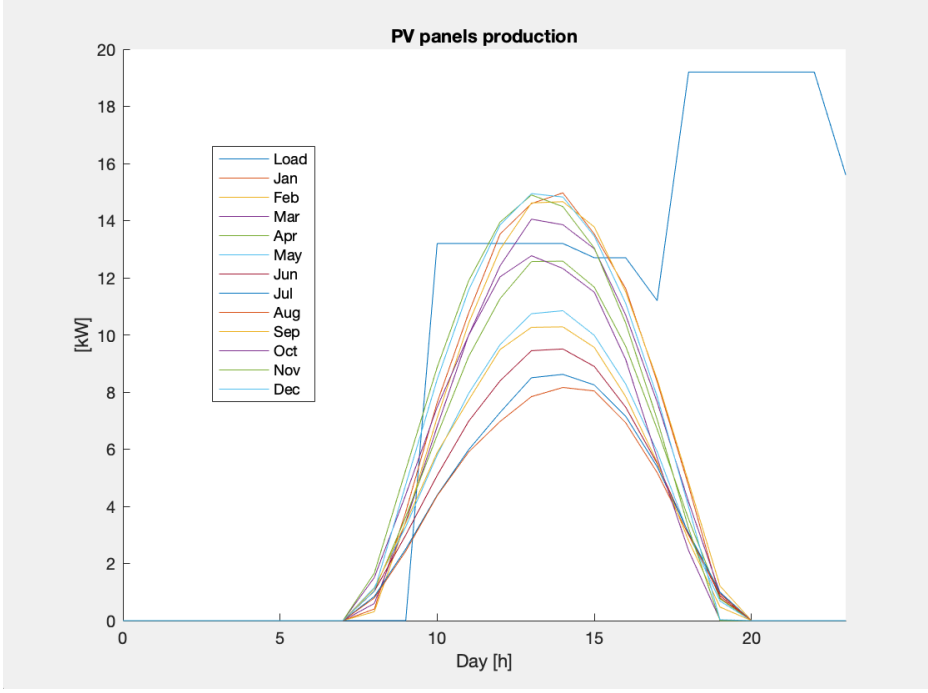

Figure 35: PV panels production and load vs hours

In the chart below they are reported both the load and the production curve of the PV panels for each month of the year (one 'average' day for each of them).
It is possible to see that the PV panels production matches pretty well the load curve during the daytime hours. At the same time the PV panels are not able to match the peak demand of the nighttime hours and then it will be required the gasifier supply. Furthermore, it is possible to see that the maximum production is achieved in December (best month) while the worst one is August. For this reason, in the months with higher production it is possible to accumulate energy through batteries and to use that in other moments.

In the chart below they are instead showed both the gasification curve and the load for each month of the year (one 'average' day for each of them).

The gasifier production curve shows a production that, as expected, is about complementary to the one of photovoltaic panels. The production is lower during the daytime, it reaches a minimum in correspondence of the maximum PV panel production and then increases more and more in the nighttime hours, covering entirely the load in the last hours of each day. It is possible to notice that in the central hours of the day, for the best months (when the PV panels production is higher), the gasifier production is null.

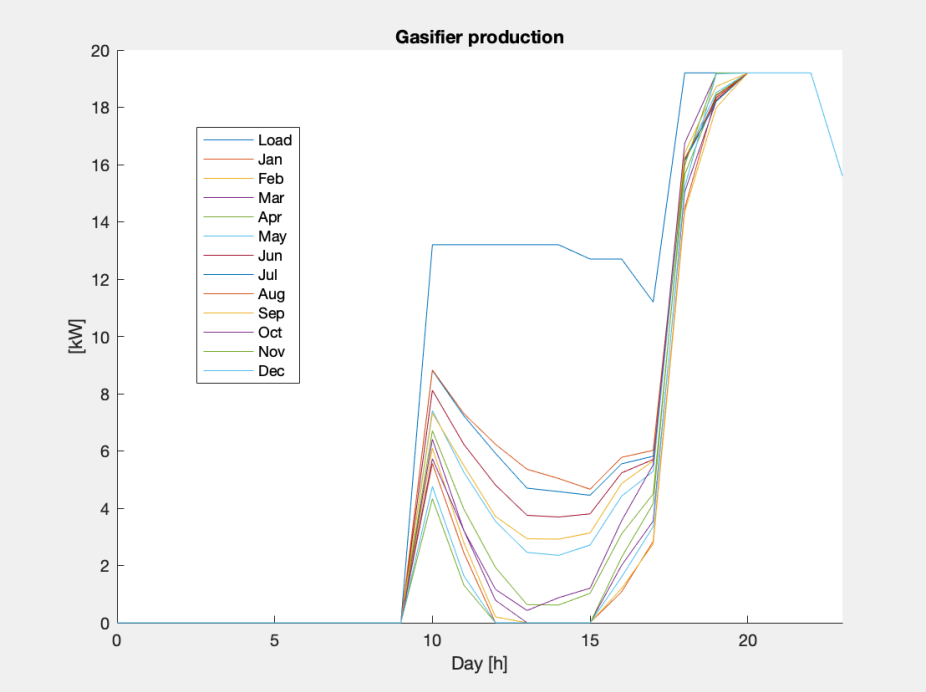

Figure 36: Downdraft gasifier production and load vs hours

Finally, it is interesting to see the share of production through PV panels and gasifier. The former produces 31564 kWh/year while the latter produces 46619 kWh/year. In the following chart it is reported the share of electricity production of both.

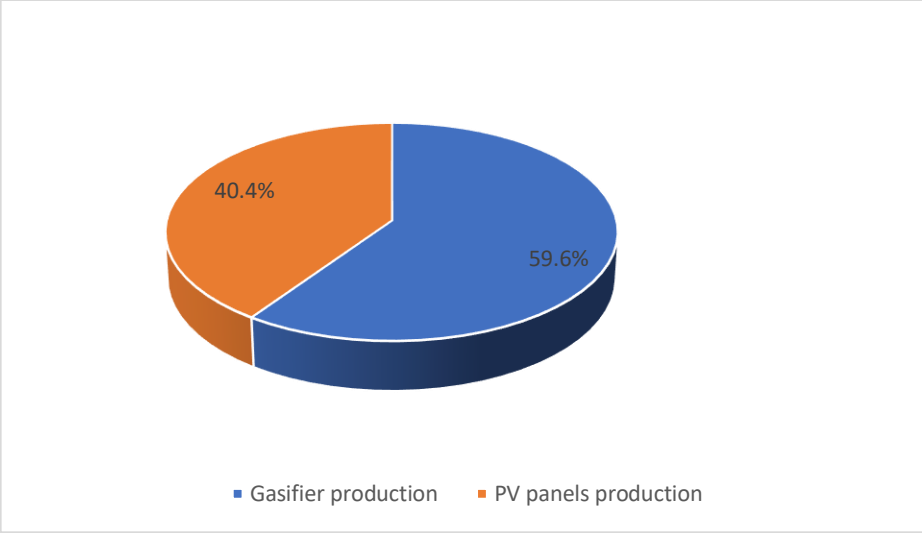

Figure 37: Share of yearly electricity production

4.6 FINAL CONFIGURATION

Overall, the final configuration consists of:

- 47 PV panels of 470 W peak each (22.09 kW_p)
- 1 Battery of 48 V and 300 Ah
- 3 inverters of 8 kW peak each
- 1 downdraft gasifier
- 1 generator
- 1 FAN
- 1 gas-water Heat Exchanger
- 1 electrical cabinet
- 49.65 tons of chicken manure needed each year
- 1.98 m^3 of biomass storage (1-week autonomy)

This optimal configuration leads to a LCOE equal to **0.1147 €/kWh**.

4.6.1 Overall costs

At this point it is very interesting to evaluate, for the optimal configuration, which is the impact of each cost on the LCOE both in terms of CAPEX and OPEX and also to evaluate which is the overall investment cost that the NGO Manos Unidas should afford to give all the services described in the section 5.2.

In the image below they are reported all the CAPEX for the optimal configuration.

Item	CAPEX
Battery	1875
FAN	160
Gasifier	40000
Generator	2500
Heat exchanger	2138
Chicken manure	0
Electrical cabinet	1471.37
Inverter	1049.9
PV panels	16450
Storage	43.64
Transport	0
Total	**65687,91**

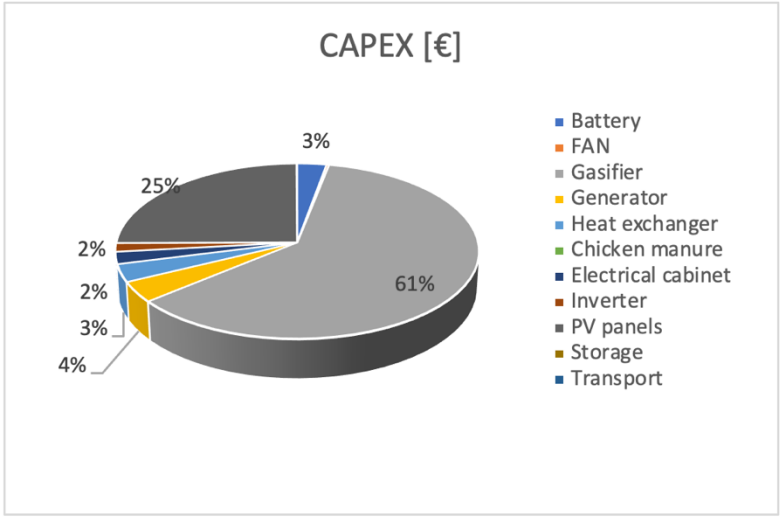

Figure 38: CAPEX in the optimal configuration

It can be noticed that the downdraft gasifier investment cost prevails over the other. Nevertheless, a not negligible contribution is also given by the PV panels investment cost. In the image below they are also reported all the OPEX for the optimal configuration.

Item	OPEX
Battery	0
FAN	0
Gasifier	2937
Generator	0
Heat exchanger	200
Chicken manure	496.52
Inverter	0
Electrical cabinet	0
PV panels	470
Storage	1.75
Transport	304.63
Total	**4409.9**

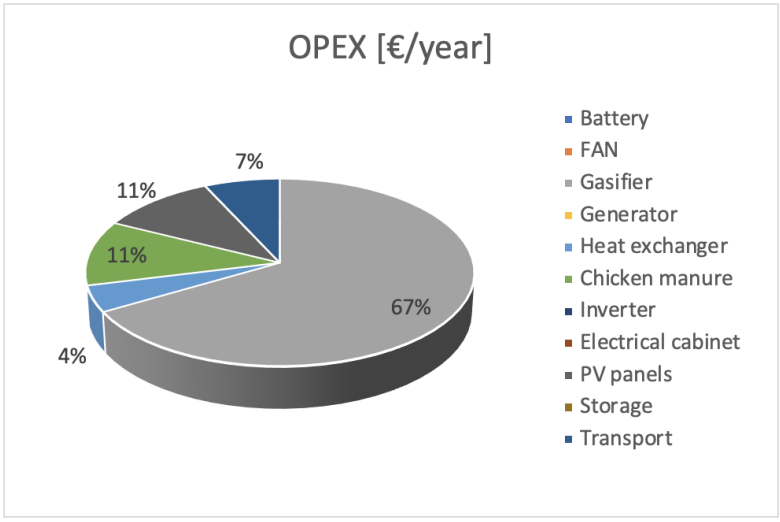

Figure 39: OPEX in the optimal configuration

For the OPEX also the major contribution is given by the gasifier. Lower contributions are also given by the chicken manure purchasing, the PV panels operation and management cost, the biomass transport cost and finally the heat exchanger operation and maintenance cost.

Finally, in the table and in the chart below it is reported the overall investment cost that should be afforded to satisfy all the needs of the selected rural community.

Table 31: Overall investment costs in the optimal configuration

Type	Cost [€/unit]	Q.tity	Total cost
Water well	6000	1	6000
Ground water tank (13000 L)	3257.5	2	6515
Tower water tank (5000 L)	863.56	4	3454.24
Tower	10000	2	20000
Hot water tank (500L)	600	2	1200
Hot water pump	45	1	45
Extraction pump (1.5 kW)	439.32	1	439.32
Sec. Pump (0.25 kW)	60	2	120
Led light (50 kW)	41.94	144	6039.36
PV panel (0.47kW)	350	47	16450

PV panel structure	130.95	8	1047.6
Electrical cabinet	1471.37	1	1471.37
Battery (300 Ah)	750	2.5	1875
Inverter (8 kW)	349.97	3	1049.91
Downdraft gasifier	40000	1	40000
Generator	2500	1	2500
Bowmann HX	2138	1	2138
Fan PX7000	160	1	160
Biom. Storage	43.65	1	43.65
		Total	**110548.45**

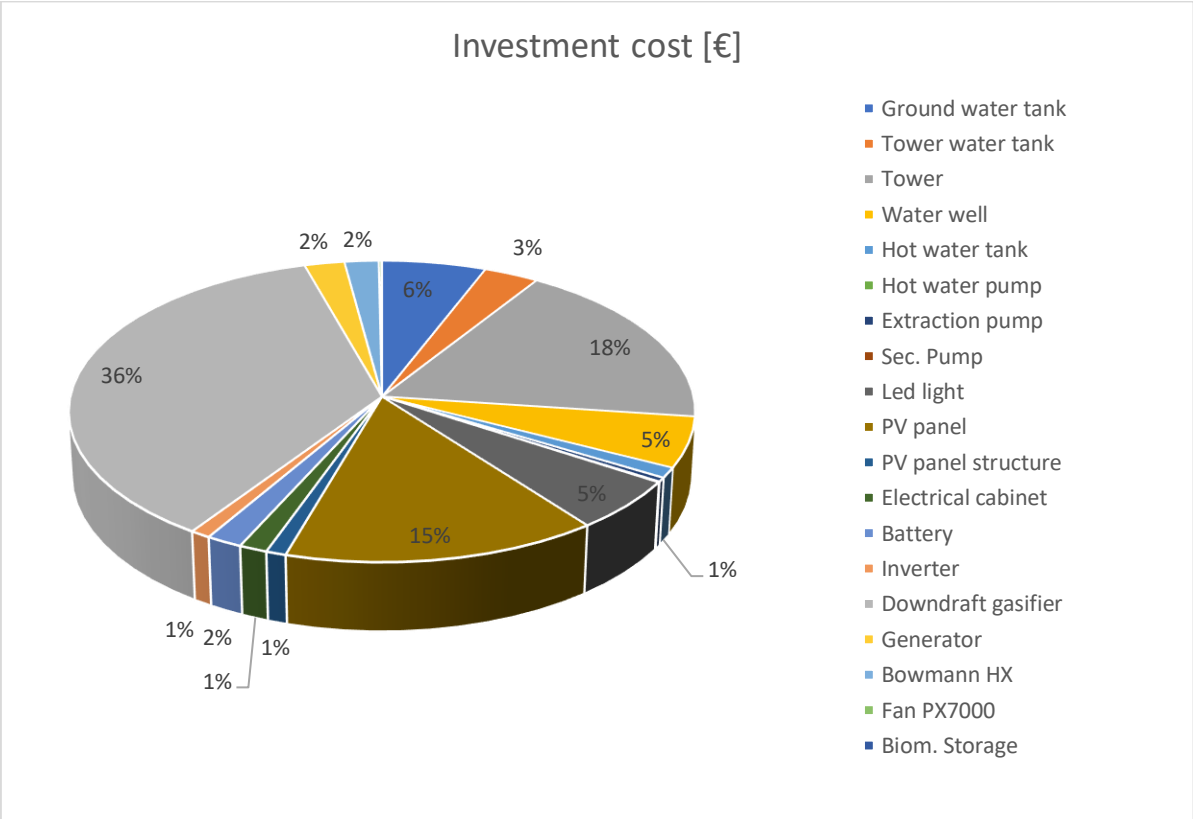

Figure 40: Overall investment costs in the optimal configuration

The major investment cost is, also in this case, due to the downdraft gasifier but significant contributions are also given by the tower construction, the PV panels investment followed by tanks and led lights investment.

Finally, the overall investment cost that Manos Unidas should afford to match all the described need of the proposed rural community is equal to **110548.45 €**. This configuration with all the described items would allow to 720 people to live in much better condition and this project aims at giving an idea of the huge potentialities that gasification, coupled with

other renewable sources, could offer to the countries and communities that are nowadays living in not acceptable conditions.

4.6.2 Actual cost of electricity and water for the community

At this point it is very interesting to see which is the specific cost of both electricity and water supply considering that the investment costs are afforded by the NGO Manos Unidas. Consequently, the community will pay just the variable costs. The price of the electricity for the rural community is calculated considering the costs reported in the following table.

Table 32: OPEX for electricity cost of the rural community

CHICKEN MANURE	CAPEX	-	-	
	OPEX	10*	€/ton	[57]
TRANSPORT	CAPEX	-	-	
	OPEX	0.386	€/L	gasoline cost [58]
		0.326	L/km	fuel consumption [59]
		1.7	€/km	truck cost [59]
		12.4	m3	truck volume
STORAGE	CAPEX	-	-	[54]
	OPEX	4%*totCAPEX	€/year	
GASIFIER	CAPEX	-	-	[50]
	OPEX	0.063	€/kWh	[60]
GENERATOR	CAPEX	-	-	[51]
	OPEX	0	€/year	
HEAT EXCHANGER	CAPEX	-	-	[53]
	OPEX	200	€/year	
FAN	CAPEX	-	-	
	OPEX	0	€/year	
ELECTRICAL CABINET	CAPEX	-	-	
	OPEX	0	€/year	
PV PANELS	CAPEX	-	-	
+ STRUCTURE	OPEX	10	€/(panel*year)	[61]
INVERTERS	CAPEX	-	-	(peak power = 8000 kW) [62]
	OPEX	included in PV OPEX		
BATTERIES	CAPEX	-	-	
	OPEX	0	0	

Then, with the optimal solution, it is obtained a cost of electricity equal to **0.0564 €/kWh.** It is the price of the electricity that the people of the selected community should afford to get the electricity (neglecting the costs for balancing the grid).

Furthermore, it is also possible to calculate the cost to get the water assuming that all the investment cost is covered by the ONG Manos Unidas. Then, assuming that the water as a resource itself is free, the price of water is just given by the pumping duty and all the calculations are reported in the following table.

Table 33: Water consumption and costs for rural community

Consumption	Well pump	10.5	kWh/day
	Secondary pump	5	kWh/day
	Tot. Pump	15.5	kWh/day
Electricity cost	Specific cost	0.0564	€/kWh
Water cost	Daily water cost	0.8742	€/day
Water consumption	Daily water needed	36000	L
Specific water cost	Daily water cost	**0.024283333**	€/1000 L
Water consumption	Yearly water needed	13140000	L
Yearly water cost	Overall water cost	**319.083**	€/year
	Family water cost	**2.659025**	€/year*family
	Person water cost	**0.443170833**	€/year*person

The important costs are underlined in bold in the table above.

4.6.3 Planimetry

Finally, the planimetry of the rural community can be represented and it is composed by:

- 120 houses (6x4 m) with 6 people each
- 80 public bathrooms (1.2x3 m)
- 144 public lights
- 47 PV panels (12.4x8.37 m)
- 1 downdraft gasifier
- 1 canopy (5x4 m) for biomass storage and other electrical components (inverters, batteries, etc.)
- 2 towers for water tanks (6x2 m)
- 2 water tanks of 13000 L
- 4 water tanks of 5000 L

The overall scheme has been realized through the software AUTOCAD and it is reported below.

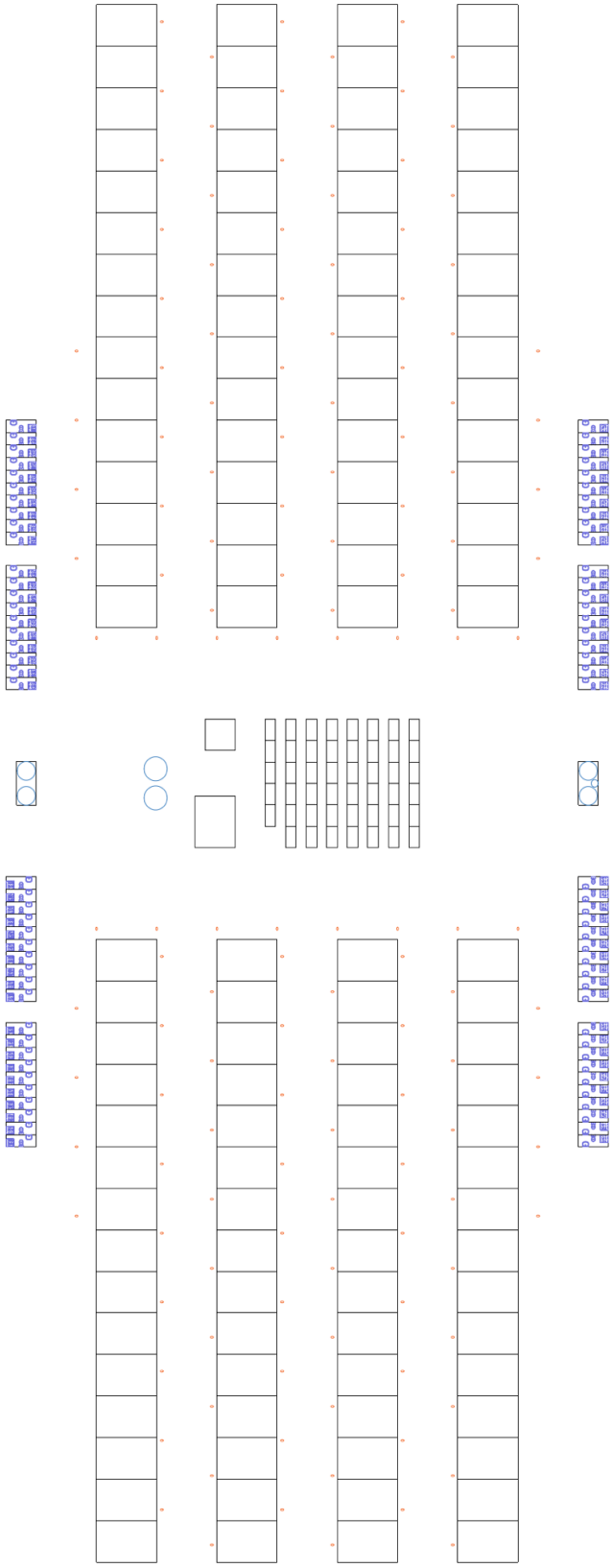

Figure 41: Planimetry of the rural community (Realized with AUTOCAD)

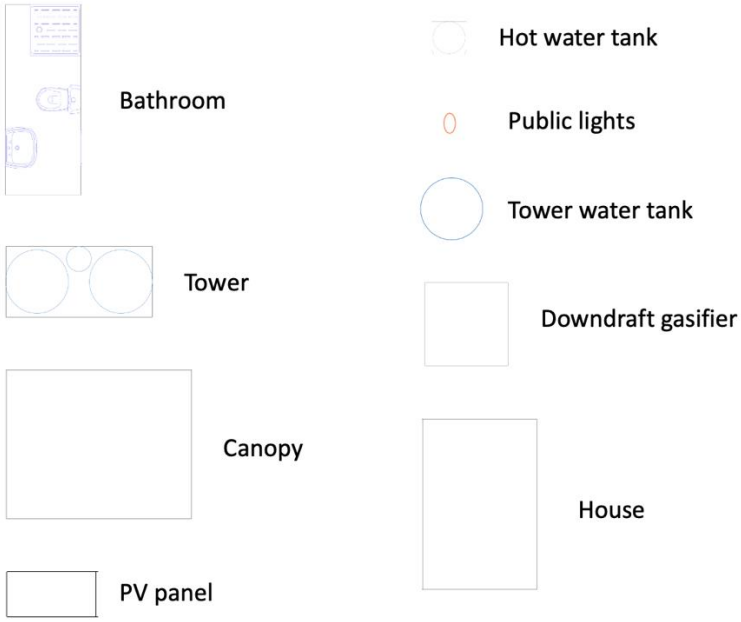

Figure 42: Planimetry legend

4.7 ELECTRICITY COST COMPARISON BETWEEN BIOMASS GASIFICATION, NATURAL GAS AND DIESEL GENERATORS

At this point that all the costs have been defined, it is very interesting to make a comparison of the cost to produce electricity between biomass gasification (syngas as fuel), natural gas and diesel generators. This allows to understand if biomass gasification is also an economical advantageous solution as well as environmentally friendly. For this reason, for the specific location, they have been searched the specific prices of each fuel and they have been selected typical generators to produce energy through them so that it is possible to evaluate the specific cost to produce a kWh of electricity. In a schematic way, they are reported all the costs and the specific consumption of each of the three solutions.

- DIESEL GENERATOR

  First, it has been considered a diesel cost equal to 1.536 €/L [65] and the diesel generator RD020 of the GENERAC company that requires 7.46 L/h [66] to produce 20 kW of electricity. The specific diesel consumption of the generator is reported in the following table.

ENGINE FUEL CONSUMPTION

		gal / hr	L / hr
RD015	25% of rated load	0.60	2.27
	50% of rated load	0.85	3.22
	75% of rated load	1.10	4.16
	100% of rated load	1.46	5.53
RD020	25% of rated load	0.77	2.9
	50% of rated load	1.03	3.90
	75% of rated load	1.46	5.53
	100% of rated load	1.97	7.46
RD030	25% of rated load	0.97	3.67
	50% of rated load	1.37	5.19
	75% of rated load	1.97	7.46
	100% of rated load	2.77	10.49
RD048 RD050	25% of rated load	1.23	4.66
	50% of rated load	2.02	7.66
	75% of rated load	3.02	11.43
	100% of rated load	4.02	15.22

Figure 43: GENERAC diesel generator specific fuel consumption

Finally, the cost to produce 20 kWh is 11.46 €, that can also be expressed as **0.573 €/kWh.** Then, considering a typical generator cost of 2500 € [51] and zero maintenance costs, a lifetime of 25 years, an interest rate equal to 0.054 [64], and 8000 equivalent hours, it is possible to calculate the LCOE as follows:

$$LCOE\left[\frac{€}{kWh}\right] = 0.573 + \frac{CAPEX * CRF}{AEP} \qquad (4.1)$$

Finally, it is obtained an LCOE equal to **0.574 €/kWh.**

- NATURAL GAS GENERATOR

In this case it has been considered a specific natural gas cost equal to 8 €/MMBtu [67] (= 0,2824 €/m^3) and the NG generator selected is the model GZ25 generator, equipped with a KOHLER GMC430-27 engine [68] whose specific natural gas consumption top produce at a full load of 20 kW is equal to 8.20 Nm^3/h. The specific NG consumption of the generator is reported in the following table.

FUEL	
Gaznat Consumption @ 110% load (m3/h)	8.80
Gaznat Consumption @ 100% load (m3/h)	8.20
Gaznat Consumption @ 75% load (m3/h)	6
Gaznat Consumption @ 50% load (m3/h)	4.30

Figure 44: GZ25 natural gas generator specific fuel consumption

Finally, the cost to produce 20 kWh is 2.32 €, that can also be expressed as **0.1158 €/kWh.**

Then, considering a typical generator cost of 2500 € [51] and zero maintenance costs, a lifetime of 25 years, an interest rate equal to 0.054 [64], and 8000 equivalent hours, it is possible to calculate the LCOE as follows:

$$LCOE\left[\frac{€}{kWh}\right] = 0.0535 + \frac{CAPEX * CRF}{AEP} \quad (4.2)$$

Finally, it is obtained an LCOE equal to **0.117 €/kWh.**

- SYNGAS GENERATOR

Finally, considering the chicken manure as a residual biomass to be gasified, it is assumed a price equal to 10 €/ton [57] and also it has been calculated that to produce 20 kWh of power they are needed 21.3 kg of biomass (Table 24).

Then the price to produce 20 kWh of electricity is 0.213 €, that can also be expressed as **0.01065 €/kWh.**

Then, considering a typical generator cost of 2500 € [51], a downdraft gasifier cost of 40000 € [50] and has OPEX equal to 0.063 €/kWh [60], a lifetime of 25 years, an interest rate equal to 0.054 [64], and 8000 equivalent hours, it is possible to calculate the LCOE as follows:

$$LCOE\left[\frac{€}{kWh}\right] = 0.01065 + \frac{CAPEX * CRF + OPEX}{AEP} \quad (4.3)$$

Finally, it is obtained an LCOE equal to **0.1039 €/kWh.**

Overall, it is possible to notice how not only the biomass gasification is a green solution that exploits residual biomasses and wastes and leads to very small amount of emissions but also is an economical and valuable solution that allows to generate electricity at lower prices than the diesel generators and natural gas ones. On the other hand, it would allow to give independency from fossil fuel supply whose availability and price is variable.

5 CONCLUSIONS

As said in the first part of the present project, even in a very technologically and scientifically evolute world, there is still a very unfair and undistributed wellness in the globe. The problem, in most of the cases, is not the unavailability of resources but rather the wrong management of them. Then, the need of finding smart solution to match the exigencies of the less lucky populations arises in a strong way. The chasing of alternative ways to provide water and electricity is becoming persistent and insistent in the last years. Indeed, it is true that the technological evolution is going faster and faster in the last years, but at the same moment it leads to a demographic growth that has never been registered in the entire life of the earth. So, there is a situation where the alternatives to provide goods are a lot but, at the same time, the demand is very high. Then it is inadmissible to waste the resources that the mankind has available. Along with the problem of scarce distribution of the goods, wellbeing and management of the resources, there is also the trouble of pollution. Indeed, differently from the past where the need of energy was accomplished using fossil fuel-based processes, today it is necessary to totally deviate the trend, using clean and environmentally friendly technologies both in the factories and in the energy farms. Never as nowadays, the world had the need of producing so much energy and never the problem of emissions was as serious as today. The world is going more and more in a direction of self-destruction because of the unresponsible behavior of the human beings that are exploiting in a wrong way the resources that the earth offers. The average global temperature has risen by 0.98 degrees Celsius since pre-industrial levels, and the trend since 2000 implies that, in the absence of intervention, it might reach +1.5 degrees Celsius between 2030 and 2050. The effects of global warming are already visible: Arctic sea ice has reduced by an average of 12.85% every decade, while coastal tide records reveal a 3.3 millimeter increase in sea level per year since 1870. The decade 2009-2019 was the warmest on record, while 2020 was the second hottest year on record, falling just short of the record established in 2016. Extreme weather phenomena, such as cyclones and floods, have grown every year from 1990 to now, impacting even unexpected times of the year compared to the past and are increasingly catastrophic. El Nio has become more irregular, causing catastrophic droughts in places already plagued by chronic dryness, such as East Africa, while the Gulf Stream is slowing and may reverse direction. Plant and animal species travel inexorably from one environment to the next, causing irreparable harm to biodiversity across the planet.

It is necessary to strongly deviate the attitude and the directives to find sustainable ways to accomplish the needs of the mankind. In this direction Europe is leading virtuous projects and initiatives.

The present project goes in direction of the energy transition discussed at length nowadays. Indeed, it aims to identify cost-effective and sustainable solutions to supply electricity and water to developing countries, in particular using a hybrid system consisting of a 20 kW downdraft gasifier and photovoltaics. The completed project will be used by the NGO Manos Unidas as a mean to estimate the costs, performance and potential of this system and will help investigate the advantages that gasification can provide in economic, environmental and exploitation terms of the residual biomass present on site. This is a pilot project that proves that downdraft gasification is not only a simple and green solution but also is very advantageous under a practical and economical point of view and it can be used and applied to every place in the world, with the proper biomass and facilities mix.

BIBLIOGRAPHY

[1] "https://support.microsoft.com/en-us/word," [Online].

[2] [Online]. Available: https://www.worldometers.info/world-population/#.

[3] [Online]. Available: https://unric.org/it/agenda-2030/#:~:text=L'Agenda%202030%20per%20lo,193%20Paesi%20membri%20dell'ONU..

[4] "IEA, data and projection: Access to electricity," [Online].

[5] "IEA, data and projections: Access to clean cooking," [Online].

[6] [Online]. Available: https://www.researchgate.net/figure/2-Heating-values-for-syngas-based-on-gasifying-medium_tbl1_269985896.

[7] [Online]. Available: https://www.semanticscholar.org/paper/Biomass-downdraft-gasifier-with-internal-cyclonic-Patil-Bhoi/726a405e93d2cf99799c4e13edfd60046c36f1dd/figure/1.

[8] [Online]. Available: https://www.researchgate.net/figure/Ultimate-and-proximate-analysis-of-sawdust-woodchip-and-coal_tbl1_273715551.

[9] [Online]. Available: https://www.researchgate.net/figure/Comparison-of-syngas-composition-and-heating-value-for-gasification-of-OPF-with-other_tbl5_275222393.

[10] [Online]. Available: https://www.researchgate.net/figure/Proximate-and-ultimate-analysis-of-hazelnut-shell-wet-basis-7-Proximate-wt_tbl1_333703761.

[11] [Online]. Available: https://www.researchgate.net/figure/Proximate-Analysis-Ultimate-Analysis-and-Calorific-Value-of-Coconut-Shell_tbl1_315852600.

[12] [Online]. Available: https://www.redalyc.org/jatsRepo/4455/445559634014/html/index.html.

[13] [Online]. Available: https://oa.upm.es/47702/1/TFG_ALEJANDRO_SANCHEZ_LARIO.pdf.

[14] [Online]. Available: https://www.researchgate.net/figure/Proximate-and-ultimate-analysis-of-pine-wood-19_tbl1_316263983.

[15] [Online]. Available: https://arro.anglia.ac.uk/id/eprint/705046/6/Pandey_2020.pdf.

[16] [Online]. Available: https://core.ac.uk/download/pdf/230206933.pdf.

[17] [Online]. Available: https://www.aeipro.com/files/congresos/2004bilbao/ciip04_0897_0905.1307.pdf.

[18] "estudio del residuo avícola procedente a la localidad de Cundinamarca," [Online]. Available: https://core.ac.uk/download/pdf/230206933.pdf.

[19] [Online]. Available: https://arro.anglia.ac.uk/id/eprint/705046/6/Pandey_2020.pdf.

[20] "Thermodynamic properties data bank, appendix A".

[21] [Online]. Available: https://www.fao.org/3/T0512S/t0512s03.htm.

[22] [Online]. Available: https://nacfe.org/technology/high-efficiency-alternator-2/#:~:text=The%20standard%20alternators%20generally%20have,the%20windings%20in%20the%20alternator. .

[23] [Online]. Available: https://mechcontent.com/volumetric-efficiency-of-ic-engine/#:~:text=In%20the%20naturally%20aspirated%20four,varies%20between%2070%20to%2080%20%25..

[24] [Online]. Available: http://www.sspd.co.za/assets/products/generators/gz25/GZ25.pdf.

[25] "https://www.allpowerlabs.com/wp-content/uploads/2012/11/GEKOneSheet10_20_15Small.pdf," [Online].

[26] "Ekman, E. and Asplund, D" A Review of Research of Peat Gasification in Finland, Technical Research Centre of Finland, Fuel and Lubricant Research Laboratory, Espoo, Finland.".

[27] "Generator Gas, The Swedish Experience From t939-1945, Solar Energy Research Institute, Golden, CO, SERI/SP 33-140, 1979.".

[28] "Jenkins, B. M., Downdraft Gasification Characteristics of Major California Residue-Derived Fuels, Ph.D. Thesis, Department of Engineering, University of California, Davis, 1 980.".

[29] [Online]. Available: https://ej-bowman.com/wp-content/uploads/2019/10/Exhaust-Gas-H.E.-Issue-M-Spanish.pdf.

[30] [Online]. Available: https://www.sciencedirect.com/topics/engineering/gasification-temperature#:~:text=The%20gas%20exit%20temperature%20of,C%20(Knoef%2C%202005)..

[31] [Online]. Available: https://emcfime.com/it/prod/px7000.html.

[32] [Online]. Available: https://www.comid.it/it/serbatoi/9678-serbatoio-poliet-cv-13000-elbi-verticale.html.

[33] [Online]. Available: https://www.comid.it/it/serbatoi/9688-serbatoio-poliet-cv-5000-elbi-verticale.html?rec_source=2&rec_scenario_id=1&prod_id=6923&vds_id=3180&rec_item_id=65753&sm_source=recommendation_frame.

[34] [Online]. Available: https://www.guardianconstructors.com/2020/05/water-tower-cost-estimate.html.

[35] [Online]. Available: https://www.alibaba.com/product-detail/HISEER-CE-500l-stainless-steel-hot_779912206.html?spm=a2700.7724857.0.0.71fe4342sG1HVp.

[36] [Online]. Available: https://www.alibaba.com/product-detail/Water-Pump-Pumps-Taizhou-Factory-2hp_1600443291295.html?spm=a2700.7735675.topad_classic.d_image.7715761cBcwcUG.

[37] [Online]. Available: https://autosolar.es/bombas-sumergibles-230v/bomba-sumergible-ideal-15kw-monofasica-230v-sli11.

[38] [Online]. Available: https://www.varo.com/p/powxg9504/article.

[39] [Online]. Available: https://www.leddiretto.it/2453-armatura-stradale-led-50w-philips-chip-ip65-ik10-asimm-70x140-135lmw.html.

[40] [Online]. Available: https://picclick.com/SunPower-Unused-470W-Mono-Solar-Panel-470-Watts-283127980373.html.

[41] [Online]. Available: https://www.efectoled.com/es/comprar-inicio-generico/63300-estructura-para-paneles-solares-30-inclinacion.html?id_c=124008&gclid=Cj0KCQjw5ZSWBhCVARIsALERCvwoN8DrEGSzbSjWRRZNwD_JSeXv5-HeT92byJ8hSahacHDw6KviqPMaAnalEALw_wcB.

[42] [Online]. Available: https://www.improvecn.com/products/303189343193927680.

[43] [Online]. Available: https://www.amazon.com/KRI%C3%8BGER-Installation-appliances-According-Standards/dp/B07MS5P2X1/ref=mp_s_a_1_1_sspa?dchild=1&keywords=4000%2Bwatt%2Binverter&qid=1634801040&sr=8-1-spons&spLa=ZW5jcnlwdGVkUXVhbGlmaWVyPUEzOUhXQ1RYNDAxQ1M1JmVuY3J5cHRlZElkPUEwMDc.

[44] [Online]. Available: https://drive.google.com/file/d/1WG8f7ZVFYS18POBiDXbl5uZgWB-tVPpB/view.

[45] [Online]. Available: https://www.alibaba.com/product-detail/Diesel-Generator-Generators-Generator-Supplier-

10_1600313172929.html?spm=a2700.pccps_detail.normal_offer.d_image.7963581cO0WI3E&s=p.

[46] [Online]. Available: https://www.solarenergypoint.it/shop/quadro-ac-full-potenza-16-20-kw-1-inverter-1-interruttore.

[47] [Online]. Available: https://www.tradewindspower.com/pdf/Parts_Specials/Bowman_May_Special.pdf.

[48] [Online]. Available: https://strathprints.strath.ac.uk/44929/1/RSER_Warehousing_publisher_version_pdf.pdf .

[49] [Online]. Available: https://cdn.enfsolar.com/Product/pdf/Crystalline/5ad7f4421dde6.pdf.

[50] [Online]. Available: https://re.jrc.ec.europa.eu/pvg_tools/en/.

[51] [Online]. Available: https://cropwatch.unl.edu/whats-feedlot-manure-worth-fertilizer.

[52] [Online]. Available: https://www.globalpetrolprices.com/Nigeria/gasoline_prices/.

[53] [Online]. Available: https://www.aci.it/fileadmin/documenti/servizi_online/Costi_chilometrici/CKI_web_dicembre_.

[54] [Online]. Available: 343046467_Economics_of_Distributed_Power_Generation_via_Gasification_of_Biomass_and_Municipal_Solid_Waste.

[55] [Online]. Available: https://www.checkatrade.com/blog/cost-guides/solar-panel-maintenance-cost/#jump-header-1 .

[56] [Online]. Available: https://www.amazon.com/KRI%C3%8BGER-Installation-appliances-According-Standards/dp/B07MS5P2X1/ref=mp_s_a_1_1_sspa?dchild=1&keywords=4000%2Bwatt%2Binverter&qid=1634801040&sr=8-1-spons&spLa=ZW5jcnlwdGVkUXVhbGlmaWVyPUEzOUhXQ1RYNDAxQ1M1JmVuY3J5cHRlZElkPUEwMDc.

[57] [Online]. Available: https://www.improvecn.com/products/303189343193927680.

[58] [Online]. Available: https://data.worldbank.org/indicator/FR.INR.RINR?locations=NG.

[59] [Online]. Available: https://www.globalpetrolprices.com/Nigeria/diesel_prices/.

[60] [Online]. Available: file:///Users/salvatorepecoraro/Downloads/10000023912.pdf.

[61] [Online]. Available: https://www.naturalgasintel.com/global-natural-gas-prices-converged-more-in-2017-as-use-of-lng-spot-prices-increased/.

[62] [Online]. Available: http://www.sspd.co.za/assets/products/generators/gz25/GZ25.pdf.

[63] [Online]. Available: https://www.nrel.gov/docs/legosti/old/3022.pdf.

[64] "http://joinville.ifsc.edu.br/~evandro.dario/Termodin%C3%A2mica/Material%20Did%C3%A1tico/Livro%20-%20Cengel/Termodinamica%20-%20Cengel%207th%20-%20espanhol.pdf," [Online].

[65] "Property data bank, Appendix A".

[66] [Online]. Available: https://www.researchgate.net/figure/Proximate-and-ultimate-analysis-of-pine-wood-19_tbl1_316263983.

[67] [Online]. Available: https://emcfime.com/it/prod/px7000.html.

[68] [Online]. Available: https://www.ieabioenergy.com/wp-content/uploads/2021/02/Emerging-Gasification-Technologies_final.pdf.

[69] [Online]. Available: https://nigerianinfopedia.com.ng/water-storage-tank-prices-in-nigeria/.

[70] [Online]. Available: https://cropwatch.unl.edu/whats-feedlot-manure-worth-fertilizer.

[71] [Online]. Available: https://www.amazon.com/KRI%C3%8BGER-Installation-appliances-According-Standards/dp/B07MS5P2X1/ref=mp_s_a_1_1_sspa?dchild=1&keywords=4000%2Bwatt%2Binverter&qid=1634801040&sr=8-1-spons&spLa=ZW5jcnlwdGVkUXVhbGlmaWVyPUEzOUhXQ1RYNDAxQ1M1JmVuY3J5cHRlZElkPUEwMDc.

APPENDIX A

During the last decades there has been a significant growth in research on biomass, conversion technologies and the final use of the products obtained. Within this, there is a greater progression in gasification given the number of advantages it presents. Simultaneously with its development, work has been done on mathematical models that allow the understanding, optimization, and management of this type of process. These models are classified into kinetic and thermodynamic.

This section focuses on the study of mathematical models. It has been tried to approach the models to the behavior of the experimental process. For this reason, it has been developed a model in which the results obtained have been compared with several experimental data.

The mathematical model developed is based on typical input parameters in gasification, such as the proximate and ultimate analysis of biomass, the equivalence ratio and the temperature. Mass balances, energy balances and equilibrium equations were proposed to predict the gas output composition and the calorific value of the gas produced. All this for a downdraft gasifier, considered in steady state.

Finally, to get more precise and meaningful results they have been compared the outcomes obtained using the mathematical correlations for the estimation of enthalpy and Gibbs free energy with the ones obtained by using the software EES® (Engineering Equation Solver) to proper estimate the enthalpy and Gibbs free energy at different temperatures.

INTRODUCTION

The development of gasification technology includes an analysis of the process on a laboratory scale and the construction of equipment on a pilot scale, until the model is implemented at an industrial level. These prototypes are also accompanied by an approach of mathematical models that describe the physicochemical, thermodynamic and thermal phenomena that occur inside the gasifier.

The limited knowledge of the complex phenomena present in the process limits and reduces technological development. The use of mathematical models allows studying the influence of the parameters involved in the process quickly and practically, becoming, then, a means to improve the efficiency of the process and make it a practical and affordable solution for the population.

Biomass gasification is a complex phenomenon in which mass transport, mass diffusion, momentum transfer and energy transfer, mainly in thermal form, occur simultaneously. It is of great importance to determine the operating conditions of the equipment, which allow obtaining fuel gases with a high calorific value. A gas with a high calorific value can release a greater amount of thermal energy by combustion.

The simulation of the biomass gasification process has great importance and can be used as a tool to better understand this complex process. Therefore, by modeling this phenomenon in a simpler and clearer way, it facilitates the detection of its weak points and how to control them. Biomass can be used in such a way that the carbon and hydrogen present in it are converted mainly into H_2, CO, CO_2, CH_4 and N_2, if said composition and its calorific value are predicted with good accuracy, the model and the simulation would be very useful.

The mathematical model that arises in this work is based on the approach of elemental balances of mass and energy, the model has been solved by means of the aforementioned balances and using equilibrium constants of characteristic reactions of the gasification process, the values of the chemical properties involved were compared with what is reported in the specialized software EES®.

With the present work, a simple functional mathematical model for a downdraft type biomass gasifier is developed. Considering the input parameters of the fuel such as the moisture content of the fuel, the elemental composition, the equivalence ratio. To predict the output composition, the proposed model was solved with a system of nonlinear equations. The results obtained by the model were compared with experimental data reported in the consulted technical literature obtained from tests carried out with different biomasses in gasifiers with similar configurations.

A mathematical model can be used as a comprehensive tool for the prediction and design of a gasification process if it has a good level of precision.

- Numerical models are cheaper and faster than experimental investigations.
- By means of a mathematical model it is possible to “see” or “access” parts of the process for which it is impossible to obtain data.
- It can be used to find optimal values in existing equipment or better in the design of new equipment.
- The modeling is not static, some parameters can be modified to extend the range of applications.

An example of the possibilities posed by the use of mathematical models can be a gasification process with a maximum concentration of hydrogen and carbon monoxide, a gas outlet temperature and a lower calorific value, for which variation in the biomass inlet conditions, a suitable air/fuel ratio and in some cases the geometries and configuration of the gasifier to be used. Through the use of mathematical models, it can be established that a lower moisture content in the fed biomass presents an increase in the calorific value of the gas obtained and vice versa. The temperature profile can also be verified throughout the process in the equipment. Modeling can contribute to the optimization of process parameters by including mass and energy balances, kinetic models, thermodynamic equilibrium. Thus, the models not only allow to verify the yields of the process but also to obtain a clear knowledge of the dynamics of the process. However, the mathematical modeling of any thermochemical process itself is not enough if there are no experimental or field data to validate the models. Indeed, it has been found that changes to the process based on results found with mathematical models start from the establishment of a base model that is compared with real conditions before making any type of modification on it.

There are different mathematical approaches to describe the gasification processes that transform input variables into desired output parameters and physical variables. The models that describe this type of phenomenon can be zero-dimensional (0-D) or dimensional models. In turn, dimensional models are classified into one, two or three dimensions (1-D, 2-D and 3-D), which depends on the number of spatial coordinates considered. Among them the most used input and output variables are: mass flows, compositions, temperatures, pressures, etc.

The 0-D models of biomass gasification are based on thermodynamic equilibrium or chemical kinetics, relating the input variables with the output variables as shown in the figure below (one-step process). So the final composition of the gas is obtained, depending on the type of biomass, humidity, air/fuel ratio and temperature. However, with this model it is not possible to evaluate the behavior of any parameter throughout the equipment

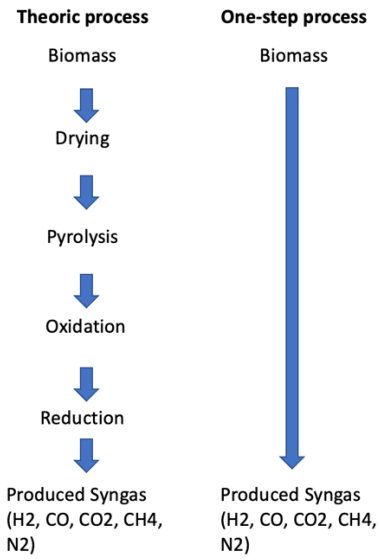

Figure 45: zero-dimensional (0-D) process

The dimensional models consider the variation of all the parameters inside the gasifier in one, two or three spatial coordinates, depending on the case. These types of models require a coupling approach between chemical kinetics and transport phenomena (mass, energy and momentum), to study the development of compounds, the thermal and dynamic state of the process in the chosen coordinates. While the 0-D models are useful for the optimization of the gasification process and plants, the dimensional ones (1-D, 2-D and 3-D) allow optimization and in turn the possibility of extracting parameters related to the design of this type of equipment.

Then, two possible approaches are possible to investigate the gasifier performances:

- **Thermodynamic equilibrium model (zero-dimensional model)**

  The thermodynamic equilibrium model is a tool used to calculate the maximum yield that can be achieved starting from a specific process. The calculations of the models are independent of the gasifier design, unlike the kinetic models mentioned above, these types of models are usually more suitable to study the influence of different fuel parameters on the process. In thermodynamic equilibrium a reaction system is in its most stable state, this condition is achieved when the entropy of the system is maximized and the Gibbs free energy is minimized. However, equilibrium cannot be achieved, this is mainly due to relatively low operating temperatures (gas outlet temperatures range from about 700°C to 1000°C).

  Chemical equilibrium is determined by any of the following ways:

- Equilibrium constants.
- Minimization of the Gibbs free energy.

Then, there are two methods for equilibrium modeling: the stoichiometric method and the non-stoichiometric method. The stoichiometric model requires clearly defined reaction mechanisms where the chemical reactions and the species involved in the process are incorporated. The non-stoichiometric equilibrium model is based on the minimization of the Gibbs free energy in the system without the need to specify the possible reactions that take place.

- **Kinetic models (dimensional models)**

The inadequacy of thermodynamic equilibrium models to relate gasifier design parameters to the final composition of the gas produced leads to the development of kinetic models to evaluate and simulate gasifier behavior. The kinetic models allow to understand design and operation parameters such as reaction speed, residence time and hydrodynamics of the reactor (superficial speed, diffusion speed and the length of the gasifier). This model offers a wide field to investigate the behavior of a gasifier through simulation and although with more precise results but computationally more complex. A large part of the models represents the modeling for the reduction reaction, and often separate pyrolysis, oxidation and reduction into sub-models. Separating the general process into sub-models helps in the simplification of the general model and also provides a better understanding of the behavior of the downdraft gasifier, the division of the sub-models can be done different forms the most used can be seen in the figure below.

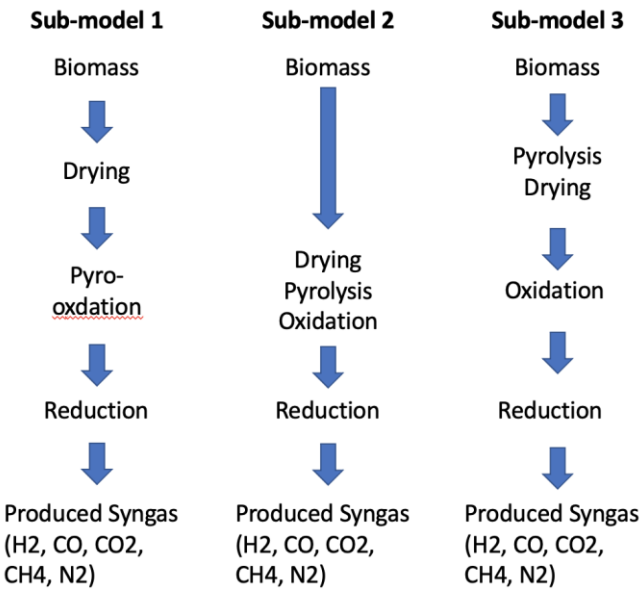

Figure 46: Dimensional model - different submodels

MODEL DEVELOPMENT METHODOLOGY

The development of a mathematical model requires a systematic approach with the scheme of postulating theories based on experimental work and assumptions. The main objective of any mathematical modeling is to create a system that is capable of performing an action similar to that of the natural system. Simulation is the result of theories and hypotheses. Therefore, it is very important to select theories and assumptions appropriate to the process to be simulated. For the model to be developed, the following assumptions have been taken into account:

- Biomass has been used as fuel.
- Atmospheric air (21% O_2, 79% N_2) has been taken as gasifying agent.
- The gasifier has been taken in a single pass at steady state.
- The model developed has been considered adiabatic and operates at 1 atm of pressure.
- The composition of the gas produced is assumed to be a mixture of C, H_2, CO, CO_2, CH_4, H_2O and N_2, although evidence of the formation of tar and other hydrocarbons is not taken into account.
- The N_2 does not participate reacting in the gasification process, the composition in the produced gas is equal to its input composition.
- There is chemical equilibrium of all species throughout the gasifier.

- The gasifier is considered dimensionless (0-D).
- The gases in the gasifier behave as an ideal gas.
- Quasi-equilibrium type gasification process with local equilibrium is considered, which allows using the values of the thermodynamic properties reported in the databases and thermodynamic tables.

Biomass compositions

After having defined all the assumptions on which the model is based, the calculation procedure can be developed and explained.

The first step is the definition of all the biomass compositions (proximate and ultimate analysis) as well as it has been done in the calculation section. Here below are reported the starting data on which all the calculations have been developed.

Table 34: Proximate analysis of the different biomasses

	Proximate analysis				
	Volatile matter	**Humidity**	**Ash**	**Fixed carbon**	**Sum**
Wood shavings	76%	6%	4%	14%	100.00%
Hazelnut shells	63%	12%	1%	24%	100.00%
Coconut shells	74.3%	7.4%	0.7%	17.6%	100.00%
Corn cob	71.4%	10.0%	1.6%	17.0%	100.00%
Rice husk	55.7%	9,4%	19.7%	15.2%	100.00%
Pine tree	67.7%	14.0%	0.4%	17.9%	100.00%
Beech wood	74.2%	8.3%	1.2%	16.3%	100.00%
Chicken manure	56.7%	29.4%	13.8%	0.1%	100.00%
Almond shell	72.3%	10.6%	1.2%	15.9%	100.00%

Table 35: Ultimate analysis of the different biomasses

	Ultimate analysis							
	C	**H**	**O**	**N**	**S**	**Cl**	**sum DAF**	**sum with ash and humidity**
Wood shavings	57.42%	4.32%	28.22%	0.81%	0.00%	0.00%	90.76%	100.00%
Hazelnut shells	40.84%	5.04%	40.12%	0.19%	0.58%	0.00%	86.78%	100.00%
Coconut shells	44.41%	6.02%	41,35%	0.09%	0.00%	0.00%	91.87%	100.00%
Corn cob	42.87%	4.99%	40.18%	0.36%	0.00%	0.00%	88.40%	100.00%
Rice husk	33.08%	3.35%	33.97%	0.29%	0.21%	0.00%	70.90%	100.00%
Pine tree	40.67%	5.58%	39.26%	0.08%	0.00%	0.00%	85.60%	100.00%
Beech wood	42.98%	5.78%	41.61%	0.16%	0.02%	0.01%	90.55%	100.00%

Chicken manure	35.00%	4.00%	15.70%	2.10%	0.00%	0.00%	56.80%	100.00%
Almond shell	51.40%	6.50%	29.60%	0.70%	0.00%	0.00%	88.20%	100.00%

Chemical formula of the biomass

Due to the high complexity to determine the chemical formula of biomass, various methods have been developed to determine the approximate equivalent formula. One of the most widely used methods is based on the use of the elemental compositions of biomass on a dry basis. To do that it is considered the following general formula for the biomass (the presence of sulfur has been ignored to reduce complexity in the calculations): $CH_xO_yN_z$.

It is taken as basis one atom of carbon C (C=1).

Then all the other coefficients are found as follows:

$$x = \frac{\%H * MM_C}{\%C * MM_H}$$

(A. 1)

$$y = \frac{\%O * MM_C}{\%C * MM_O}$$

(A. 2)

$$z = \frac{\%N * MM_C}{\%C * MM_N}$$

(A. 3)

Molecular mass of the biomass

The molecular mass of the biomass is then calculated as follows:

$$MM_{biomass} = C * MM_C + x * MM_H + y * MM_O + z * MM_N$$

(A. 4)

Humidity content of the biomass

The moisture content of biomass is normally presented in mass fraction. However, the kmol of water per kmol of biomass is required for stoichiometric calculations. When the moisture

content (MC) of the biomass is known, the amount of water (w) entering the system can be determined as follows.

$$MC = \frac{w * MM_{H_2O}}{MM_{biomass} + w * MM_{H_2O}}$$

(A. 5)

Clearing from the previous equation the following is obtained:

$$w = \frac{MC * MM_{biomass}}{MM_{H_2O} * (1 - MC)}$$

(A. 6)

Heating value of the biomass

The calorific value in biomass is the amount of heat released during complete combustion, there are several approximate methods to calculate the calorific value such as experimental methods and unified correlations based on the latest analysis of biomass. The following correlation has been used to estimate the heating value of the biomass [69].

$$HHV\ \left[\frac{MJ}{kg}\right] = 34.1 * \%C + 132.2 * \%H - 1.53 * \%Ash - 12 * \%(O + N)$$

(A. 7)

Formation enthalpy of the biomass

The enthalpy of formation of the biomass is necessary to make the energy balance of the gasification system. It is calculated under the premise of complete combustion, considering the following reaction.

$$CH_xO_yN_z + n * (O_2 + 3{,}76N_2) \rightarrow CO_2 + aH_2O + bN_2$$

Where x, y, z are known and a, b, n are computed making respectively the mass balance of H, O and N:

$$a = \frac{x}{2}$$

(A. 8)

$$n = 1 + \frac{a}{2} - \frac{y}{2}$$

(A. 9)

$$b = \frac{z}{2} + 3{,}76 * n$$

(A. 10)

Finally, the enthalpy of formation of the biomass can be calculated according to the following formula.

$$\Delta h^{\circ}_{biom}\left[\frac{MJ}{kmol}\right] = LHV_{biom}\left[\frac{MJ}{kg}\right] * MM_{biom}\left[\frac{kg}{kmol}\right] + h^{\circ}_{f,CO_2} + a * h^{\circ}_{f,H_2O}$$

(A. 11)

The enthalpy of formation for each biomass is reported in the table below.

Table 36: Enthalpy of formation for all the biomasses

	Δh°_{biom}
	[MJ/kmol]
Wood shavings	-116.78
Hazelnut shells	-171.06
Coconut shells	-160.54
Corn cob (dry)	-150.21
Rice husk	-107.47
Pine tree (dry)	-98.99
Beech wood	-179.55
Chicken manure	-281.82
Almond shell	-240.98

Gasification air

The equivalence ratio refers to the ratio between the actual air fuel ratio and the stoichiometric air-fuel ratio, as already mentioned above.

The air-fuel ratio fed in the gasifier is an operational parameter for the model, it can be manipulated for experimental purposes, while the stoichiometric air-fuel ratio is a constant for biomass and is calculated with the equation:

$$\left(\frac{A}{F}\right)_{stoich} = \left(1 + \frac{x}{4} + \frac{z}{2} - \frac{y}{2}\right) * (1 + 3{,}76)$$

(A. 12)

Where $\left(1 + \frac{x}{4} + \frac{z}{2} - \frac{y}{2}\right)$ is the amount of oxygen required for complete combustion, on a molar basis it is the oxygen required per 1 kmol of biomass.

When the equivalence ratio is known, it is possible to estimate the amount of air fed on a molar basis as a precursor to the stoichiometric equation to calculate the amount of air shown below.

$$m = \left(1 + \frac{x}{4} + \frac{z}{2} - \frac{y}{2}\right) * ER$$

(A. 13)

Mass and energy balance

Before being able to make the mass and energy balance of the gasification process, it has to be properly defined the gasification reaction that is assumed to occur within the gasifier. The formulation of the gasification process is based on empirical assumptions that were supported by experimental results of biomass gasification. According to the literature, the chemical reaction that governs the gasification process is defined as:

$$CH_xO_yN_z + w(H_2O) + m(O_2 + 3{,}76N_2) \rightarrow n_{H_2}H_2 + n_{CO}CO + n_{H_2O}H_2O + n_{CO_2}CO_2 + n_{CH_4}CH_4 + n_{N2}N_2$$

Applying the mass conservation principle, mass balances were carried out for each of the biomass components C, H, N, O:

$$Carbon\ balance\colon\ 1 = n_{CO} + n_{CO_2} + n_{CH_4}$$

(A. 14)

$$Hydrogen\ balance:\ \ x + 2w = 2n_{H2} + 2n_{H_2O} + 4n_{CH_4}$$

(A. 15)

$$Oxygen\ balance:\ \ y + 2m + w = n_{CO} + 2n_{CO2} + n_{H2O}$$

(A. 16)

$$Nitrogen\ balance:\ \ z + 3.76 * 2 * m = 2 * n_2$$

(A. 17)

For oxygen, the reactants appear both in the biomass and in the air and at the outlet in CO, CO_2 and H_2O, as the gasification process is carried out with oxygen deficiency, it is considered that at the outlet of the gas there is no presence of oxygen (O_2).

Concerning the energy balance, in this model, it is assumed that reagents enter at standard conditions (25°C and 1.0 atm) and that the products come out at an assumed temperature T and 1.0 atm. The figure below shows a general scheme of the energy balance.

Figure 47: General diagram of the energy balance for a reacting system

Then, the energy balance is made by putting equal the enthalpy of the reactants to the one of the products (HR=HP) according to the following expressions:

$$HR = \Delta h^{\circ}_{biom} + m\left(h^{\circ}_{f,O_2} + 3.76h^{\circ}_{f,N_2}\right) + wh^{\circ}_{f,H_2O}$$

(A. 18)

$$HP = n_{H_2}\left(h^{\circ}_{f,H_2} + \Delta h^{\circ}_{H_2}\right) + n_{CO}\left(h^{\circ}_{f,CO} + \Delta h^{\circ}_{CO}\right) + n_{H_2O}\left(h^{\circ}_{f,H_2O} + \Delta h^{\circ}_{H_2O}\right) + n_{CO_2}\left(h^{\circ}_{f,CO_2} + \Delta h^{\circ}_{CO_2}\right) + n_{CH_4}\left(h^{\circ}_{f,CH_4} + \Delta h^{\circ}_{CH_4}\right) + n_{N_2}\left(h^{\circ}_{f,N_2} + \Delta h^{\circ}_{N_2}\right)$$

(A. 19)

Chemical equilibrium

For the present model, it has been assumed that all the gasification system reaches the equilibrium. All the gases involved have been considered as ideal and at a pressure of 1 atm. Consequently, it is possible to impose the equilibrium for all the reactions considered within the gasification systems.
The equilibrium constant general expression for each chemical reaction can be written as follows:

$$K_p = \Pi_i (x_i)^{\nu_i} * \left(\frac{p}{p^\circ}\right)^{\Sigma \nu_i} = \Pi_i \left(\frac{n_i}{n_{tot}}\right)^{\nu_i} * \left(\frac{p}{p^\circ}\right)^{\Sigma \nu_i}$$

(A. 20)

Where x_i is the mole fraction of species i in the produced gas mixture, ν_i is the stoichiometric number, p° is the standard pressure, 1 atm, and n_{tot} are the total moles produced.

The value of the K_p has been defined as a function of the temperature and the Gibbs free energy, whose expression is reported here below.

$$lnK_{eq} = -\frac{\Delta G_r^\circ}{RT}$$

(A. 21)

Where $\Delta G_r^\circ = \Sigma_i \upsilon_i \Delta g_{f,i}^\circ$ is the Gibbs free energy of the considered reaction.
The Gibbs free energy for a particular species is stated as:

$$g_j^\circ(T) = h_j(T) - T * s_j(T)$$

(A. 22)

Where h is the enthalpy and s is the entropy.
For the considered system, finally, the equation to calculate the Gibbs free energy of a reaction can be expressed as follows:

$$\Delta G_r^\circ = \Sigma_i v_i \{[h_{f,i}^\circ + (h_i(T) - h_i(298K))] - T[s_{f,i}^\circ + (s_i(T) - s_i(298K))\}$$

(A. 23)

Where $h_{f,i}^\circ$ and $s_{f,i}^\circ$ are respectively the standard enthalpy and entropy of formation, while $h_i(T)$ and $s_i(T)$ are respectively the enthalpy and the entropy at a given temperature T.

Correlations and estimation of enthalpy and Gibbs free energy

The calculation procedure described above is based on the values of enthalpy and Gibbs free energy that each species has at each temperature. In this direction, to proper evaluate the syngas composition, the correct and precise estimation of these properties plays a paramount role to obtain accurate results and, consequently, reduce the error of the outcomes. For better understanding how the accuracy of calculations improves the obtained results, they have been compared two possible alternatives to estimate the enthalpy and the Gibbs free energy:

1. Estimation through empirical correlations.
2. Punctual values through the software EES.

1) Estimation through empirical correlations.

This first approach bases the estimation of the enthalpy and of the Gibbs free energy on empirical correlations. Consequently, both the properties are expressed as a polynomial function of temperature in which each term of each component is defined by coefficients. Accordingly, here below are reported the equations used to estimate the Gibbs free energy and the enthalpy as a function of the temperature.

$$\Delta G_{f,T}^\circ = \Delta G_{f,298K}^\circ - a * T * \ln(T) - b * T^2 - \frac{c}{2} * T^3 - \frac{d}{3} * T^4 + \frac{e}{2 * T} + f + g * T$$

(A. 24)

Table 37: Empirical coefficients for Gibbs free energy estimation [64]

Component	a	b	c	d	e	f	g

CO_2	$-1{,}949\cdot10^{-2}$	$3{,}122\cdot10^{-5}$	$-2{,}448\cdot10^{-8}$	$6{,}946\cdot10^{-12}$	-489,100	5,270	-0,1207
H_2O	$-8{,}950\cdot10^{-3}$	$-3{,}672\cdot10^{-6}$	$5{,}209\cdot10^{-9}$	$-1{,}478\cdot10^{-12}$	0,00	2,868	-0,01720
CO	$5{,}619\cdot10^{-3}$	$-1{,}190\cdot10^{-5}$	$6{,}383\cdot10^{-9}$	$-1{,}846\cdot10^{-12}$	-489,100	0,868	-0,06131
CH_4	$-4{,}620\cdot10^{-2}$	$1{,}130\cdot10^{-5}$	$1{,}319\cdot10^{-8}$	$-6{,}647\cdot10^{-12}$	-489,100	14,11	-0,2234

The values of the Gibbs free energy at standard conditions are reported in the table below [70].

Table 38: Gibbs free energy at standard conditions

	$DG°_{f,i}$ (298K)
H_2	0
CO	-137400
CO_2	-394600
H_2O (g)	-228800
CH_4	-50870
N_2	0
O_2	0

The only estimation that is not available is the one of the H2. Then it is computed through another correlation path, which is described here below.
The enthalpy and entropy are firstly computed and finally the Gibbs free energy is found [70]:

The following expression for the Cp is given.

$$c_p\left[\frac{kJ}{kmol*K}\right] = a + b*T + c*T^2 + d*T^3$$

(A. 25)

Given the Cp function it is then possible to compute the enthalpy and the entropy at a given temperature according to the following equations:

$$\Delta H_T^\circ = \int_{298K}^{T} c_p dT = a(T-298) + \frac{b}{2}(T^2 - 298^2) + \frac{c}{3}(T^3 - 298^3) + \frac{d}{4}(T^4 - 298^4)$$

(A. 26)

$$\Delta S_T^\circ = \int_{298K}^{T} \frac{c_p}{T} dT = \Delta S_{f,298K}^\circ + \mathrm{a} * \ln\left(\frac{T}{298}\right) + b(T-298) + \frac{c}{2}(T^2 - 298^2) + \frac{d}{3}(T^3 - 298^3)$$

(A. 27)

Finally, the Gibbs free energy is computed as follows:

$$\Delta G_T^\circ = \Delta H_T^\circ + T * \Delta S_T^\circ$$

(A. 28)

Table 39: Empirical coefficients of hydrogen for enthalpy, entropy and Gibbs free energy estimation

	a	b	c	d
H_2	27,14	$9{,}2743 \cdot 10^{-3}$	$-1{,}381 \cdot 10^{-5}$	$7{,}645 \cdot 10^{-9}$

2) Punctual values through the software EES.

This second approach is more rigorous than the first one because in this case the values obtained for both enthalpy and Gibbs free energy are taken in a punctual way from the software EES under the assumption that all the gases behave as ideal. In particular, they are taken the values of these properties for the following temperatures: 800 K, 900 K, 1000 K, 1100 K, 1200 K, 1300 K.

In the tables below, all the punctual values (for each component and for each of the considered temperatures) are reported. The enthalpy is given in [J/kg], while the entropy is given in [J/kgK].

Table 40: Enthalpy punctual values with software EES [J/kg]

Tout [K]	800	900	1000	1100	1200	1300
H_2	7.281E+06	8.761E+06	1.026E+07	1.177E+07	1.330E+07	1.485E+07
CO	-3.403E+06	-3.289E+06	-3.172E+06	-3.053E+06	-2.932E+06	-2.810E+06

CO_2	-8.422E+06	-8.304E+06	-8.182E+06	-8.058E+06	-7.931E+06	-7.802E+06
H_2O (g)	-1.242E+07	-1.220E+07	-1.198E+07	-1.175E+07	-1.150E+07	-1.126E+07
CH_4	-3.097E+06	-2.685E+06	-2.244E+06	-1.775E+06	-1.280E+06	-7.622E+05
N_2	5.376E+05	6.509E+05	7.662E+05	8.835E+05	1.003E+06	1.124E+06
O_2	4.957E+05	6.017E+05	7.094E+05	8.186E+05	9.292E+05	1.041E+06

Table 41: Entropy punctual values with software EES [J/kgK]

Tout [K]	800	900	1000	1100	1200	1300
H_2	7.906E+04	8.080E+04	8.238E+04	8.382E+04	8.516E+04	8.640E+04
CO	8.111E+03	8.247E+03	8.370E+03	8.483E+03	8.588E+03	8.686E+03
CO_2	5.849E+03	5.988E+03	6.117E+03	6.235E+03	6.345E+03	6.448E+03
H_2O (g)	1.242E+04	1.267E+04	1.291E+04	1.313E+04	1.334E+04	1.354E+04
CH_4	1.452E+04	1.501E+04	1.547E+04	1.592E+04	1.635E+04	1.676E+04
N_2	7.886E+03	8.020E+03	8.141E+03	8.253E+03	8.357E+03	8.453E+03
O_2	7.371E+03	7.496E+03	7.609E+03	7.713E+03	7.809E+03	7.899E+03

Finally, the Gibbs free energy is computed as: $\Delta G_T^\circ = \Delta H_T^\circ + T * \Delta S_T^\circ$

(A. 29)

Table 42: Gibbs free energy punctual values with software EES [J/kg]

Tout [K]	800	900	1000	1100	1200	1300
H_2	-5.597E+07	-6.396E+07	-7.212E+07	-8.043E+07	-8.889E+07	-9.746E+07
CO	-9.892E+06	-1.071E+07	-1.154E+07	-1.238E+07	-1.324E+07	-1.410E+07
CO_2	-1.310E+07	-1.369E+07	-1.430E+07	-1.492E+07	-1.555E+07	-1.618E+07
H_2O (g)	-2.235E+07	-2.361E+07	-2.489E+07	-2.620E+07	-2.751E+07	-2.886E+07
CH_4	-1.472E+07	-1.619E+07	-1.772E+07	-1.929E+07	-2.090E+07	-2.256E+07
N_2	-5.771E+06	-6.567E+06	-7.375E+06	-8.195E+06	-9.025E+06	-9.865E+06
O_2	-5.401E+06	-6.145E+06	-6.900E+06	-7.666E+06	-8.442E+06	-9.228E+06

It is useful, in developing the calculations, to have the values specific to the moles. Then, all the values reported above are divided by the molecular mass of each component to get the following values:

Table 43: Enthalpy punctual values with software EES [kJ/kmol]

Tout [K]	800	900	1000	1100	1200	1300
H_2	1.456E+04	1.752E+04	2.052E+04	2.354E+04	2.660E+04	2.970E+04

CO	-9.528E+04	-9.209E+04	-8.882E+04	-8.548E+04	-8.210E+04	-7.868E+04
CO_2	-3.706E+05	-3.654E+05	-3.600E+05	-3.546E+05	-3.490E+05	-3.433E+05
H_2O (g)	-2.236E+05	-2.196E+05	-2.156E+05	-2.115E+05	-2.070E+05	-2.027E+05
CH_4	-4.955E+04	-4.296E+04	-3.590E+04	-2.840E+04	-2.048E+04	-1.219E+04
N_2	1.505E+04	1.822E+04	2.145E+04	2.474E+04	2.808E+04	3.147E+04
O_2	1.586E+04	1.925E+04	2.270E+04	2.620E+04	2.974E+04	3.331E+04

Table 44: : Gibbs free energy punctual values with software EES [kJ/kmol]

Tout [K]	**800**	**900**	**1000**	**1100**	**1200**	**1300**
H_2	-1.119E+05	-1.279E+05	-1.442E+05	-1.609E+05	-1.778E+05	-1.949E+05
CO	-2.770E+05	-2.999E+05	-3.232E+05	-3.468E+05	-3.707E+05	-3.949E+05
CO_2	-5.765E+05	-6.025E+05	-6.292E+05	-6.563E+05	-6.840E+05	-7.121E+05
H_2O (g)	-4.023E+05	-4.249E+05	-4.480E+05	-4.715E+05	-4.952E+05	-5.195E+05
CH_4	-2.355E+05	-2.591E+05	-2.835E+05	-3.086E+05	-3.344E+05	-3.609E+05
N_2	-1.616E+05	-1.839E+05	-2.065E+05	-2.295E+05	-2.527E+05	-2.762E+05
O_2	-1.728E+05	-1.966E+05	-2.208E+05	-2.453E+05	-2.701E+05	-2.953E+05

PROPOSED MODELS

The development of this kind of model is strictly related to the assumptions that have been made. It depends on many parameters, such us the gasification reaction that is considered, the equilibrium reactions involved, the molecules exiting from the gasifier, the temperature, the equivalence ratio, the estimation method for the main thermodynamic properties.

To proper develop the model and to find the best among the multiple options, they have been compared lots of cases and they have been carefully analyzed in terms of outcomes and convergency. Overall, they have been analyzed 18 cases. Among them, three possible gasification reactions have been considered and 5 reactions have been selected to impose the equilibrium. They are divided in three macro cases, according to the gasification reaction products assumed.

- **Gasification reaction 1**

$$CH_xO_yN_z + w(H_2O) + a(O_2 + 3.76N_2) \rightarrow n_C C + n_{H_2} H_2 + n_{CO} CO + n_{H_2O} H_2O + n_{CO_2} CO_2 + n_{CH_4} CH_4 + n_{N2} N_2$$

Together with this gasification reaction, they are considered the following reactions within the gasifier to impose the equilibrium.

a. $C + 2H_2 \rightarrow CH_4$

$$K_{eq}(T) = e^{-\frac{\left(g^{\circ}_{CH_4}(T) - 2g^{\circ}_{H_2}(T)\right)}{RT}}$$

(A. 30)

$$K_p = \Pi_i(x_i)^{\nu_i} * \left(\frac{p}{p^{\circ}}\right)^{\Sigma\nu_i} = \frac{n_{CH_4}}{n_{H_2}^2} * n_{tot}$$

(A. 31)

b. $C + H_2O \rightarrow CO + H_2$

$$K_{eq}(T) = e^{-\frac{\left(g^{\circ}_{CO}(T) + g^{\circ}_{H_2}(T) - g^{\circ}_{H_2O}(T)\right)}{RT}}$$

(A. 32)

$$K_p = \Pi_i(x_i)^{\nu_i} * \left(\frac{p}{p^{\circ}}\right)^{\Sigma\nu_i} = \frac{n_{CO} * n_{H_2}}{n_{H_2O}} * \frac{1}{n_{tot}}$$

(A. 33)

c. $C + CO_2 \rightarrow 2CO$

$$K_{eq}(T) = e^{-\frac{\left(2g^{\circ}_{CO}(T) - g^{\circ}_{CO_2}(T)\right)}{RT}}$$

(A. 34)

$$K_p = \Pi_i(x_i)^{\nu_i} * \left(\frac{p}{p^{\circ}}\right)^{\Sigma\nu_i} = \frac{n_{CO}^2}{n_{CO_2}} * \frac{1}{n_{tot}}$$

(A. 35)

- **Gasification reaction 2**

$$CH_xO_yN_z + w(H_2O) + a(O_2 + 3{,}76N_2) \rightarrow n_{H_2}H_2 + n_{CO}CO + n_{H_2O}H_2O + n_{CO_2}CO_2 + n_{CH_4}CH_4 + n_{N2}N_2$$

Together with this gasification reaction, they are considered the following reactions within the gasifier to impose the equilibrium.

d. $H_2O + CO \rightarrow CO_2 + H_2$

$$K_{eq}(T) = e^{-\frac{\left(g^{\circ}_{CO_2}(T) + g^{\circ}_{H_2}(T) - g^{\circ}_{CO}(T) - g^{\circ}_{H_2O}(T)\right)}{RT}}$$

(A. 36)

$$K_p = \Pi_i(x_i)^{\nu_i} * \left(\frac{p}{p^{\circ}}\right)^{\Sigma\nu_i} = \frac{n_{CO_2} * n_{H_2}}{n_{CO} * n_{H_2O}}$$

(A. 37)

e. $CO_2 + CH_4 \rightarrow 2H_2 + 2CO$

$$K_{eq}(T) = e^{-\frac{\left(2g^{\circ}_{H_2}(T) + 2g^{\circ}_{CO}(T) - g^{\circ}_{CO_2}(T) - g^{\circ}_{CH_4}(T)\right)}{RT}}$$

(A. 38)

$$K_p = \Pi_i(x_i)^{\nu_i} * \left(\frac{p}{p^{\circ}}\right)^{\Sigma\nu_i} = \frac{n_{CO}^2 * n_{H_2}^2}{n_{CO_2} * n_{CH_4}} * \frac{1}{n_{tot}^2}$$

(A. 39)

- **Gasification reaction 3**

$$CH_xO_yN_z + w(H_2O) + a(O_2 + 3.76N_2) \rightarrow n_{H_2}H_2 + n_{CO}CO + n_{CO_2}CO_2 + n_{CH_4}CH_4 + n_{N2}N_2$$

After having introduced the gasification reactions, it is possible to list all the eighteen cases taken into account:

- **Gasification reaction 1**

1. Gasification reaction 1 & empirical correlations (ER variable)
    - 7 unknowns: nC, nH_2, nCO, nH_2O, nCO_2, nCH_4, a
    - 7 equations: 4 mass balances (C, H, O, N) + 3 equilibrium equations (a, b, c)
2. Gasification reaction 1 & EES data (ER variable)
    - 7 unknowns: nC, nH_2, nCO, nH_2O, nCO_2, nCH_4, a
    - 7 equations: 4 mass balances (C, H, O, N) + 3 equilibrium equations (a, b, c)
3. Gasification reaction 1 & empirical correlations (ER variable)
    - 7 unknowns: nC, nH_2, nCO, nH_2O, nCO_2, nCH_4, a
    - 7 equations: 4 mass balances (C, H, O, N) + 2 equilibrium equations (a, b) + energy balance
4. Gasification reaction 1 & EES data (ER variable)
    - 7 unknowns: nC, nH_2, nCO, nH_2O, nCO_2, nCH_4, a
    - 7 equations: 4 mass balances (C, H, O, N) + 2 equilibrium equations (a, b) + energy balance
5. Gasification reaction 1 & empirical correlations (ER fixed)
    - 6 unknowns: nC, nH_2, nCO, nH_2O, nCO_2, nCH_4
    - 6 equations: 4 mass balances (C, H, O, N) + 2 equilibrium equations (a, b)
6. Gasification reaction 1 & EES data (ER fixed)
    - 6 unknowns: nC, nH_2, nCO, nH_2O, nCO_2, nCH_4
    - 6 equations: 4 mass balances (C, H, O, N) + 2 equilibrium equations (a,b)
7. Gasification reaction 1 & empirical correlations (ER fixed)
    - 6 unknowns: nC, nH_2, nCO, nH_2O, nCO_2, nCH_4
    - 6 equations: 4 mass balances (C, H, O, N) + 1 equilibrium equation (a) + energy balance
8. Gasification reaction 1 & EES data (ER fixed)
    - 6 unknowns: nC, nH_2, nCO, nH_2O, nCO_2, nCH_4
    - 6 equations: 4 mass balances (C, H, O, N) + 1 equilibrium equations (a) + energy balance

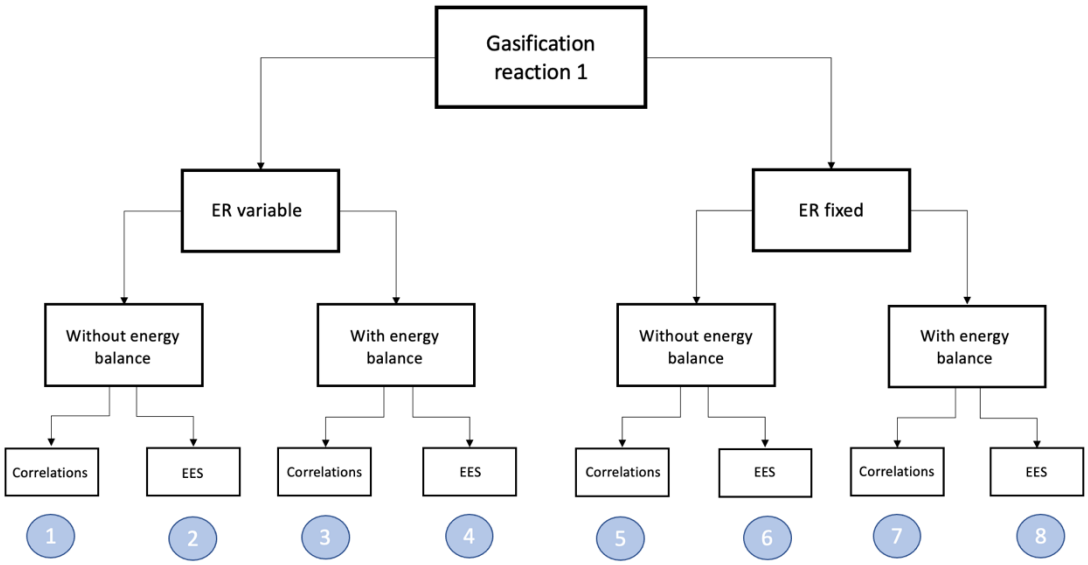

Figure 48: Model development scheme for gasification reaction 1

- **Gasification reaction 2**

9. Gasification reaction 2 & empirical correlations (ER variable)
    - 6 unknowns: nH_2, nCO, nH_2O, nCO_2, nCH_4, a
    - 6 equations: 4 mass balances (C, H, O, N) + 2 equilibrium equations (d, e)
10. Gasification reaction 2 & EES data (ER variable)
    - 6 unknowns: nH_2, nCO, nH_2O, nCO_2, nCH_4, a
    - 6 equations: 4 mass balances (C, H, O, N) + 2 equilibrium equations (d, e)
11. Gasification reaction 2 & empirical correlations (ER variable)
    - 6 unknowns: nH_2, nCO, nH_2O, nCO_2, nCH_4, a
    - 6 equations: 4 mass balances (C, H, O, N) + 1 equilibrium equation (d) + energy balance
12. Gasification reaction 2 & EES data (ER variable)
    - 6 unknowns: nH_2, nCO, nH_2O, nCO_2, nCH_4, a
    - 6 equations: 4 mass balances (C, H, O, N) + 1 equilibrium equation (d) + energy balance
13. Gasification reaction 2 & EES data (ER fixed)
    - 5 unknowns: nH_2, nCO, nH_2O, nCO_2, nCH_4
    - 6 equations: 4 mass balances (C, H, O, N) + 1 equilibrium equation (d) + $\%CH_4$ min constraint

14. Gasification reaction 2 & empirical correlations (ER fixed)
    - 5 unknowns: nH_2, nCO, nH_2O, nCO_2, nCH_4
    - 6 equations: 4 mass balances (C, H, O, N) + 1 equilibrium equation (d) + $\%CH_4$ min constraint
15. Gasification reaction 2 & empirical correlations (ER fixed)
    - 5 unknowns: nH_2, nCO, nH_2O, nCO_2, nCH_4
    - 5 equations: 4 mass balances (C, H, O, N) + energy balance
16. Gasification reaction 2 & EES data (ER fixed)
    - 5 unknowns: nH_2, nCO, nH_2O, nCO_2, nCH_4
    - 5 equations: 4 mass balances (C, H, O, N) + energy balance
17. Gasification reaction 2 & EES data (ER fixed)
    - ***5 unknowns: nH_2, nCO, nH_2O, nCO_2, nCH_4***
    - ***6 equations: 4 mass balances (C, H, O, N) + 2 equilibrium equations***

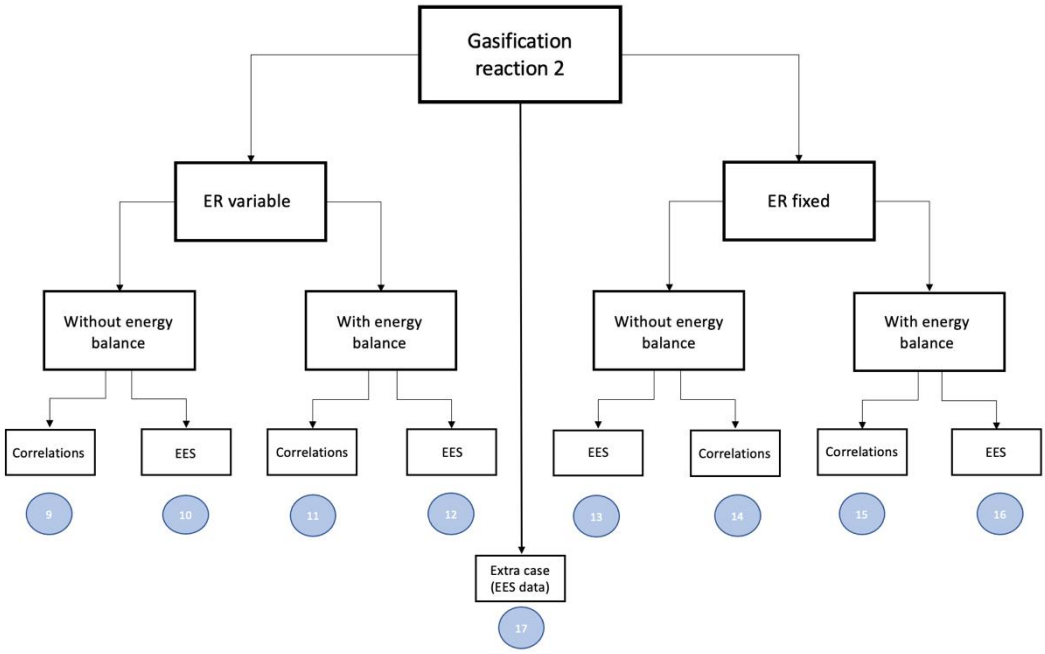

Figure 49: Model development scheme for gasification reaction 2

➢ Gasification reaction 3

18. Gasification reaction 3 & ER variable
    - 5 unknowns: nH_2, nCO, nCO_2, nCH_4, a

- 5 equations: 4 mass balances (C, H, O, N) + %CO = 11.9

Looking carefully at each of the proposed models, many considerations and critical issues arises. In particular, the following peculiarities are evidenced:

- The models that use the punctual values (EES software) to compute the thermodynamic properties (enthalpy, entropy, Gibbs free energy) lead to much more precise results and lower percentage errors than the ones using correlations, both in terms of syngas composition and heating value of the exiting gases. It is because the correlations in most of the cases are imprecise and very approximative, sometimes maybe wrong. Then using punctual values of the main thermodynamic properties allows to mitigate this problem.
- The models that involve the energy balance are very unstable and, in most of the cases, they do not even converge on a solution. It is because the energy balance strictly depends on the considered gasification reaction and, consequently, on the different species that are assumed to be formed because of the gasification. Since the considered gasification reaction is a simplified one, they are not considered the less relevant hydrocarbons, the sulfuric compounds and the other minor gases exiting from the gasifier. This leads to an approximate energy balance that in most of the cases does not give any solution.
- The models accounting the gasification reaction 1, thus viewing solid carbon at the outlet of the gasifier, lead to more aleatory results and to higher error in both the prediction of the outlet composition and the heating value of the syngas.
- The models that introduce the additional constraint on the equivalent ratio, thus fixing the equivalent ratio equal to the one typical of the downdraft gasifier, are much more precise and consistent with respect to the ones that have the ER as a free parameter. That underlines, once again, that the model responds very well to any approach to the real conditions.
- The models accounting the gasification reaction 2, thus not considering solid carbon at the outlet of the gasifier, in the cases 13 and 14, present more than one solution. Thus, it is necessary to introduce one additional constraint to the usual number of equations (equal to the number of unknowns) to get the desired solution. In the specific case, it has been decided to fix the lower percentage value of the methane exiting the gasifier.

- The model accounting the gasification reaction 3, thus the case 18, is a very simplified model and it is just based on the mass balance. Beyond this, one more equation/constraint is needed to close the system, the additional constraint consists in fixing the percentage of the CO equal to the average among all the biomasses experimental data. In the case, it has been chosen to fix the CO amount, rather than the others, because it presents the lower variability range among all the gases (from 10% to 14%). Therefore, this last simplified model is aloof from the reality, and it not based on the thermodynamic equilibrium, leading to very meaningless results. Furthermore, it does not even depend on paramount parameters such us the temperature and the equivalent ratio.

MODELS' RESULTS

Outcomes at fixed temperature and equivalent ratio

By the careful analysis of all the above-mentioned considerations, one additional case (case 17) has been introduced. It complies with the need of obtaining a unique solution without introducing any additional constraint on the minimum amount of methane present in the outlet gas, thus it mitigates the problem of relying on the bibliography and/or on the experimental data, that in many cases are not available. Consequently, the case 17 is over constrained by introducing one more equilibrium equation, thus considering, at the same time, two equilibrium equations (reactions d and e).
Overall, the best outcomes are obtained with the case 13 and 17.

13. Gasification reaction 2 & EES data (ER fixed)
    a. 5 unknowns: nH_2, nCO, nH_2O, nCO_2, nCH_4
    b. 6 equations: 4 mass balances (C, H, O, N) + 1 equilibrium equation (d) + $\%CH_4$ min constraint

17. Gasification reaction 2 & EES data (ER fixed)
    - 5 unknowns: nH_2, nCO, nH_2O, nCO_2, nCH_4
    - 6 equations: 4 mass balances (C, H, O, N) + 2 equilibrium equations

Before showing all the results obtained, it is necessary to specify how any simulation has been made, which are the input parameters involved, how the output results are obtained, how the percentage errors are computed and how the lower heating value of the syngas is estimated.

For all the biomasses, since they were not provided the information about the gasification main parameters (temperature and equivalent ratio), the gasification has been considered to occur at an equilibrium temperature T equal to 1000 K and at an equivalent ratio ER equal to 0.3, except for the corn cob for which it was known that the experiment has been made at a T temperature of 900 K and an ER equal to 0.39.

Finally, once each simulation is developed and the outlet gas composition is known, it is possible to estimate the syngas LHV [69] and, consequently, it is possible to compute the percentage error on the prediction of each gas component and of the lower heating value. Here below all the used formula are depicted.

$$error_i[\%] = \frac{x_{i,model}[\%] - x_{i,experimental}[\%]}{x_{i,experimental}[\%]}$$

(A. 40)

$$LHV_{syngas}\left[\frac{MJ}{kg}\right] = 11.2 * \%H_2 + 13.1 * \%CO + 37.1 * \%CH_4$$

(A. 41)

$$error_{LHV}[\%] = \frac{LHV_{model} - LHV_{experimental}}{LHV_{experimental}}$$

(A. 42)

After having defined the calculation procedure, the following results are listed and depicted below, starting from each biomass.

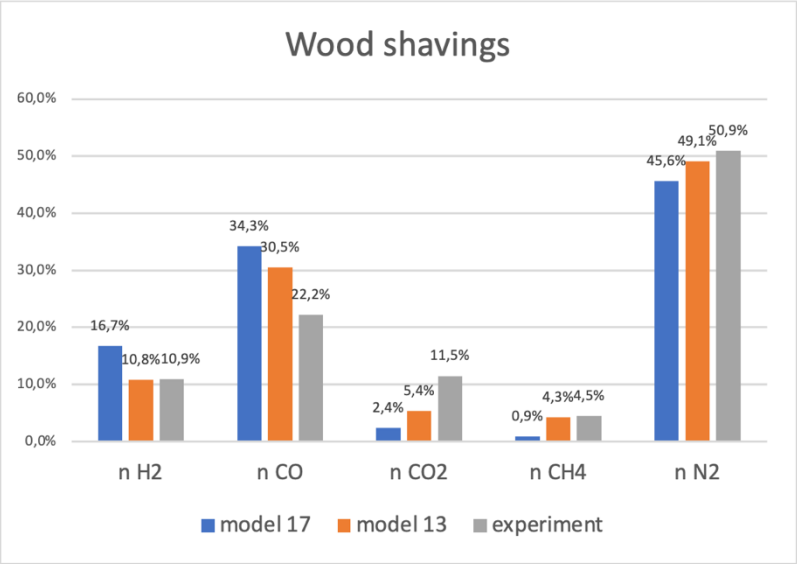

err mod 17	err mod 13	
53,5%	**1,1%**	n H2
54,4%	**37,2%**	n CO
78,8%	**53,2%**	n CO2
79,2%	**5,0%**	n CH4
10,4%	**3,5%**	n N2
15,7%	**17,0%**	LHV
55,3%	20,0%	Avg

Figure 50: Comparison of the syngas composition between models and experimental data - Wood shavings (ER=0.3; T=1000K)

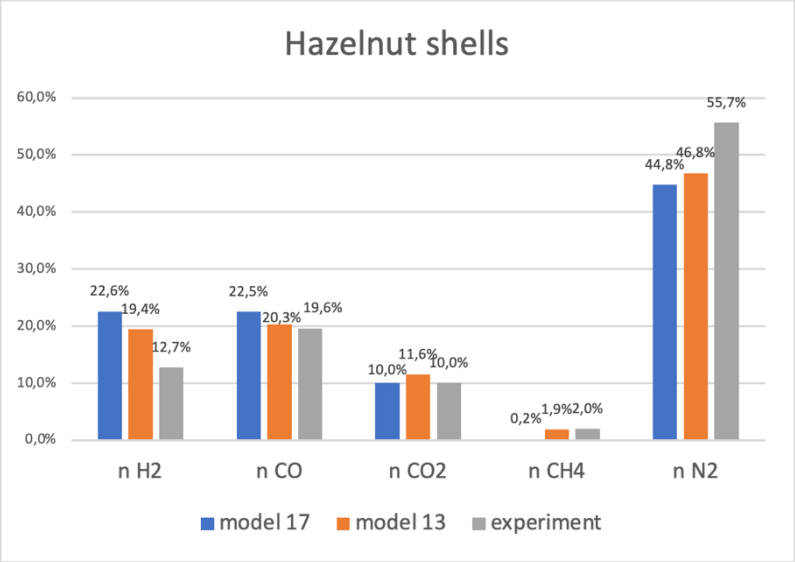

err mod 17	err mod 13	
77,8%	**53,0%**	n H2
14,7%	**3,7%**	n CO
0,0%	**15,5%**	n CO2
91,1%	**5,2%**	n CH4
19,6%	**16,0%**	n N2
17,1%	**17,1%**	LHV
40,6%	18,7%	Avg

Figure 51: Comparison of the syngas composition between models and experimental data - Hazelnut shells (ER=0.3; T=1000K)

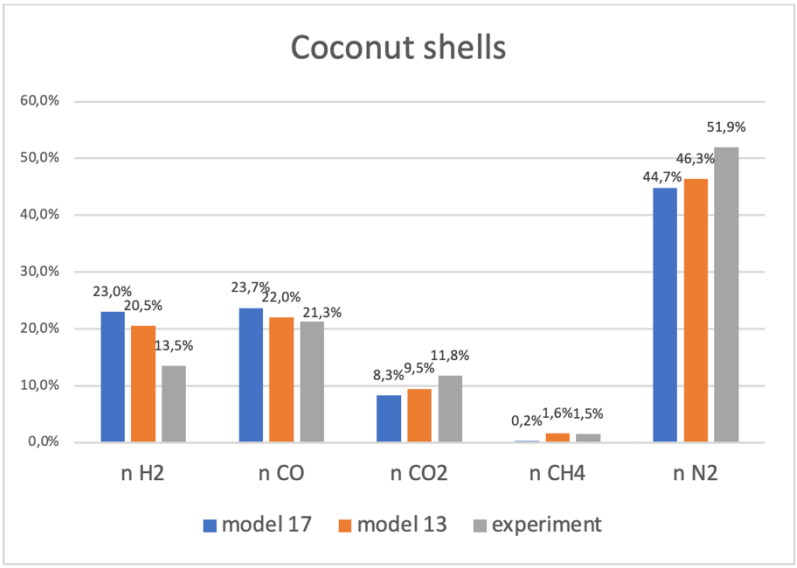

err mod 17	err mod 13	
70,6%	**52,1%**	n H2
11,2%	**3,5%**	n CO
29,6%	**19,7%**	n CO2
83,5%	**7,1%**	n CH4
13,8%	**10,7%**	n N2
18,9%	**19,0%**	LHV
41,7%	**18,6%**	Avg

Figure 52: Comparison of the syngas composition between models and experimental data - Coconut shells (ER=0.3; T=1000K)

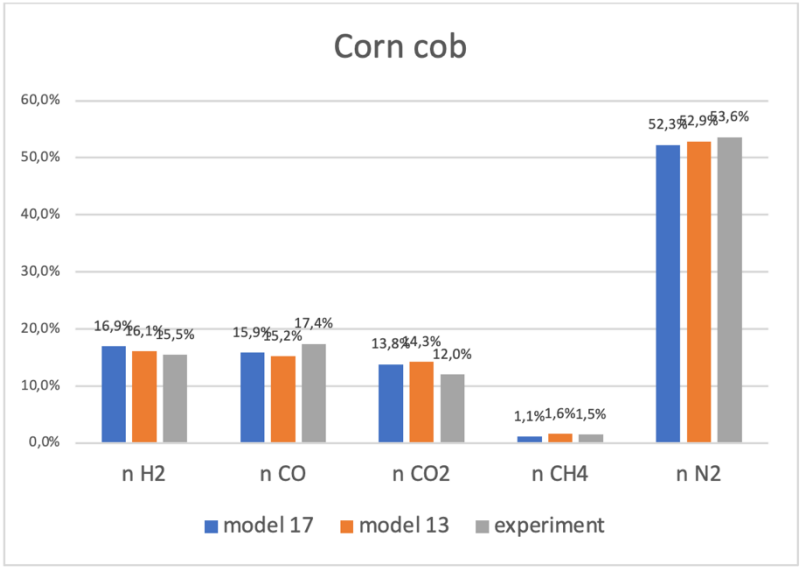

err mod 17	err mod 13	
9,2%	**3,6%**	n H2
8,9%	**12,7%**	n CO
14,9%	**18,9%**	n CO2
23,4%	**8,2%**	n CH4
2,5%	**1,4%**	n N2
3,8%	**4,0%**	LHV
11,8%	**9,0%**	Avg

Figure 53: Comparison of the syngas composition between models and experimental data - Corn cob (ER=0.39; T=900K)

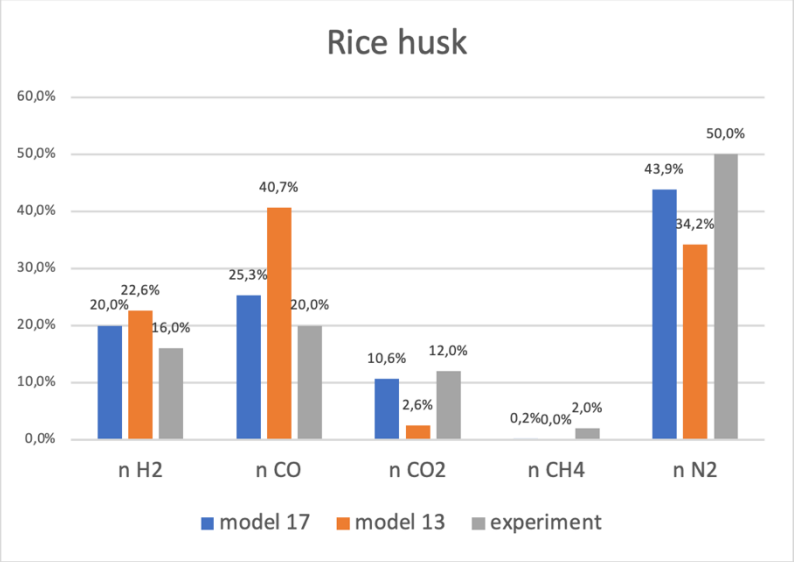

err mod 17	err mod 13	
25,0%	**41,2%**	n H2
26,7%	**103,5%**	n CO
11,3%	**78,7%**	n CO2
91,7%	**100,0%**	n CH4
12,3%	**31,7%**	n N2
9,0%	**52,5%**	LHV
33,4%	71,0%	Avg

Figure 54: Comparison of the syngas composition between models and experimental data - Rice husk (ER=0.3; T=1000K)

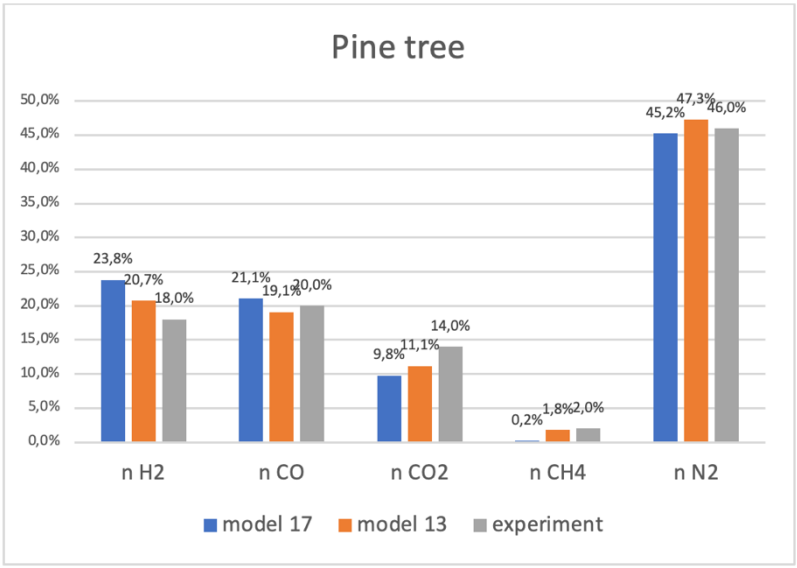

err mod 17	err mod 13	
32,0%	**15,2%**	n H2
5,3%	**4,7%**	n CO
30,3%	**20,5%**	n CO2
91,1%	**10,0%**	n CH4
1,7%	**2,7%**	n N2
2,0%	**2,1%**	LHV
32,1%	10,6%	Avg

Figure 55: Comparison of the syngas composition between models and experimental data - Pine tree (ER=0.3; T=1000K)

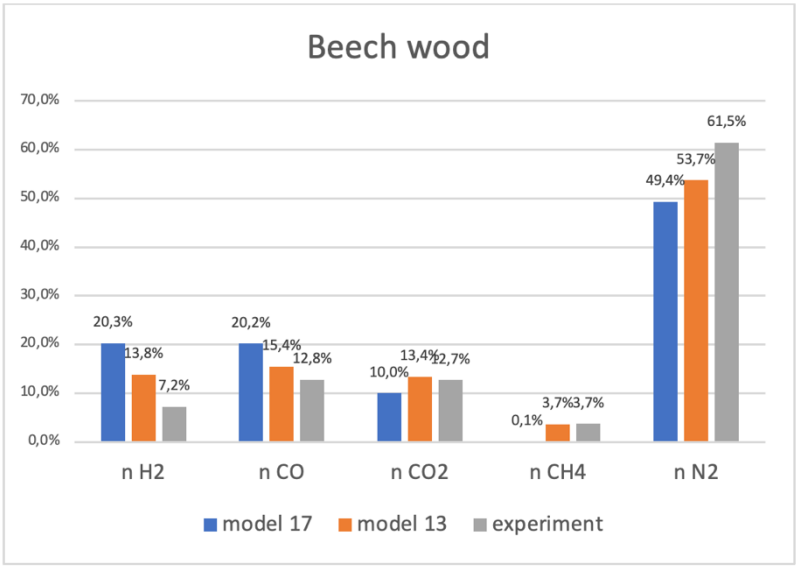

err mod 17	err mod 13	
182,2%	**91,6%**	n H2
57,8%	**20,6%**	n CO
21,2%	**5,2%**	n CO2
96,9%	**1,1%**	n CH4
19,7%	**12,6%**	n N2
28,7%	**27,7%**	LHV
75,5%	**26,2%**	Avg

Figure 56: Comparison of the syngas composition between models and experimental data - beech wood (ER=0.3; T=1000K)

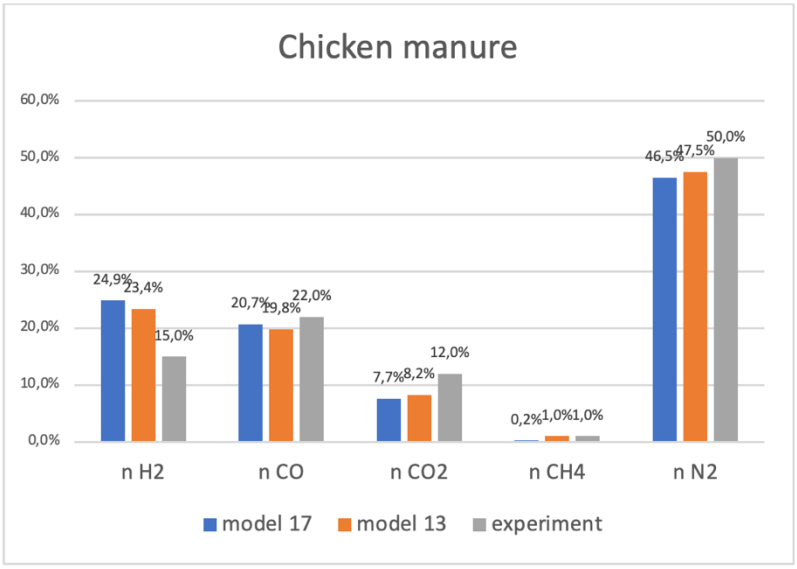

err mod 17	err mod 13	
66,0%	**56,3%**	n H2
6,0%	**10,1%**	n CO
36,2%	**31,4%**	n CO2
76,0%	**1,6%**	n CH4
7,0%	**4,9%**	n N2
13,3%	**13,4%**	LHV
38,2%	**20,9%**	Avg

Figure 57: Comparison of the syngas composition between models and experimental data - Chicken manure (ER=0.3; T=1000K)

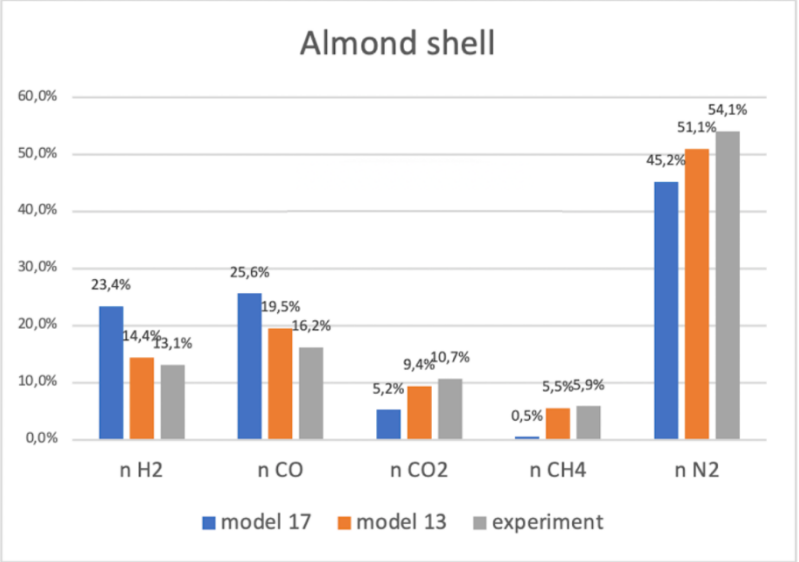

err mod 17	err mod 13	
78,8%	**10,3%**	n H2
58,3%	**20,6%**	n CO
51,1%	**11,8%**	n CO2
91,9%	**6,5%**	n CH4
16,4%	**5,6%**	n N2
6,6%	**7,7%**	LHV
59,3%	11,0%	Avg

Figure 58: Comparison of the syngas composition between models and experimental data - Almond shell (ER=0.3; T=1000K)

Overall, they are reported the average results in the following table.

Table 45: Comparison of the syngas composition between models and experimental data - Average results

Components	model 17	model 13	experiment	err mod 17	err mod 13
n H2	21.3%	18.0%	13.5%	66.1%	36.0%
n CO	23.2%	22.5%	19.1%	27.0%	24.1%
n CO2	8.6%	9.5%	11.9%	30.4%	28.3%
n CH4	0.4%	2.4%	2.7%	80.5%	16.1%
n N2	46.4%	47.7%	52.6%	11.5%	9.9%
			Avg	43.1%	**22.9%**
LHV syngas [MJ/kg]	**5.582**	**5.843**	**5.007**	**12.8%**	17.8%

Together with the syngas composition, it is very interesting to see how the LHV of the syngas differs between the models and the experimental data. Below are reported and depicted all the outcomes for each biomass.

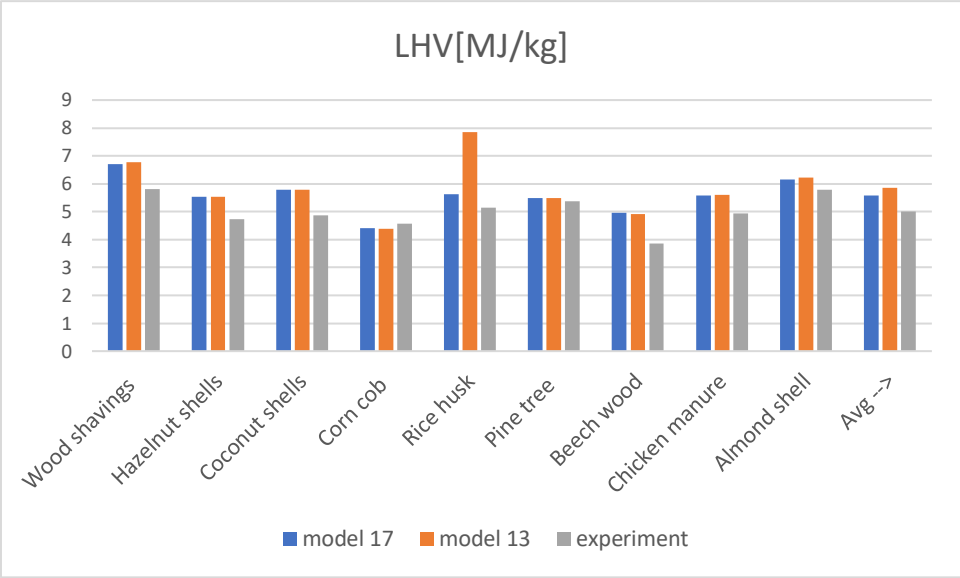

Figure 59: Comparison of the syngas LHV between models and experimental data

In the following table all the punctual values and the errors are reported.

Table 46: Comparison of the syngas LHV between models and experimental data

-	LHVsyngas [MJ/kg]			[%]	
Biomsses	**model 17**	**model 13**	**experiment**	**err mod 17**	**err mod 13**
Wood shavings	6.711	6.783	5.799	**15.7%**	**17.0%**
Hazelnut shells	5.539	5.541	4.732	**17.1%**	**17.1%**
Coconut shells	5.775	5.783	4.859	**18.9%**	**19.0%**
Corn cob	4.400	4.389	4.572	**3.8%**	**4.0%**
Rice husk	5.620	7.861	5.154	**9.0%**	**52.5%**
Pine tree	5.486	5.488	5.378	**2.0%**	**2.1%**
Beech wood	4.964	4.925	3.856	**28.7%**	**27.7%**
Chicken manure	5.589	5.592	4.933	**13.3%**	**13.4%**
Almond shell	6.159	6.225	5.778	**6.6%**	**7.7%**
Avg -->	5.582	5.843	5.007	**12.8%**	**17.8%**

It can be noted that in all the cases the LHV predicted by the models is a bit higher than the one that comes out from the experiments. It is because the H_2 percentage in the models is always higher than the one of the experiments and, also, the CO percentage is higher in most of the cases. The biggest error is registered on the rice husk (model 13) because the CO percentage is very high and it makes the LHV grow a lot. Moreover, for both models (13 and 17), the values of LHV of beech wood predicted by the models detach more than the

other cases because both the H_2 and CO percentage are pretty much higher than the one registered in the experiments. Overall, the model 17 results to be better to predict the LHV value since the higher amount of H_2 and CO are somehow compensated by a lower percentage of methane (err = 12,8%); on the other hand, the model 13 results to be better to predict the syngas composition (mean err = 22,9%).

It must be carefully underlined that the only biomass for which more detailed information were given upon the gasification process (Temperature and equivalent ratio) was the corn cob. In this case the prediction of both the syngas composition and the LHV is very precise and led to very satisfying results.

Overall, the model 17 has been selected and developed to estimate the change of the syngas composition as a function of the main parameters, such as temperature, equivalent ratio, moisture content, gasification agent (pure oxygen vs air). It has been done because the model 17 is more useful than the model 13 in the prediction of the syngas composition variation because it leads by itself to a unique solution, without the needing of introducing the minimum CH_4 percentage constraint, and so it can be used even if it is not known any information about the syngas composition.

In the following section, therefore, it will be analyzed how the syngas composition, and consequently the LHV, changes varying the main parameters above-mentioned. In particular, it will be analyzed the biomass of reference for this project (Chicken manure) using the model 17 for the reasons just described.

Syngas composition varying ER at fixed temperature (T = 1000 K)

The first sensitivity analysis that has been made is the one that looks out how syngas composition (from chicken manure) changes varying the equivalent ratio ER. For this analysis it has been fixed the temperature at a typical gasification value of 1000 K, while the ER has been ranged between 0.1 and 0.8.

Table 47: Syngas composition at T=1000 K fixed and ER from 0,1 to 0,8 – Model 17

T = 1000 K	ER							
Syngas	**0.1**	**0.2**	**0.3**	**0.4**	**0.5**	**0.6**	**0.7**	**0.8**
n H_2	36.7%	31.3%	24.9%	19.3%	14.6%	10.6%	7.2%	3.7%
n CO	34.5%	27.1%	20.7%	15.5%	11.4%	8.0%	5.3%	2.7%
n CO_2	2.8%	5.2%	7.7%	9.7%	11.3%	12.5%	13.5%	12.3%
n H_2O	2.3%	4.6%	7.1%	9.3%	11.1%	12.7%	14.1%	13.3%
n CH_4	4.0%	1.0%	0.2%	0.1%	0.0%	0,0%	0.0%	0.0%
n N_2	19.7%	30.9%	39.4%	46.2%	51.7%	56.1%	59.9%	63.0%

It is more useful and intuitive to see how each molecule percentage in the outlet gas changes, within this range of ER, in a chart. To proper evaluate the validity of the model, it has been compared the graph obtained through the model with the one obtained through experiments [69].

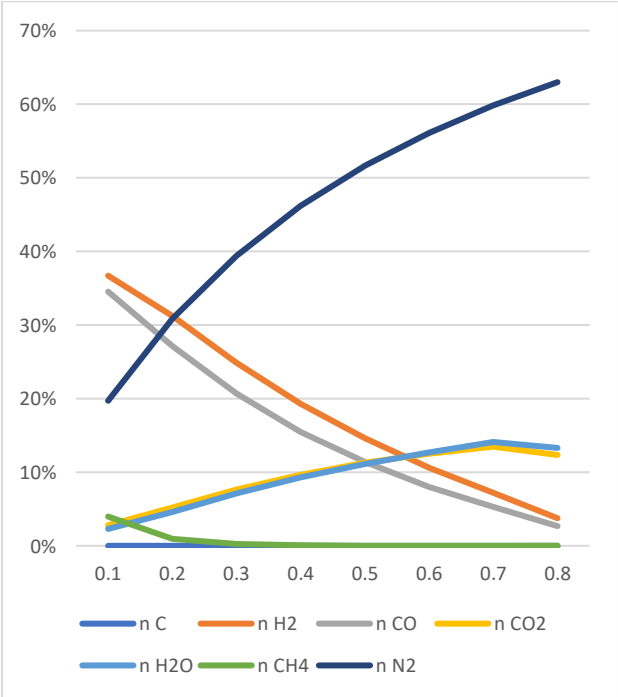

Figure 60: Syngas composition at T=1000 K fixed and ER from 0,1 to 0,8 – Model 17

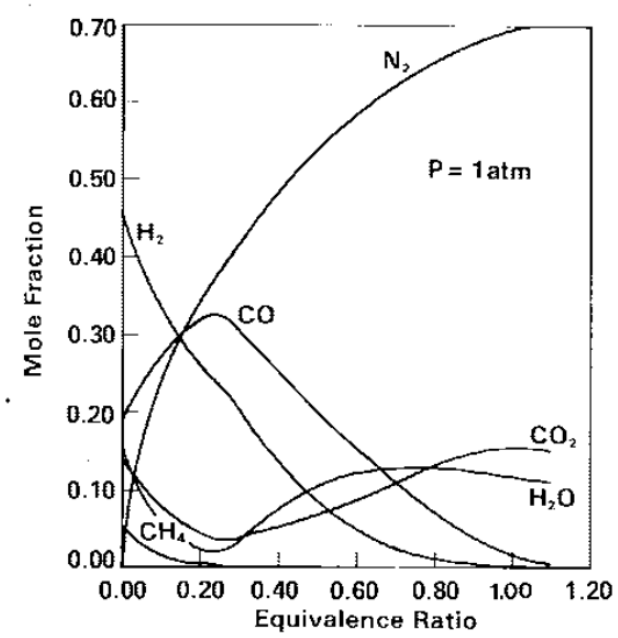

Figure 61: Syngas composition at T=1000 K fixed and ER from 0.1 to 0.8 – Experiments [8]

It can be noted that the model emulates in a satisfying way the behavior of the experimental results. Looking carefully, the N_2 trend is practically the same in both cases, the H_2 and CO have the same trend as the ones of the experiment except for low ER, where the CO is decreasing while in the real case it has a maximum around 0.3. Same consideration can be made for both CO_2 and H_2O that in the model are increasing with ER, while in the real case in the first part they show a minimum. For CO, CO_2 and H_2O, anyway, it can be seen that their values are pretty close to the ones of the experiments at each ER. Concerning the CH_4, it can be noted that both the trend and the percentage value are practically the same.

Syngas composition varying T at fixed equivalent ratio (ER = 0.1, 0.25, 0.3, 0.4)

The second sensitivity analysis that has been made is the one that looks out how syngas composition (from chicken manure) changes varying the equilibrium temperature. This analysis has been made fixing the equivalent ratio ER equal to different values (0.21, 0.25, 0.3, 0.4). It allowed to see how the temperature of the process affects the gas composition at

different values of the equivalent ratio. Here below they are reported all the tables with the punctual values.

Table 48: Syngas composition varying T at fixed equivalent ratio (ER = 0.4)

ER = 0.4	T [K]					
Syngas	**800**	**900**	**1000**	**1100**	**1200**	**1300**
n H_2	12.3%	18.8%	19.3%	18.2%	17.4%	16.6%
n CO	5.8%	12.7%	15.5%	16.7%	17.6%	18.4%
n CO_2	16.8%	11.9%	9.7%	8.5%	7.6%	6.8%
n H_2O	9.1%	8.3%	9.3%	10.4%	11.3%	12.0%
n CH_4	5.1%	1.1%	0.1%	0.0%	0.0%	0.0%
n N_2	50.9%	47.1%	46.2%	46.2%	46.2%	46.2%

Table 49: Syngas composition varying T at fixed equivalent ratio (ER = 0.3)

ER = 0.3	T [K]					
Syngas	**800**	**900**	**1000**	**1100**	**1200**	**1300**
n H_2	12.9%	21.9%	24.9%	24.3%	23.5%	22.8%
n CO	7.3%	16.4%	20.7%	22.0%	22.8%	23.5%
n CO_2	17.5%	10.9%	7.7%	6.4%	5.6%	4.9%
n H_2O	7.9%	6.9%	7.1%	8.0%	8.8%	9.5%
n CH_4	8.5%	2.6%	0.2%	0.0%	0.0%	0.0%
n N_2	45.9%	41.3%	39.4%	39.3%	39.2%	39.2%

Table 50: Syngas composition varying T at fixed equivalent ratio (ER = 0.25)

ER = 0.25	T [K]					
Syngas	**800**	**900**	**1000**	**1100**	**1200**	**1300**
n H_2	13.1%	23.2%	28.0%	27.9%	27.3%	26.7%
n CO	8.2%	18.5%	23.7%	25.1%	25.8%	26.5%
n CO_2	17.9%	10.4%	6.5%	5.2%	4.5%	3.9%
n H_2O	7.3%	6.2%	5.9%	6.6%	7.2%	7.8%
n CH_4	10.9%	3.9%	0.5%	0.0%	0.0%	0.0%
n N_2	42.7%	37.8%	35.4%	35.1%	35.1%	35.1%

Table 51: Syngas composition varying T at fixed equivalent ratio (ER = 0.21)

ER = 0,21	T [K]					
Syngas	**800**	**900**	**1000**	**1100**	**1200**	**1300**
n H_2	13.1%	24.2%	30.6%	31.2%	30.7%	30.2%
n CO	9.1%	20.3%	26.4%	27.9%	28.6%	29.1%
n CO_2	18.3%	10.0%	5.5%	4.2%	3.6%	3.1%
n H_2O	6.7%	5.6%	4.9%	5.3%	5.8%	6.3%
n CH_4	13.2%	5.3%	0.8%	0.1%	0.0%	0.0%
n N_2	39.6%	34.6%	31.8%	31.4%	31.3%	31.3%

Also in this case, it is more explicative to look out the syngas composition change with temperature through the charts. In that way it is possible to see in an easier way the trend of the various components of which the syngas is composed of.

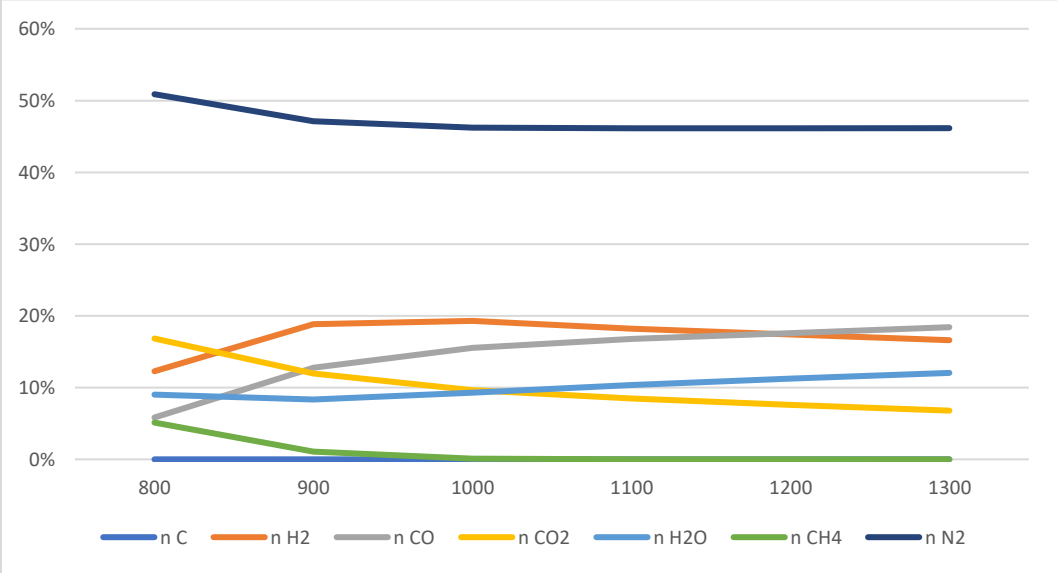

Figure 62: Syngas composition varying T at fixed equivalent ratio (ER = 0.4)

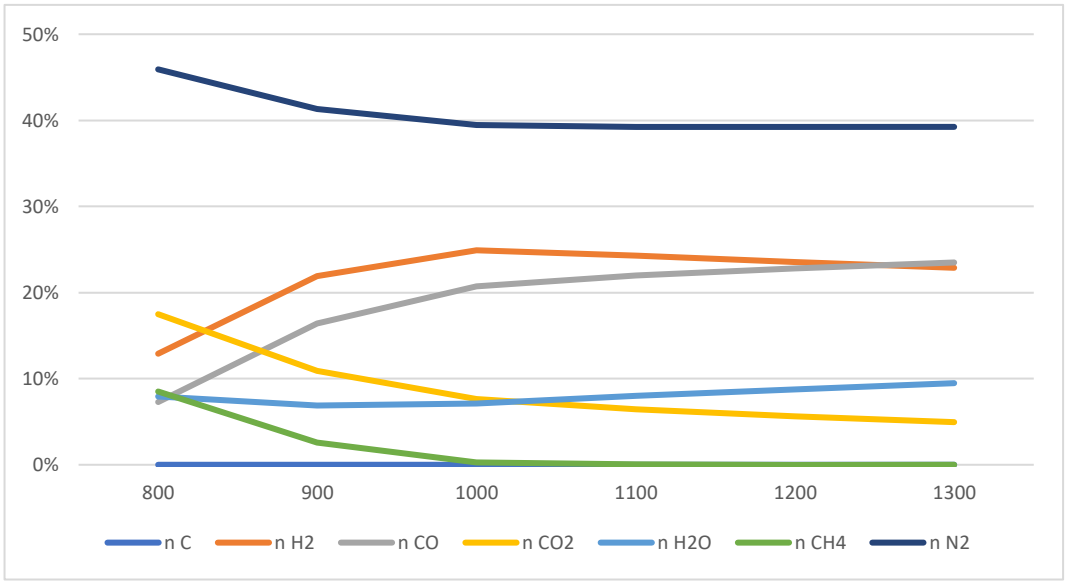

Figure 63: Syngas composition varying T at fixed equivalent ratio (ER = 0.3)

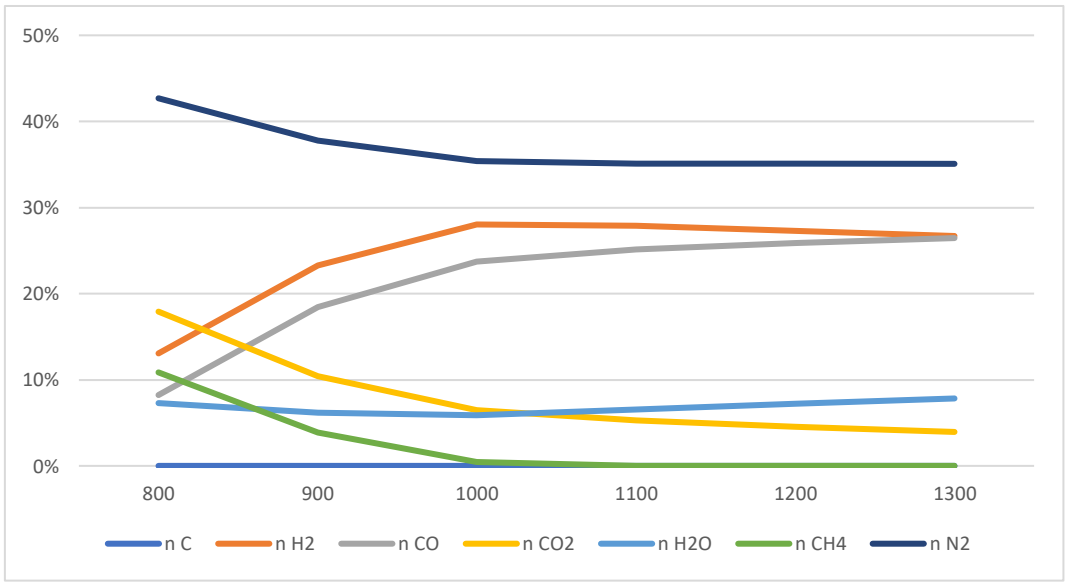

Figure 64: Syngas composition varying T at fixed equivalent ratio (ER = 0.25)

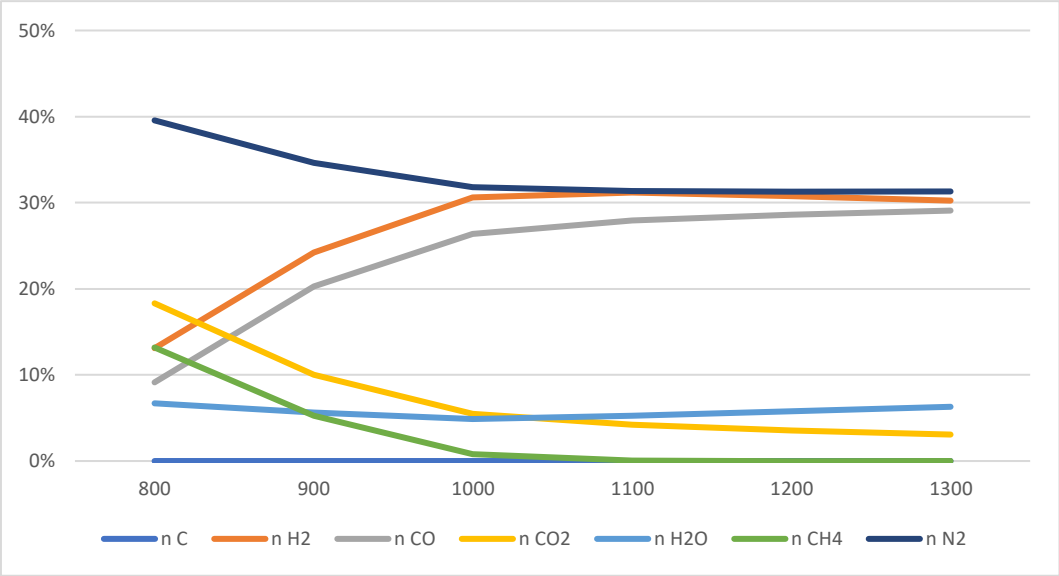

Figure 65: Syngas composition varying T at fixed equivalent ratio (ER = 0.21)

First observation that can be made concerns the fact that decreasing the equivalent ratio, thus the amount of air, the percentage of nitrogen decreases in favor of the growth of the amount of both CO and H_2. This, in principle, would increase the heating value of the syngas but, on the other hand, an important decrease of methane is shown, so the advantage of growing CO and H_2 is somehow counteracted by the decrease of CH_4. The CO_2 percentage keeps almost the same for each ER, it is shown just a slight decrease for lower ER while the amount of H_2O shows a pretty evident decrease at lower ER.

Now, looking on the other way, it is possible to see how the com ponents of the syngas have all the same trend, whatever the ER, changing the temperature. So that the considerations made on a fixed equivalent ratio hold true also for other values of ER. In all the cases the percentage of N_2, CH_4, CO_2 decreases with temperature, while the CO and H_2 percentages increase with temperature. Concerning the H_2O, the trend is not monotonous, indeed it decreases until a certain temperature, reaches a minimum, and then grows up increasing the temperature. This minimum is shifted towards higher temperatures for lower ER.

Syngas LHV varying T at fixed equivalent ratio (ER = 0.3)

After having seen closer how each component of the obtained gas changes varying the temperature and the ER, it is interesting to watch out the influence on the heating value, since it is crucial in understanding the amount of energy that can be obtained from the

gasification process. In. this direction, it has been studied, for chicken manure, how the LHV is affected by a change of temperature, holding constant the ER to a typical value of 0.3. The important thing to see in this case is not the value itself of the syngas LHV (it has already been analyzed above) but rather the trend to see if it effectively matches with the experimental results [69].

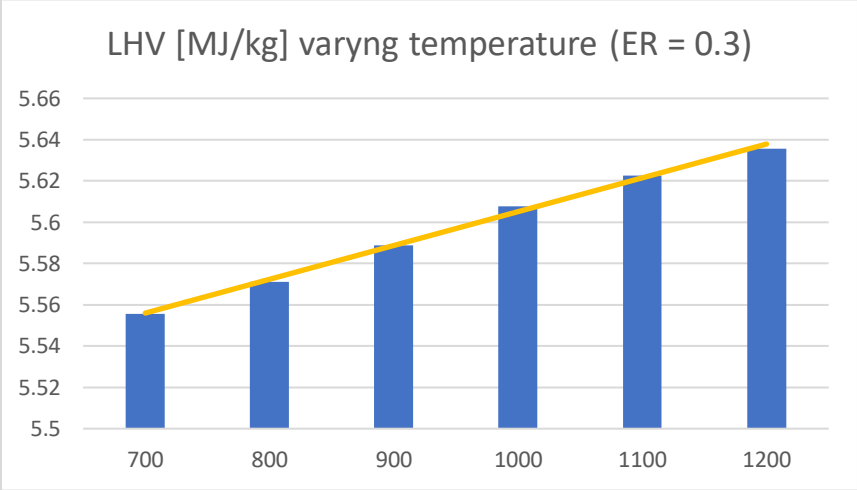

Figure 66: Syngas LHV [MJ/kg] varying T at fixed equivalent ratio (ER = 0.3) – Model 17

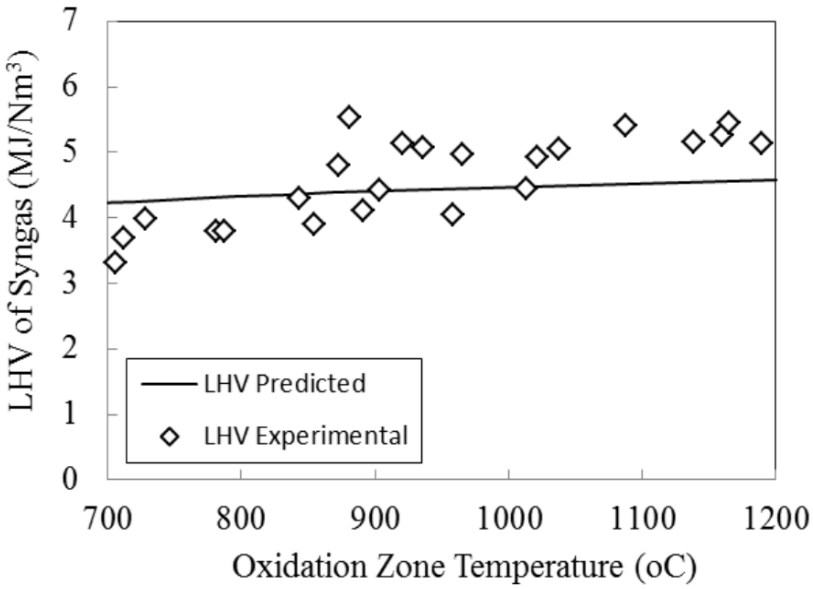

Figure 67: Syngas LHV [MJ/Nm3] varying T at fixed equivalent ratio (ER = 0.3) – Experiments [8]

It can be seen that in both the model and the experiments, the LHV of the syngas increases with the temperature keeping constant the equivalent ratio. It has to be underlined, on the other hand, that the LHV is more sensible to temperature changes in the experiments, hence the temperature impression results to be a bit more significant in the experiments.

Syngas LHV varying ER at fixed temperature (T = 1000 K), air vs pure oxygen

The syngas LHV change can be seen also on the other way around, that is changing the equivalent ratio ER at fixed temperature. Furthermore, it is very interesting to see how the syngas LHV changes when using pure oxygen rather than ambient air. Then, the gasification reaction has been modified in order to use pure oxygen and to watch out the outcomes. The temperature has been fixed at a typical value of 1000 K and the equivalent ratio has been ranged from 0.1 to 0.6. Here below the results obtained are shown.

Table 52: Syngas LHV varying ER at fixed temperature (T = 1000 K), air vs pure oxygen

T = 1000 K	ER					
	0.1	**0.2**	**0.3**	**0.4**	**0.5**	**0.6**
LHV with air [MJ/kg]	10.108	7.402	5.589	4.216	3.128	2.243
LHV with O2 [MJ/kg]	11.808	10.486	9.165	7.838	6.502	5.159

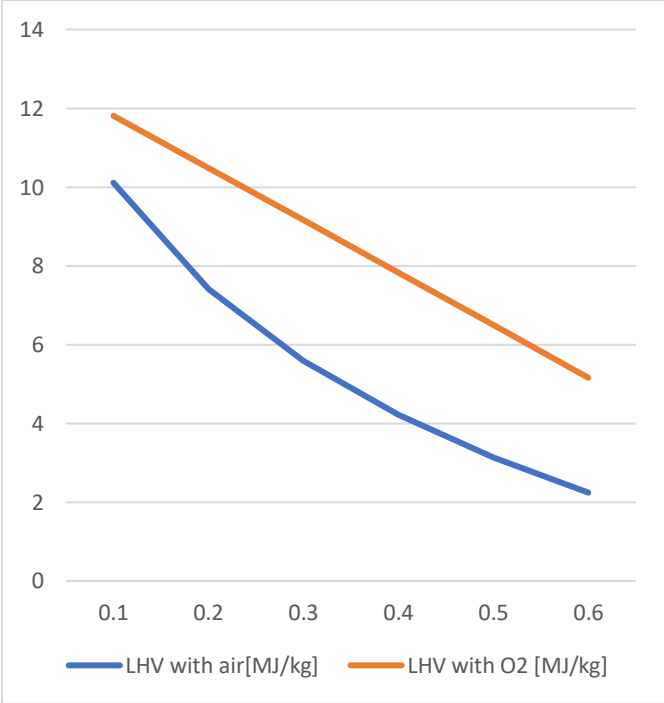

Figure 68: Syngas LHV varying ER at fixed temperature (T = 1000 K), air vs pure oxygen – Model 17

Also in this case, it is interesting to compare the results obtained through the model with the experimental ones that are reported in the following chart [69].

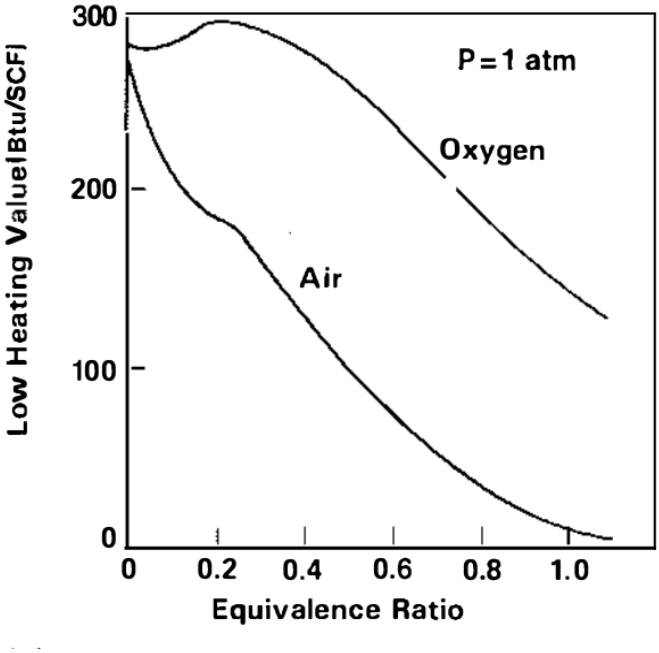

Figure 69: Syngas LHV varying ER at fixed temperature (T = 1000 K), air vs pure oxygen – Experiments [8]

It can be noted that the trend for the gasification with air is very similar to the one of the experiments, while the one using oxygen presents a different trend in the left part (low ER). Indeed, the experiments evidence a non-monotonous trend (having a maximum around ER equal to 0.3) while, according to the model, the LHV of the syngas decreases in a linear way. Overall, the results are satisfying also in this case since the model predict in a good way the LHV value of the syngas, evidencing that using air the LHV of the syngas is much higher and, on the other hand, emulates pretty well the trend of the experiments, especially with air.

Syngas composition and LHV varying the MC at fixed T and ER (T = 1000 K, ER = 0.3)

It is very interesting to watch out how the biomass moisture content affects the syngas composition and, consequently the LHV. The biomass of interest of this study, the chicken manure, has a very high moisture content. For this reason, it might be convenient to dry it before being introduced in the gasifier. Therefore, it has been assumed to reduce the moisture content of the chicken manure from its initial value of 29.4% to 15%. All the other

components have been rescaled accordingly. The table below shows the difference of the two compositions.

Table 53: Chicken manure composition - before and after drying

Chicken Manure	Volatile matter	Humidity	Ashes	Fixed carbon
Before drying	56.7%	29.4%	13.8%	0.1%
After drying	68.3%	15.0%	16.6%	0.1%

According to these initial compositions, it has been found the syngas composition at a typical temperature of 1000 K and at a typical equivalent ratio ER equal to 0.3. The results are depicted in the following table and chart.

Table 54: Syngas composition and LHV of chicken manure varying the MC (29.4% vs 15%)

	MC 15%	MC 29.4%
n H_2	22,9%	23.4%
n CO	25.7%	19.8%
n CO_2	4.8%	8.2%
n CH_4	0.5%	1.0%
n N_2	46.1%	47.5%
LHV syngas [MJ/kg]	**6.108**	**5.592**

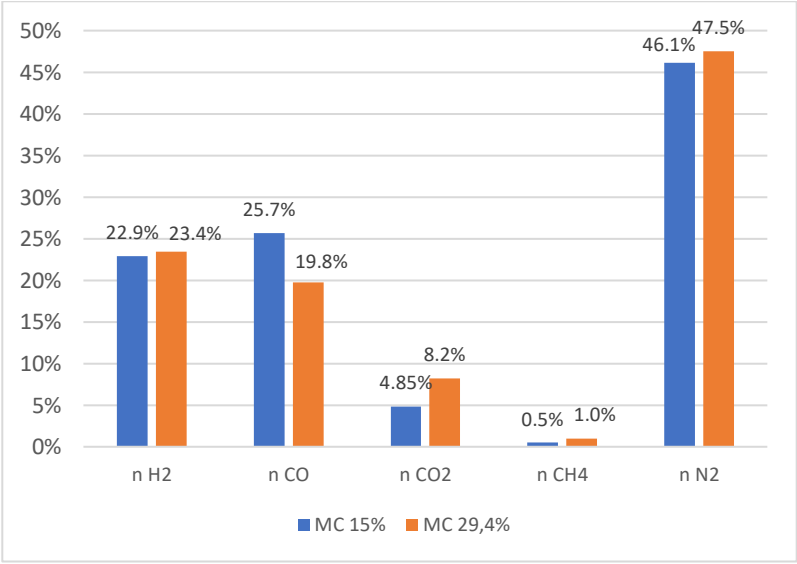

Table 55: Syngas composition and LHV of chicken manure varying the MC (29.4% vs 15%)

The important outcome of this comparison regards the LHV change. Indeed, it is possible to note that, with the dry chicken manure, the CO percentage increase in the syngas prevails over the modest decrease of H_2 and CH_4, thus leading to a LHV increase of 9.2%. Therefore, it could be interesting, according to the model, to dry the biomass before gasifying in order to achieve a higher efficiency of the process.

ADVANTAGES, DRAWBACKS AND FINAL CONSIDERATIONS

The described model results to be satisfying and very useful to approximatively predict the gasification process outcomes starting from each biomass at defined input parameters, such as the temperature and the equivalent ratio. It is for sure approximative due to the simplifying hypothesis on which it is based that, consequently, cannot lead to very rigorous results as it happens with the experimental analysis. The reality is much more complex than the model. The species involved are much more than the ones considered, the process happens in various steps, each of them at a different temperature, the biomass undergoing the gasifier is not uniformly distributed, it has not a regular composition and it has not even the same temperature in a singular section due to temperature gradients, the gases are not homogeneously distributed. Furthermore, there are lots of type of downdraft gasifier, that work following the same principles but, at the same time, they are all different among themselves since each brand and each type has his own design, not to mention the fact that also the same gasifier does not work in the same way during the entire lifetime due to degradation phenomena or fouling of some components.

All of this to underline that a simple model cannot never substitute or be as precise as the observation and measurements of the reality but is a very useful and helpful tool for estimating the yield starting from a specific model. It has the big advantages of being free, quick, and easy to perform once it is developed. On the other hand, it is not even easy to get reliable information upon the gasification results. There are a lot of publications but, in most of the cases, they are not specified the equipment, the conditions and the input parameters through which the gasification occurs. Also, to evaluate the errors in the prediction of the syngas composition for each biomass, they are not known neither the parameters under which the gasification happens nor if the experiments have been developed in a proper way. Overall, comparing the results with the available information and experimental data, the model is a good option and approach whenever there is the need of obtaining quick and

cheap information upon a process and to evaluate, approximatively, the yield that is possible to obtain starting from each condition and biomass.

COMPARISON WITH CIEMAT MODEL

After having shown all the results and highlighted all the features of the proposed mode, it is useful to compare its outcomes with the ones obtained with the CIEMAT model. The CIEMAT (Center for Energy, Environmental and Technological Research) is a public research organization attached to the Ministry of Science and Innovation through the general secretariat for research, focused mainly on the fields of energy and the environment and technological fields related to both.

The CIEMAT model is also a 0-D model developed in more than one step. It is based on the same principles as the model proposed in this project, but it uses different equations, reactions, and steps. This model has been used to compare the results obtained with chicken manure for different values of temperature (800 °C, 850 °C, 900 °C) and different values of equivalent ratio (0.21, 0.25, 0.3, 0.4) and, furthermore, reducing the moisture content until 15%, at fixed ER of 0.3 for the above-mentioned values of temperature. Below it is reported the syngas composition for all the described cases.

Table 56: Syngas composition varying ER obtained with the CIEMAT model - T=800°C

	ER = 0.21	ER = 0.25	ER = 0.3	ER = 0.4
n H_2	29.5%	26.1%	22.4%	15.9%
n CO	20.9%	18.5%	15.7%	11.1%
n CO_2	9.5%	10.6%	11.7%	13.7%
n CH_4	2.7%	2.6%	2.4%	2.2%
n N_2	37.3%	42.1%	47.7%	57.1%

Table 57: Syngas composition varying ER obtained with the CIEMAT model - T=850°C

	ER = 0.21	ER = 0.25	ER = 0.3	ER = 0.4
n H_2	29.1%	25.7%	21.9%	15.4%
n CO	21.7%	19.3%	16.5%	11.8%
n CO_2	8.9%	9.9%	11.1%	13.2%

n CH_4	2.7%	2.6%	2.5%	2.2%
n N_2	37.5%	42.4%	47.9%	57.4%

Table 58: Syngas composition varying ER obtained with the CIEMAT model - T=900°C

	ER = 0,21	**ER = 0,25**	**ER = 0,3**	**ER = 0,4**
n H_2	28.7%	25.3%	21.4%	14.9%
n CO	22.4%	20.0%	17.2%	12.4%
n CO_2	8.4%	9.4%	10.6%	12.7%
n CH_4	2.7%	2.6%	2.5%	2.2%
n N_2	37.7%	42.6%	48.2%	57.7%

Table 59: Syngas composition varying T obtained with the CIEMAT model – ER=0.3, MC=15%

	T = 800 °C	**T = 850 °C**	**T = 900 °C**
n H_2	19.7%	19.4%	19.0%
n CO	19.5%	20.2%	20.8%
n CO_2	8.8%	8.3%	7.9%
n CH_4	2.5%	2.5%	2.5%
n N_2	49.3%	49.5%	49.7%

To better understand which are the differences between the two models, it has been reported the difference, in percentage, of the model developed in that project minus the one of CIEMAT. In the following tables all the results are reported.

Table 60: Syngas composition difference between the proposed model and the CIEMAT model – T=800°C

	ER = 0.21	ER = 0.25	ER = 0.3	ER = 0.4
n H_2	1.8%	1.9%	2.2%	2.7%
n CO	6.8%	6.4%	6.0%	5.4%
n CO_2	-5.1%	-5.1%	-5.0%	-5.0%
n CH_4	-2.6%	-2.5%	-2.4%	-2.2%
n N_2	-0.8%	-0.7%	-0.6%	-0.8%

Table 61: Syngas composition difference between the proposed model and the CIEMAT model - T =850°C

	ER = 0.21	ER = 0.25	ER = 0.3	ER = 0.4
n H_2	2.0%	2.1%	2.2%	2.7%
n CO	6.4%	6.0%	5.7%	5.2%
n CO_2	-4.9%	-4.9%	-4.9%	-4.9%
n CH_4	-2.7%	-2.6%	-2.4%	-2.2%
n N_2	-0.8%	-0.6%	-0.5%	-0.6%

Table 62: Syngas composition difference between the proposed model and the CIEMAT model - T=900°C

	ER = 0.21	ER = 0.25	ER = 0.3	ER = 0.4
n H_2	2.2%	2.2%	4.3%	7.9%
n CO	6.0%	5.7%	6.8%	8.9%
n CO_2	-4.7%	-4.7%	-6.2%	-8.8%
n CH_4	-2.7%	-2.6%	-2.5%	-2.2%
n N_2	-0.7%	-0.5%	-2.4%	-5.7%

Table 63: Syngas composition difference between the proposed model and the CIEMAT model - ER=0.3, MC=15%

	T = 800 °C	T = 850 °C	T = 900 °C
n H_2	3.4%	3.6%	3.8%
n CO	7.1%	6.7%	6.4%
n CO_2	-4.7%	-4.6%	-4.4%
n CH_4	-2.4%	-2.5%	-2.5%
n N_2	-3.2%	-3.2%	-3.2%

Thanks to this comparison, it is possible to see that that the percentage of both H_2 and CO is higher in the proposed model with respect to the CIEMAT one. In particular, the H_2 percentage difference increases with higher ER and temperature, while for the CO is the opposite. On the other hand, the percentage of CO, CH_4 and N_2 is lower in the proposed model. It can be seen that the CH_4 difference increases with both higher T and ER, while both the CO_2 and N_2 differences increase with higher ER and lower T.

Finally, the percentage error of the two models with the experimental data is calculated at a temperature equal to 800 °C and an equivalent ratio equal to 0.3.

Table 64: Syngas composition and LHV error between models and experimental data - T=800°C, ER=0.3

	Model 17	CIEMAT model	Experiments	%err model 17	%err CIEMAT model
n H_2	24.5% ↑	22.4% ↑	15.0%	63.4%	49.0%
n CO	21.7% ↓	15.7% ↓	22.0%	1.3%	28.4%
n CO_2	6.7% ↓	11.7% ↓	12.0%	44.1%	2.3%
n CH_4	0.0% ↓	2.4% ↑	1.0%	96.5%	144.2%
n N_2	47.0% ↓	47.7% ↓	50.0%	5.9%	4.7%
			Avg -->	42.2%	45.7%
LHV syngas [MJ/kg]	5.603 ↑	5.473 ↑	4.933	13.6%	10.9%

Overall, the results show that the proposed model results to be (at least for chicken manure and at those T and ER) more precise than the CIEMAT one in terms of syngas composition, but it leads to a higher overestimation of the syngas lower heating as a consequence of an higher percentage of both H_2 and CO.

LIST OF FIGURES

LIST OF TABLES